RO 2

ROMANIAN ACADEMY

ROMANIAN ASTRONOMICAL JOURNAL

Vol. 16, No. 2
2006

EDITURA ACADEMIEI ROMÂNE

ROMANIAN ACADEMY

ROMANIAN ASTRONOMICAL JOURNAL

The ROMANIAN ASTRONOMICAL JOURNAL appears twice a year. Orders from abroad (issues or subscriptions) should be sent to:
EDITURA ACADEMIEI ROMÂNE, Calea 13 Septembrie nr. 13, sector 5, 050711, Bucharest, Romania, Phone: +(4021) 318 81 46, +(4021) 318 81 06, Fax: +(4021) 318 24 44, E-mail: edacad@ear.ro, Web: www.ear.ro
RODIPET S.A., Piaţa Presei Libere nr. 1, sector 1, P.O. Box 33-57, Bucharest, Romania, Phone: +(4021) 318 70 00, +(4021) 318 70 01, Fax: +(4021) 318 70 02, +(4021) 318 70 03 E-mail: rodipet@rodipet.ro
ORION PRESS IMPEX 2000, P.O. Box 77-19, sector 3, Bucharest, Romania, Phone: +(4021) 0311044668; Phone/Fax:+(4021) 610 67 65; +(4021) 210 67 87, E-mail: office@orionpress.ro

The manuscripts, the books and journals proposed in exchange and the mail should be sent to the Editorial Board.

Editorial Board's Address:

ROMANIAN ASTRONOMICAL JOURNAL
Astronomical Institute of the Romanian Academy
Str. Cuţitul de Argint 5
040557 Bucharest 28
Phone: +(4021) 335 68 92, +(4021) 335 80 10
Phone/Fax: +(4021) 337 33 89
E-mail: roaj@aira.astro.ro
http://www.astro.ro/~roaj/
Romania

Calea 13 Septembrie nr. 13, sector 5, Bucureşti, tel. +(4021) 318 81 46
E-mail: edacad@ear.ro
Internet: http://www.ear.ro/

ROMANIAN
ASTRONOMICAL
JOURNAL

Vol. 16, No. 2, 2006

CONTENTS

ON THE SUN'S MOTION WITH RESPECT TO NEARBY STARS

ADINA IONESCU [1], MARIAN DORU ŞURAN [2]

[1] *"Octav Onicescu" National College*
Str. Trivale 29, Bucharest, Romania
E-mail: adina_2301@yahoo.com

[2] *Astronomical Institute of the Romanian Academy*
Str. Cuţitul de Argint 5, 040557 Bucharest, Romania
E-mail: suran@aira.astro.ro

Abstract. We determine the Sun's motion with respect to the neighbouring stars, using a kinematical selection obtained via a combination of Hipparcos catalogue and Barbier-Brossat catalogue of radial velocities. The Sun' velocity is determined by the methods of spatial velocities, radial velocities, and proper motions. We point out that there are no significant differences between the results obtained by the application of these three methods. Because the results in literature were obtained via studies made on a limited number of stars, we consider a number of stars as large as possible, with known radial velocities and parallaxes. Here we extend the previous results, determining the Sun's motion with respect to stars situated at different distances. The Sun's velocity is also determined as function of the color index for the stellar population situated in the central region and for those stellar populations belonging to ZAMS, TAMS, and AGB regions.

Key words: stellar dynamics – Sun's motion.

1. INTRODUCTION

To determine the Sun's motion with respect to the stars and the velocity ellipsoid, different methods (based on total velocities, radial velocities, and proper motions) were used. Parenago (1950) determined the velocity components for 3000 stars belonging to the flat, intermediate, and spherical sub-systems, getting the apex of the Sun's motion and the velocity of the Sun for each homogeneous group of stars. He indicated the existence of a change of all kinematical components for F-type stars. As to stars of G, K, M types, the kinematical elements remain practically unchanged.

Delhaye (1965) done the most complete synthesis of the results obtained until 1961 through the determination of the Sun's motion and of the velocity ellipsoid for stars of different spectral types. Wielen (1982) completed later the results synthesized by Delhaye, correcting the $v_{\odot}$ component of the Sun's velocity with respect to the local standard of the rest (LSR), namely with respect to the local centroid.

At present the dynamical definition of LSR is in use, LSR meaning the system of the rest centered in the Sun that moves on a circular orbit around the galactic center (e.g., Illingworth and Clark 2000).

The most used procedures to determine the velocity components of the Sun with respect to LSR is to consider distinct stellar populations with different velocity dispersions, to calculate the mean motion of each stellar population with respect to the Sun, and to extrapolate to zero the velocity dispersion. Through this method, by eliminating very young stars from the selection, Dehnen and Binney (1998) obtained the values $u_{\odot} = 10.00 \pm 0.3$ km/s, $v_{\odot} = 5.25 \pm 0.62$ km/s, $w_{\odot} = 7.17 \pm 0.38$ km/s for the components of the Sun's motion with respect to LSR. Different authors obtained approximately the same results for $u_{\odot}$ and $w_{\odot}$, but for the $v_{\odot}$ component some authors obtained values of 10–20 km/s (e.g., Mignard 2000). This was due to an increase of the tangential velocities for very small values of the dispersion, that leads (by extrapolation) to some high values of $v_{\odot}$. Since the small dispersions correspond to very young stars that are not in kinematical equilibrium, according to Dehnen and Binney (1998), these should be excluded from the selection when the extrapolation method of velocity dispersion to zero is applied. Mignard (2000) determined the velocity components of the Sun, showing that the values obtained for $u_{\odot}$ and $w_{\odot}$ vary depending on the kinematical selection studied. Using only populations of dwarf early stars and giants of K and M types with galactic longitude less than 30° (in module), Mignard (2000) obtained $v_{\odot} \approx 10-12$ km/s for the young population and $v_{\odot} \approx 15-18$ km/s for the old population which belongs to the PMS. The difference between the values obtained by Dehnen and Binney (1998) and Mignard (2000) is due to the different kinematical selections taken into consideration and to the existing selection effects.

Thus, the Sun's velocity given for LSR depends on the kinematical selection studied and on the methods used, its determination being still uncertain.

The results obtained until now concerning the velocity distribution of the stars differ from one author to another, because of the use of different observational data and different methods; moreover, the conditions imposed to parameters were never standardized. Thus, for the stars of B and A type, younger than 5×10^7 years situated in the Gould Belt at a distance $r < 500$ pc from the Sun, Palouš (1985) obtained a vertex deviation $l_V \approx 90°$ by the proper motion method, and $l_V = -26°$ by the radial velocity method.

In this paper we try to extend the previous researches, determining the Sun's motion with respect to the stars situated at different distances (however nearby). The Sun's velocity is got, as depending on the color index, by the three above mentioned methods applied to the stellar population belonging to PMS, ZAMS, TAMS regions and horizontal branch (stars of III class of luminosity with $0.6 \le B-V \le 0.9$ and $M_V < 4$), AGB region (stars with $0.9 \le B-V \le 1.7$ and $-2 < M_V < 2$).

2. OBSERVATIONAL DATA

In this study, we use the astrometrical data (positions, parallaxes, and proper motions) from *Hipparcos Catalogue* (ESA 1997) and the radial velocities from the *General Catalogue of Mean Radial Velocities* (Barbier-Brossat and Figon 2000).

The distance r of the stars from the Sun has been calculated by means of the trigonometric parallaxes from *Hipparcos Catalogue*. The observational data are given in the galactic system.

To remove the existing parallax errors, the condition: $\sigma_\pi / \pi < 0.1$ has been imposed. The clusters of stars and the multiple and variable stars have been eliminated, because their kinematics contains additional motions. We adopted the 3σ accuracy condition.

Accordingly, the coordinates of each star and the components of the proper motion have been determined for each volume element considered. We took into account the components of the proper motion corrected for the effects of the galactic rotation, where for Oort's constants A and B the following values have been adopted: $A = 14.82$ km s^{-1} kpc^{-1} and $B = -12.37$ km s^{-1} kpc^{-1}.

For each star, the components (u, v, w) of the spatial velocity have been determined as:

$$\begin{aligned} u &= -kr\mu_l \cos b \sin l - kr\mu_b \sin b \cos l + V_r \cos b \cos l, \\ v &= kr\mu_l \cos b \cos l - kr\mu_b \sin b \sin l + V_r \cos b \sin l, \\ w &= kr\mu_b \cos b + V_r \sin b, \end{aligned} \tag{1}$$

where V_r is the radial velocity and $k = 4.738$ km s^{-1}/("/year).

For N stars from the volume element taken into account, the velocity components of the centroid along the axes of coordinates were determined as:

$$\begin{aligned} u_0 &= (1/N)\sum_{i=1}^{N} u_i, \\ v_0 &= (1/N)\sum_{i=1}^{N} v_i, \\ w_0 &= (1/N)\sum_{i=1}^{N} w_i, \end{aligned} \tag{2}$$

centroid meaning the point that moves in the system with the mean value of the velocities of the stars from the volume element taken into account.

3. DETERMINATION OF THE SUN'S MOTION BY THE METHOD OF SPATIAL VELOCITIES

Knowing the spatial velocities of the stars, the most simple determination method of the Sun's motion elements could be applied.

For a random star from a volume element considered, discarding the indices for simplicity, we have

$$\mathbf{r} = -\mathbf{r}_{\odot} + \mathbf{r}', \tag{3}$$

where **r** represents the position vector of the star with respect to the Sun, $\mathbf{r}_{\odot}$ is the position vector of the Sun with respect to the centroid and **r'** is the position vector of the star with respect to the centroid.

Differentiating (3) with time, the Sun's velocity with respect to the centroid is obtained as the difference between the peculiar velocity of the star and the velocity of the star:

$$\mathbf{V}_{\odot} = \mathbf{V}' - \mathbf{V}. \tag{4}$$

Supposing for simplicity that the volume element contains N stars of equal masses and taking into account that the velocity of centroid $\mathbf{V}_0 = (1/N)\sum_{i=1}^{N}\mathbf{V}_i$ and $\sum_{i=1}^{N}\mathbf{V}'_i = \sum_{i=1}^{N}\mathbf{V}_i - N\mathbf{V}_0 = 0$, from (4) results

$$\mathbf{V}_{\odot} = -(1/N)\sum_{i=1}^{N}\mathbf{V}_i,$$

which is equivalent with $\mathbf{V}_{\odot} = -\mathbf{V}_0$. From here the components of the Sun's velocity are obtained in the directions of the axes of coordinates: $u_{\odot} = -u_0$, $v_{\odot} = -v_0$, $w_{\odot} = -w_0$ and $|\mathbf{V}_{\odot}| = (u_{\odot}^2 + v_{\odot}^2 + w_{\odot}^2)^{1/2}$.

The Sun's motion with respect to the stars is determined completely if the coordinates of apex are known, apex meaning the point where the direction of the Sun's local motion cuts the celestial sphere.

The coordinates (L, B) of the solar apex are determined easily from the following relations:

$$\tan L = v_{\odot}/u_{\odot},$$
$$\tan B = w_{\odot}/(u_{\odot}^2 + v_{\odot}^2)^{1/2}. \tag{5}$$

In this paper, the elements of the Sun's motion have been determined by the method of spatial velocities for cubical volume elements, centered in the Sun, of edge (in pc) $a \in \{40, 60, 80, 100, 120, 160, 320, 500, 1000, 1500\}$. The results obtained are presented in Table 1.

Table 1

The Sun's velocity for cubical volume elements, centered in the Sun, of edge *a*.

a	N	$u_{\odot}$ (km/s)	$v_{\odot}$ (km/s)	$w_{\odot}$ (km/s)	$V_{\odot}$ (km/s)	L (°)	B (°)
40	882	8.0	20.5	6.9	23.0	67	18
60	1858	9.2	20.8	7.5	23.9	68	19
80	2904	9.2	21.3	7.9	24.5	67	19
100	4014	10.8	21.4	7.8	25.2	63	18
120	4938	10.7	20.9	7.8	24.7	61	18
160	6662	10.2	19.9	7.7	23.6	62	19
320	12257	9.2	17.7	7.2	21.2	61	20
500	15754	8.9	17.1	7.1	20.5	61	20
1000	18773	8.7	16.7	7.1	20.1	61	21
1500	20026	8.5	16.7	7.1	20.0	61	21

The components of the Sun's motion have been determined also depending on the colour index for the stellar population situated in the central zone, which belongs to ZAMS, TAMS and AGB regions. For a selection of N stars, the mean square deviation for each component of the velocity has been calculated:

$$\sigma_{u_{\odot}} = \sigma_1 / \sqrt{N}\,, \qquad \sigma_{v_{\odot}} = \sigma_2 / \sqrt{N}\,, \qquad \sigma_{w_{\odot}} = \sigma_3 / \sqrt{N}\,,$$

where

$$\sigma_1^2 = \sum_{i=1}^{N} u_i'^2 / N\,, \quad \sigma_2^2 = \sum_{i=1}^{N} v_i'^2 / N\,, \quad \sigma_3^2 = \sum_{i=1}^{N} w_i'^2 / N$$

are the dispersions with respect to the components of the stars velocities.

Figure 1 (see Section 4) presents the results obtained for the Sun's velocity determined depending on the color index, for the population of stars which belongs to ZAMS, TAMS and AGB regions, situated in cubical volume elements, centered in the Sun, of edge $a \in \{80, 160, 320, 500, 1000, 1500\}$.

4. DETERMINATION OF THE SUN'S MOTION BY THE METHOD OF RADIAL VELOCITIES

In the galactic system of coordinates, let us consider a macroscopic volume element. For a star from the volume element considered, the projection of relation (4) on the heliocentric distance of the star given by the unit vector $\mathbf{r}/|\mathbf{r}|$ of components ($\cos l \cos b$, $\sin l \cos b$, $\sin b$) leads to

$$u_{\odot} \cos l \cos b + v_{\odot} \sin l \cos b + w_{\odot} \sin b = V_r' - V_r\,, \tag{6}$$

where V_r' is the star's peculiar radial velocity and V_r represents the observed radial velocity of the celestial object.

Considering V_r' as an accidental error, this term can be neglected in equation (6), and, supposing V_r' included in V_r, we obtain

$$u_{\odot}\cos l \cos b + v_{\odot}\sin l \cos b + w_{\odot}\sin b = -V_r .$$

Denoting by (l_i, m_i, n_i), $i = \overline{1,n}$ the director cosines of the heliocentric directions of n stars from the volume element considered with respect to the coordinate axes, the equations of condition

$$l_i u_{\odot} + m_i v_{\odot} + n_i w_{\odot} = -V_{r,i}, \quad i = \overline{1,n}$$

form a system of n algebraic equations with three unknowns, which can be solved by the least squares method.

In this paper, we intended to determine the Sun's velocity depending on the colour index by the method of radial velocities, with a high accuracy, as well as possible. Thus, we determined the Sun's velocity with respect to the stellar populations from ZAMS and TAMS regions, with respect to the stars of type AGB, and also with respect to the stars from the whole kinematical selection considered, for different cubical volume elements centered in the Sun, of edge $a \in \{80, 160, 320, 500, 1000, 1500\}$.

Introducing Gauss' notations

$$\begin{aligned} l_1 l_1 + l_2 l_2 + \ldots + l_n l_n &= [ll], \\ l_1 m_1 + l_2 m_2 + \ldots + l_n m_n &= [lm], \\ &\ldots\ldots\ldots\ldots, \end{aligned}$$

the normal system

$$\begin{aligned} [ll]\, u_{\odot} + [lm]\, v_{\odot} + [ln]\, w_{\odot} &= [lV_r]\,, \\ [ml]\, u_{\odot} + [mm]\, v_{\odot} + [mn]\, w_{\odot} &= [mV_r]\,, \\ [nl]\, u_{\odot} + [nm]\, v_{\odot} + [nn]\, w_{\odot} &= [nV_r]\,, \end{aligned} \tag{7}$$

was obtained. Solving it, we obtained the components of the Sun's velocity, $u_{\odot} \pm \sigma_{u_{\odot}}$, $v_{\odot} \pm \sigma_{v_{\odot}}$, $w_{\odot} \pm \sigma_{w_{\odot}}$, where the mean square deviations of each component are given by the relations

$$\sigma^2_{u_{\odot}} = \frac{\Delta_{11}}{\Delta}\sigma^2, \quad \sigma^2_{v_{\odot}} = \frac{\Delta_{22}}{\Delta}\sigma^2, \quad \sigma^2_{w_{\odot}} = \frac{\Delta_{33}}{\Delta}\sigma^2, \tag{8}$$

$\Delta_{11}, \Delta_{22}, \Delta_{33}$ being the algebraic complements of the main diagonal of the determinant Δ of the normal system, and $\sigma = [\sum_{i=1}^{n} \delta_i^2 /(n-3)]^{1/2}$, $\delta_i = l_i u_\odot + m_i v_\odot + n_i w_\odot - V_{r,i}$, $i = \overline{1,n}$.

The stars for which the deviation $\delta_i > 3\sigma$, $i = \overline{1,n}$, were removed; by solving the new system via the least squares method, we have obtained the components of the Sun's velocity and the mean square deviations on each component.

The existing diferences between the values obtained for the Sun's velocity by the method of spatial velocities and by the method of radial velocities are insignificant in general, as it is shown in Fig. 1.

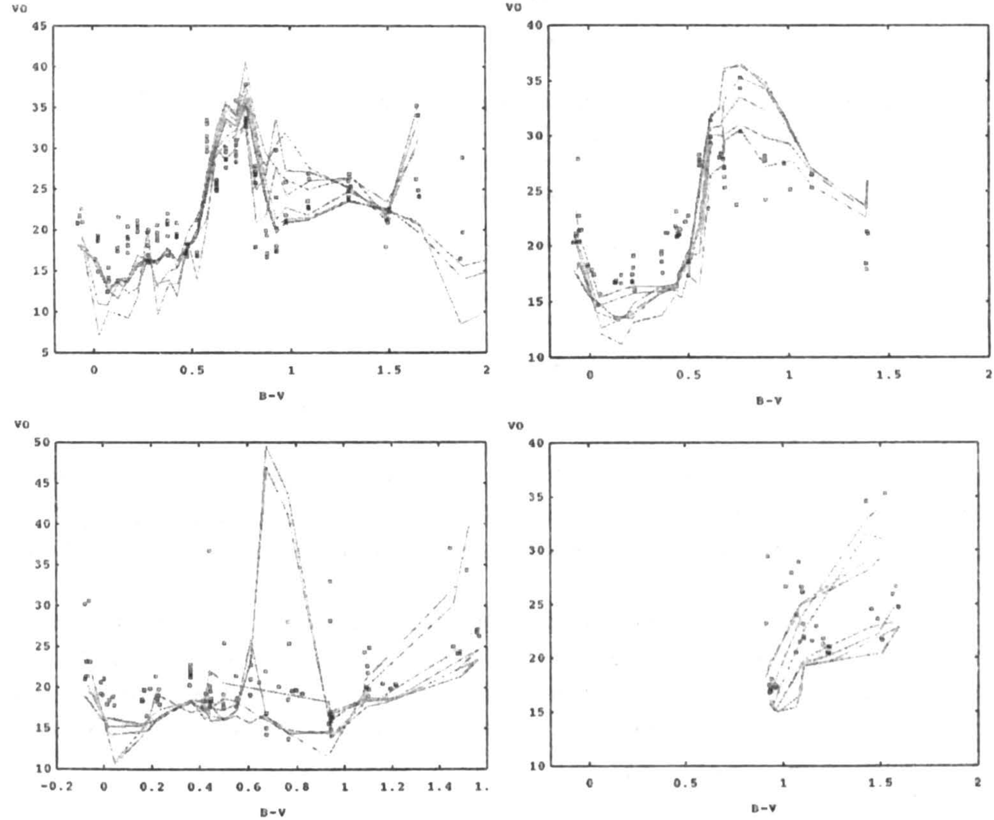

Fig. 1 − The Sun's velocity determined by the method of radial velocities and by the method of spatial velocities for cubical volume elements centered in the Sun. Dotted line: the Sun's velocity obtained by the method of radial velocities. Full line: the Sun's velocity obtained by the method of spatial velocities. In the upper side, to the left: the Sun's velocity for the stars from the whole selection considered. In the upper side, to the right: the Sun's velocity for the stars situated in ZAMS region. Bottom, to the left: the Sun's velocity for the stars situated in TAMS region. Bottom, to the right: the Sun's velocity for the stars of AGB type.

5. DETERMINATION OF THE SUN'S MOTION BY THE METHOD OF PROPER MOTIONS

The Sun's motion with respect to the stars can be studied also by the method of proper motions, using the projections of the yearly motions of the stars on the plane tangent to the celestial sphere. Below, by this method, we determine the Sun's motion with respect to the stellar populations situated in different cubical volume elements, centered in the Sun, of the same edge as in the previous sections.

For a star situated in the considered volume element, we obtain the components (V_l, V_b) of the velocity in the galactic system:

$$V_l = -u\sin l + v\cos l,$$
$$V_b = -u\cos l\sin b - v\sin l\sin b + w\cos b.$$

Expressing V_l and V_b depending on the proper motions $V_l = kr\mu_l\cos b$, $V_b = kr\mu_b$, and taking into account relation (4), we obtain

$$kr\mu_l\cos b = u_\odot\sin l - v_\odot\cos l + \varepsilon_l,$$
$$kr\mu_b = u_\odot\cos l\sin b + v_\odot\sin l\sin b - w_\odot\cos b + \varepsilon_b, \qquad (9)$$

where

$$\varepsilon_l = -u'\sin l + v'\cos l,$$
$$\varepsilon_b = -u'\cos l\sin b - v'\sin l\sin b + w'\cos b.$$

Discarding the quantities ε_l and ε_b, which can be treated as accidental errors, equations (9) written for n stars from the volume element form a system of $2n$ algebraic equations with three unknowns. Solving this system, the components of the Sun's velocity are determined.

Similar with the case of the determination of the Sun's motion by the method of radial velocities, solving the system (9) by the least squares method, we have obtained the components of the Sun's velocity and the mean square deviations of each component given by the relations (8), where the mean square deviation in this case is $\sigma = [\sum_{i=1}^{2n}\delta_i^2/(2n-3)]^{1/2}$, with

$$\delta_i = u_\odot\sin l - v_\odot\cos l - kr\mu_l\cos b,\quad i=\overline{1,n},$$
$$\delta_i = u_\odot\cos l\sin b + v_\odot\sin l\sin b - w_\odot\cos b - kr\mu_b,\quad i=\overline{n+1,2n}.$$

The stars for which the deviation $\delta_i > 3\sigma$, $i=\overline{1,2n}$, were removed. Solving the new system, the components of the Sun's velocity and the mean square deviations of each component have been obtained by the least squares method. The Sun's velocity determined by the method of proper motions with respect to the stars belonging to ZAMS and TAMS regions, with respect to the stars of AGB type, and with respect to all stars from the kinematical selection considered is represented in the Fig. 2, in comparison with the Sun's velocity obtained by the method of radial velocities with respect to the same stellar populations. As Figs. 1 and 2 show, there are no significant differences between the results obtained by the methods of spatial velocities, radial velocities and proper motions. The Sun's velocity varies depending on the kinematical selection studied.

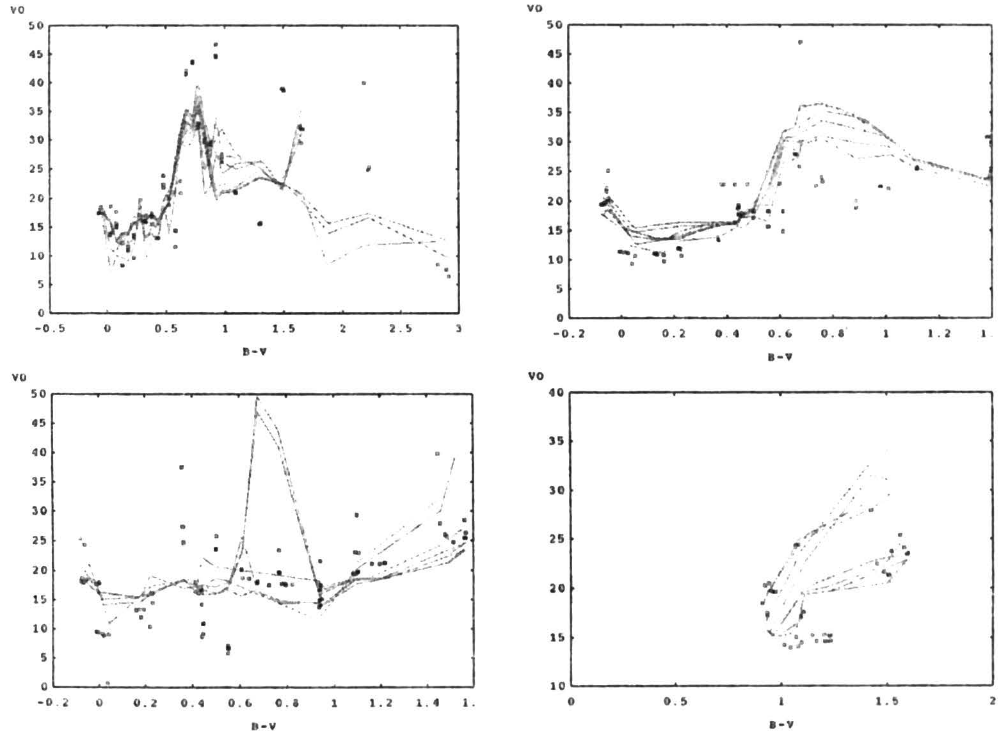

Fig. 2 – The Sun's velocity determined by the method of proper motions and by the method of spatial velocities for cubic volume elements centered in the Sun. Dotted line: the Sun's velocity obtained by the method of proper motions. Full line: the Sun's velocity obtained by the method of spatial velocity. In the upper side, to the left: Sun's velocity for the stars from the whole selection considered. In the upper side, to the right: Sun's velocity for the stars from ZAMS region. Bottom, to the left: Sun's velocity for the stars from TAMS region. Bottom, to the right: Sun's velocity for the stars of AGB type.

6. CONCLUSIONS

We have determined the Sun's motion with respect to the stars from the kinematical selections considered, by the methods of spatial velocities, radial velocities and proper motions, proving that there are no significant differences between the results obtained by the application of these methods.

The study was made with respect to a greater number of parameters, taking into account the distribution of the stars in the Galaxy, heliocentric distance, radial velocity, colour index, spectral class, magnitude and ages of the stars.

The Sun's velocity has been determined in the central zone depending on the colour index and heliocentric distance, for the stellar populations which belong to ZAMS and TAMS regions and to AGB zone, situated at different distances $r \leq 750$ pc from the Sun. We have proved that the results obtained depend on the kinematical selection studied.

We have confirmed and enriched the results existing in the literature that were obtained in some partial studies performed about the central zone depending on a part of the mentioned parameters, on a much limited number of observational data, at a small distance from the Sun.

Acknowledgments. The authors thank Professor Ieronim Mihăilă for his direct contribution to this paper, for his guidance and trust.

REFERENCES

Barbier-Brossat, M., Figon, P.: 2000, *Astron. Astrophys. Suppl. Ser.*, **142**, 217.
Dehnen, W., Binney, J.: 1998, *Mon. Not. Roy. Astron. Soc.*, **298**, 387.
Delhaye, J.: 1965, *Galactic Structure*, University of Chicago Press, Chicago, London.
ESA: 1997, *The Hipparcos and Tycho Catalogues*, ESA SP Series.
Illingworth, V., Clark, J. O. E: 2000, *The Facts On File Dictionary of Astronomy*, New York, Inc., Science Online, www.factsonfile.com.
Mignard, F.: 2000, *Astron. Astrophys.*, **354**, 522.
Palouš, J.: 1985, *Bull. Astron. Inst. Czechosl.*, **36**, 261.
Parenago, P. P: 1950, *Astron. Zh.*, **27**, 150.
Wielen, R.: 1982, in *Landolt-Börnstein*, Group 6: *Astronomy*, Vol. **2**, Springer-Verlag, New York, p. 208.

Received on 12 July 2006

ESTIMATION OF ASTROPHYSICALLY USEFUL PARAMETERS FOR SnF AND ScF MOLECULES

PONSAMY SRI RAMACHANDRAN [1], RAMACHANDRAN SHANMUGAVEL [1], NARAYANAN RAJAMANICKAM [1], SOMASHEKAR PUNDALIKARAO BAGARE [2]

[1] *Physics Research Centre, VHNSN College*
Virudhunagar, 626 001, India
E-mail: nrmanickam@rediffmail.com

[2] *Indian Institute of Astrophysics*
Kodaikanal and Bangalore, 560 034, India
E-mail: bagare@iiap.ernet.in

Abstract. The calculation of Franck-Condon factors and *r*-centroids are of interest to study the electronic transition between bound molecular states. Franck-Condon factors and *r*-centroid values estimated using the most reliable numerical integration procedure for the bands of $A^2\Sigma - X^2\Pi_{3/2}$, $A^2\Sigma - X^2\Pi_{1/2}$, $B^2\Sigma - X^2\Pi$, $C^2\Delta - X^2\Pi_{3/2}$, and $C^2\Delta - X^2\Pi_{1/2}$ systems of the astrophysical molecule SnF and $B^2\Sigma - X^2\Pi_{3/2}$, $C\Sigma - X^2\Pi_{1/2}$, and $E^2\Sigma - X^2\Pi$. systems of ScF using a suitable potential.

Key words: astrophysics – molecules SnF and ScF – Franck-Condon factors; *r*-centroids.

1. INTRODUCTION

The spectral intensity distribution in the electronic states of a molecule requires knowledge of electronic transition probabilities, which are to a good approximation proportional to the Franck-Condon (FC) factors. The FC factors give the molecular information required to evaluate the band intensities in absorption and emission. The theoretical prediction of intensity distribution in the spectra of many diatomic molecules, which are of interest in astrophysics, is necessary for an understanding of the physical-chemical conditions of the emitting sources.

A precise knowledge of FC factors and *r*-centroids are essential to understand and to estimate many important aspects of the astrophysical molecules, such as radiative lifetime, variation of electronic transition moment with internuclear separation, vibrational temperature of the source and relative band strengths. The FC factors are useful in studies of radiative transfer in the atmospheres of stellar and other astronomical objects, which contain molecular species (Nicholls et al. 1981).

Rom. Astron. J., Vol. **16**, No. 2, p. 123–132, Bucharest, 2006

The molecular spectrum of the SnF molecule and its significance in astrophysics due to its presence in the stellar spectrum were dealt with in detail elsewhere (Singh et al. 1965). The abundances of a number of elements detected in HST GHRS spectra (Hobbs et al. 1993) have clarified the depletion pattern seen in moderately dense interstellar clouds. In addition, the heavy elements Ga, Ge, As, Si, Kr, Sn, Tl and Pb provide probes of nucleosynthetic processes other than those responsible for the lighter elements. Comparison of the depletion properties of Si, Ge, Sn and Pb, all in the same group IV A with similar chemical behaviour, may provide valuable information regarding various processes through to occur on the surfaces of dust grains in the ISM.

The SnF molecule is a diatomic halide of fourth group and having the same structure of SiF, GeF and PbF. Singh and Rai (1965) reported the presence of the SnF molecule in stellar region. The variation of chemical equilibria in stellar atmospheres is still one of the basic obstacles to understanding the atmospheres of cool stars. The atmospheres of cool stars are complicated systems of chemical equilibria in which about a hundred elements are mixed and there are many possible chemical reactions to form molecules. The interstellar matter has different types of molecules wherein the heavy molecules of interest are much denser and so the dust is densest. Especially, the role of the diatomic molecules in stellar atmospheres for various values of H, C, N, O and F with other elements has been limited to the evaluation of some of the equilibrium constants. Peery (1979) reported the presence of SnH molecule in the spectrum of cool carbon stars. Based on the estimates of abundances of Sn, the fluorides of fourth group halides are expected to be present in stellar and cool stars.

The presence of Sc I and Sc II lines has been identified in the stellar spectrum and cool carbon stars (Peery 1979). Angular size and effective temperature for cool carbon stars show a significant elemental abundance for Sc. Schadee (1964) identified that the ScO, TiO and ZrO molecules are to be present in the Sun. Since oxides of Sc are among the most readily formed diatoms in sunspots (Wöhl 1971) and in M-type stars (Nicholls 1977), fluorides of Sc are also expected to be present in these astrophysical objects. Further, Sauval and Tatum (1984) predicted the possible presence of ScF molecules in stellar and cometary spectra. Their relative abundances in the interstellar medium give estimates of stellar activity like nature of stellar wind and the elemental abundances of cool stars.

There has been no report on the FC factors and r-centroids for the band systems $A^2\Sigma - X^2\Pi_{3/2}$, $A^2\Sigma - X^2\Pi_{1/2}$, $B^2\Sigma - X^2\Pi$, $C^2\Delta - X^2\Pi_{3/2}$ and $C^2\Delta - X^2\Pi_{1/2}$ systems of SnF molecule and $B^2\Sigma - X^2\Pi_{3/2}$, $C\Sigma - X^2\Pi_{1/2}$ and $E^2\Sigma - X^2\Pi$ systems of ScF molecule, to our best knowledge, in the literature. Therefore the reliable values of FC factors and r-centroids for these band systems of astrophysically important molecules SnF and ScF have been determined in this study by using a numerical integration procedure adopting a suitable potential.

2. FRANCK-CONDON FACTORS AND *r*-CENTROIDS

The wave mechanical formulation of the FC principle leads to: the absorption intensity $I_{v'v''}$ of a molecular band for a $v'-v''$ electronic transition is proportional to the product of the number of molecules present in the particular state, the photon energy and the rate of absorption. Thus

$$I_{v'v''} = DN_{v''}\,E_{v'v''}\,R_e^2(\bar{r}_{v'v''})\,q_{v'v''}, \tag{1}$$

where D is a constant partly depending on the geometry of the apparatus, $N_{v''}$ the population of the level v'', $E_{v'v''}$ the energy quantum, $q_{v'v''}$ the Franck-Condon factor, $\bar{r}_{v'v''}$ the *r*-centroid, and R_e the electronic transition moment.

The intensities of diatomic molecular bands in absorption are controlled by the square of the overlap integral. The square of the coefficients used in the linear combination tells us about the degree of overlap between the excited state wave function and the ground state wave function. The square of the overlap integral is termed as FC factor:

$$q_{v'v''} = \left|\langle\psi_{v'}|\psi_{v''}\rangle\right|^2, \tag{2}$$

where $\psi_{v'}$ and $\psi_{v''}$ are the vibrational eigenfunctions for the upper and lower states, respectively, between which the transition takes place. The *r*-centroid is a unique value of internuclear separation associated with a $v'-v''$ band and is defined as

$$\bar{r}_{v'v''} = \frac{\langle\psi_{v'}|r|\psi_{v''}\rangle}{\langle\psi_{v'}|\psi_{v''}\rangle}. \tag{3}$$

Morse's (1929) potential energy curves for diatomic molecules are required in order to evaluate the FC factors, especially for vibrational transition involving between their various low quantum number electronic states (Sri Ramachandran et al. 2004). The computation of the FC factor is made by Bates' (1949) method of numerical integration according to the detailed procedure provided by Partel et al. (2000). Morse wave functions were calculated at intervals of 0.01 Å for the range of r respectively from 1.71 Å to 2.49 Å, from 1.74 Å to 2.37 Å, from 1.69 Å to 2.14 Å, from 1.74 Å to 2.17 Å and from 1.74 Å to 2.11 Å for every observed vibrational level of $A^2\Sigma-X^2\Pi_{3/2}$, $A^2\Sigma-X^2\Pi_{1/2}$, $B^2\Sigma-X^2\Pi$, $C^2\Delta-X^2\Pi_{3/2}$ and $C^2\Delta-X^2\Pi_{1/2}$ states of the SnF molecule and from 1.64 Å to 2.21 Å, from 1.66 Å to 2.36 Å and from 1.69 Å to 2.08 Å for the band $B^2\Sigma-X^2\Pi_{3/2}$, $C\Sigma-X^2\Pi_{1/2}$ and $E^2\Sigma-X^2\Pi$ systems of the ScF molecule, respectively. Once the appropriate wave functions are obtained, the FC factors can be evaluated by integrating the expression (1). The definition of r-centroids offers a method of computing them directly. Integrals in equations (1) and (2) for the FC factors ($q_{v'v''}$) and r-centroids ($\bar{r}_{v'v''}$) were computed numerically and the results are presented in Tables 1–8 for the respective bands of the SnF and ScF molecules. The wavelengths ($\lambda_{v'v''}$) data (Jenkins and Rochester 1937; McLeod and Weltner 1966) are also included in the tables. The molecular constants used in the present study are collected from the compilations of Huber and Herzberg (1979), and Dai and Balasubramanian (1994).

3. RESULTS AND DISCUSSION

The FC factors of the SnF molecule indicate that the most intense bands are the (1,0), (0,1) and (0,0) for the $A^2\Sigma - X^2\Pi_{3/2}$ and $A^2\Sigma - X^2\Pi_{1/2}$ systems; the (0,0), (2,1), (1,2), (1,0) and (0,1) for the $B^2\Sigma - X^2\Pi$ system; the (0,0), (1,1) and (3,2) for the $C^2\Delta - X^2\Pi_{3/2}$ and $C^2\Delta - X^2\Pi_{1/2}$ systems, whereas all other observed bands are weak.

For $A^2\Sigma - X^2\Pi_{3/2}$ and $A^2\Sigma - X^2\Pi_{1/2}$ band systems of the SnF molecule, it is found that $r_e' > r_e''$ and hence the r-centroid values increase with increasing wavelength, which is expected to be red degraded band system. For $B^2\Sigma - X^2\Pi$, $C^2\Delta - X^2\Pi_{3/2}$ and $C^2\Delta - X^2\Pi_{1/2}$ band systems, it is found that $r_e' < r_e''$ and r-centroid values increase with decreasing wavelength, hence the bands are degraded towards the ultraviolet.

The sequence difference is found to be varying between 0.003 Å to 0.04 Å, and 0.002 to 0.02 for $A - X$ and $C - X$ sub-band systems of the SnF molecule, respectively; hence the potentials are so wide. In the case of the $B - X$ band system, the sequence difference is found to be constant and is about 0.01 Å, which suggests that the potentials are not so wide.

In the case of the $B - X$ system of the ScF molecule, the FC factors imply that the (0,1), (2,0) and (1,0) bands are intense, and other bands are weak. For the $C - X$ system, the FC factors indicate that (0,0) and (1,0) bands are intense. Similarly, in the case of the $E - X$ band system, the (1,0), (2,0), (3,0) and (0,0) bands are intense and all other bands are weak.

The sequence differences for all these band systems ($B - X$, $C - X$ and $E - X$) of the ScF molecule is found to be a constant, and is about 0.01 Å. Further, $r_e' > r_e''$ and hence the r-centroids values increase with an increase in wavelength, which is expected in the red degraded band system.

Table 1

Franck-Condon factors and *r*-centroids of A-X3/2 bands of SnF

		v″ = 0	v″ = 1	v″ = 2	v″ = 3	v″ = 4
v′ = 0	a) b) c)	0.300 1.990 2927.80	0.353 2.040 2978.17	0.219 2.083 3029.81	0.092 2.126	0.029 2.167
v′ = 1	a) b) c)	0.361 1.955 2871.36	0.013 2.025 2919.77	0.101 2.050 2969.47	0.227 2.095 3020.18	0.179 2.137
v′ = 2	a) b) c)	0.219 1.918 2817.36	0.109 1.962	0.138 2.023	*	0.112 2.106 3011.34
v′ = 3	a) b) c)	0.088 1.878 2765.96	0.235 1.930 2810.83	*	0.139 2.034	0.048 2.078
v′ = 4	a) b) c)	0.026 1.832	0.179 1.892 2759.93	0.121 1.938 2804.18	0.044 2.016 2849.47	0.057 2.044 2895.74
v′ = 5	a) b) c)	0.006 1.775 2670.45	0.081 1.849 2711.33	0.198 1.905 2754.01	0.023 1.928 2797.64	0.099 2.021 2841.50
v′ = 6	a) b) c)	0.001 1.695	0.025 1.798	0.141 1.865	0.146 1.914 2748.04	0.002 2.118 2791.18
v′ = 7	a) b) c)	*	0.006 1.729	0.061 1.818	0.172 1.879 2700.4	0.067 1.917 2742.22
v′ = 8	a) b) c)	*	0.001 1.618	0.018 1.759	0.106 1.837	0.160 1.891 2695.36
v′ = 9	a) b) c)	*	*	0.004 1.670	0.042 1.784	0.142 1.853
v′ = 10	a) b) c)	*	*	*	0.011 1.710	0.074 1.806
v′ = 11	a) b) c)	*	*	*	*	0.025 1.743
v′ = 12	a) b) c)	*	*	*	*	0.006 1.644
		v″ = 5	v″ = 6	v″ = 7	v″ = 8	v″ = 9
v′ = 0	a) b) c)	0.007 2.208	0.001 2.249	*	*	*

$v'=1$	a)	0.084	0.028	0.007	0.001	
	b)	2.178	2.218	2.260	2.302	*
	c)					
$v'=2$	a)	0.194	0.141	0.063	0.020	0.005
	b)	2.148	2.188	2.229	2.270	2.312
	c)					
$v'=3$	a)	0.019	0.142	0.170	0.104	0.041
	b)	2.117	2.159	2.199	2.240	2.281
	c)	3001.27				
$v'=4$	a)	0.107	0.003	0.067	0.161	0.139
	b)	2.088	2.130	2.170	2.210	2.250
	c)					
$v'=5$	a)	0.003	0.106	0.040	0.013	0.119
	b)	2.050	2.099	2.140	2.184	2.221
	c)	2887.95				
$v'=6$	a)	0.098	0.012	0.061	0.082	0.001
	b)	2.031	2.073	2.110	2.151	2.173
	c)		2880.08			
$v'=7$	a)	0.036	0.054	0.052	0.015	0.095
	b)	2.022	2.043	2.082	2.120	2.163
	c)	2784.56		2872.37		
$v'=8$	a)	0.012	0.072	0.011	0.079	
	b)	1.887	2.024	2.055	2.093	*
	c)	2736.42	2778.26			
$v'=9$	a)	0.113	0.001	0.078	0.001	0.073
	b)	1.899	2.209	2.033	2.058	2.104
	c)	2690.12	2730.61	2771.98		
$v'=10$	a)	0.156	0.054	0.023	0.054	0.020
	b)	1.867	1.898	2.040	2.045	2.075
	c)		2684.97	2724.85	2765.61	
$v'=11$	a)	0.109	0.138	0.012	0.051	0.020
	b)	1.825	1.879	1.859	2.034	2.059
	c)			2679.75	2719.18	
$v'=12$	a)	0.048	0.135	0.098		0.063
	b)	1.771	1.842	1.885	*	2.040
	c)					2713.53

Table 2

Franck-Condon factors and *r*-centroids of A-X1/2 bands of SnF

		$v''=0$	$v''=1$	$v''=2$	$v''=3$	$v''=4$	$v''=5$	$v''=6$
$v'=0$	a)	0.315	0.355	0.212	0.086	0.026	0.006	0.001
	b)	1.992	2.042	2.086	2.129	2.171	2.212	2.253
	c)	3141.13	3199.66	3259.90				
$v'=1$	a)	0.363	0.008	0.115	0.231	0.172	0.078	0.025
	b)	1.956	2.032	2.052	2.097	2.140	2.181	2.222
	c)	3076.22	3132.27	3190.00	3249.29			
$v'=2$	a)	0.212	0.124	0.130	0.001	0.125	0.195	0.134
	b)	1.917	1.963	2.025	2.044	2.108	2.151	2.192
	c)	3014.59	3068.30		3180.41	3238.5		

v′ = 3	a)	0.082	0.240	0.002	0.145	0.039	0.027	0.151
	b)	1.876	1.929	1.902	2.035	2.081	2.119	2.162
	c)			3060.41			3228.52	
v′ = 4	a)	0.023	0.172	0.135	0.034	0.068	0.101	0.001
	b)	1.828	1.890	1.938	2.020	2.046	2.090	2.138
	c)			3000.15	3052.48			
v′ = 5	a)	0.005	0.074	0.200	0.032	0.094	0.008	0.110
	b)	1.768	1.846	1.903	1.933	2.023	2.053	2.101
	c)						3097.67	
v′ = 6	a)	0.001	0.022	0.133	0.157		0.103	0.007
	b)	1.685	1.792	1.862	1.913	*	2.032	2.077
	c)							3089.06

Table 3

Franck-Condon factors and *r*-centroids of B-X bands of SnF

		v″ = 0	v″ = 1	v″ = 2
v′ = 0	a)	0.615	0.293	0.076
	b)	1.917	1.863	1.808
	c)	2593.84	2635.64	
v′ = 1	a)	0.303	0.158	0.326
	b)	1.979	1.924	1.872
	c)	2556.45	2595.50	2633.94
v′ = 2	a)	0.071	0.354	0.010
	b)	2.040	1.987	1.926
	c)		2557.98	
v′ = 3	a)	0.010	0.156	0.283
	b)	2.099	2.047	1.995
	c)			2559.68
v′ = 4	a)	0.001	0.034	0.223
	b)	2.160	2.107	2.055
	c)			
v′ = 5	a)		0.005	0.069
	b)	*	2.167	2.114
	c)			
v′ = 6	a)			0.012
	b)	*	*	2.174
	c)			

Table 4

Franck-Condon factors and *r*-centroids of C-X3/2 bands of SnF

		v″ = 0	v″ = 1	v″ = 2	v″ = 3	v″ = 4
v′ = 0	a)	0.784	0.179	0.032	0.005	
	b)	1.926	1.841	1.784	1.730	*
	c)	2195.34	2223.49	2252.14		
v′ = 1	a)	0.205	0.473	0.240	0.068	0.014
	b)	2.013	1.939	1.842	1.786	1.731
	c)	2163.15		2218.23		

ν' = 2	a)	0.012	0.322	0.296	0.245	0.095
	b)	2.152	2.024	1.956	1.842	1.788
	c)	2132.67	2158.75			2240.94
ν' = 3	a)		0.027	0.393	0.196	0.226
	b)	*	2.173	2.036	1.979	1.840
	c)					

Table 5

Franck-Condon factors and *r*-centroids of C-X1/2 bands of SnF

		ν″ = 0	ν″ = 1	ν″ = 2
ν' = 0	a)	0.767	0.191	0.036
	b)	1.927	1.846	1.789
	c)	2348.90		
ν' = 1	a)	0.218	0.438	0.252
	b)	2.011	1.940	1.848
	c)		2344.06	
ν' = 2	a)	0.015	0.336	0.256
	b)	2.137	2.022	1.957
	c)		2308.37	
ν' = 3	a)		0.033	0.394
	b)	*	2.156	2.033
	c)			2303.99

Table 6

Franck-Condon factors and *r*-centroids of B-X bands of ScF

		ν″ = 0	ν″ = 1
ν' = 0	a)	0.114	0.271
	b)	1.853	1.887
	c)	9405.00	
ν' = 1	a)	0.231	0.155
	b)	1.826	1.858
	c)	8909.00	
ν' = 2	a)	0.249	0.006
	b)	1.800	1.826
	c)	8468.00	
ν' = 3	a)	0.191	0.041
	b)	1.775	1.808
	c)	8079.00	8572.49
ν' = 4	a)	0.115	0.126
	b)	1.750	1.782
	c)	7727.00	
ν' = 5	a)	0.058	0.149
	b)	1.725	1.757
	c)	7405.00	
ν' = 6	a)	0.026	0.116
	b)	1.700	1.732
	c)	7111.00	

Table 7

Franck-Condon factors
and *r*-centroids of C-X bands of ScF

		$v'' = 0$
$v' = 0$	a) b) c)	0.1636 1.848 6277.50
$v' = 1$	a) b) c)	0.275 1.818 6010.50
$v' = 2$	a) b) c)	0.250 1.790 5810.00
$v' = 3$	a) b) c)	0.164 1.763 5623.50
$v' = 4$	a) b) c)	0.086 1.736 5450.00
$v' = 5$	a) b) c)	0.039 1.710 5288.50
$v' = 6$	a) b) c)	0.015 1.6840 5138.00
$v' = 7$	a) b) c)	0.006 1.658 4997.50
$v' = 8$	a) b) c)	0.002 1.638 4864.00

Table 8

Franck-Condon factors
and *r*-centroids of E-X bands of ScF

		$v'' = 0$
$v' = 0$	a) b) c)	0.447 1.829 4792.00
$v' = 1$	a) b) c)	0.339 1.785 4657.00
$v' = 2$	a) b) c)	0.145 1.743 4531.00
$v' = 3$	a) b) c)	0.045 1.703 4415.00

The legend: a) = $q_{v'v''}$; b) = $\bar{r}_{v'v''} A^0$; c) = $\lambda_{v'v''} A^0$; * = $q_{v'v''} = 0$ is valid for all the above tables.

REFERENCES

Bates, D. R.: 1949, *Proc. Roy. Soc.*, **A196**, 217.

Dai, D., Balasubramanian, K.: 1994, *Chem. Phys. Lett.*, **224**, 423.

Hobbs. L. M., Welty. D. E., Morton. D. C., Spitzer. L., York. D. G.: 1993, *Astrophys. J.*, **411**, 750.

Huber. K. P., Herzberg, G.: 1979, *Molecular Spectra and Molecular Structure*, Vol. **4**. *Constants of Diatomic Molecules*. Van Nostrand Reinhold, New York.

Jenkins. F. A., Rochester, G. D.: 1937. *Phys. Rev.*, **52**, 1135.

McLeod. D., Jr., Weltner, W., Jr.: 1966, *J. Phys. Chem.*, **70**, 3293.

Morse. P. M.: 1929: *Phys. Rev.*, **34**, 57.

Nicholls, R. W.: 1977, *Ann. Rev. Astron. Astrophys.*, **15**, 197.

Nicholls, R. W.: 1981, *Astrophys. J. Suppl. Ser.*, **47**, 279.

Partel. F., Fernandez Gomez. M., Lopez Gonzalez, J. J., Rajamanickam, N.: 2000, *Astrophys. Space Sci.*, **272**, 345.

Peery, B. F., Jr.: 1979, *Publ. Astron. Soc. Japan*, **31**, 461.

Sauval, A. J., Tatum, J. B.: 1984, *Astrophys. J. Suppl. Ser.*, **56**, 193.

Schadee, A.: 1964, *Bull. Astron. Inst. Netherlands*, **17**, 311.

Singh. R. B., Rai, D. K.: 1965, *Ind. J. Pure Appl. Phys.*, **4**, 102.

Sri Ramachandran, P., Rajamanickam, N., Bagare, S. P., Balachandra Kumar, K.: 2004, *Astrophys. Space Sci.*, **295**, 443.

Wöhl, H.: 1971, *Solar Phys.*, **16**, 362.

Received on 31 July 2006

STUDY OF THE MASSIVE X-RAY BINARY LSI+65°010

DANA VICAŞ, JING-ZHI YAN, QING-ZHONG LIU

Purple Mountain Observatory, Chinese Academy of Sciences, Space Astronomy
West Beijing Rd. 2, Nanjing, Jiangsu 210008, China
E-mail: dana.vicas@gmail.com

Abstract. We investigate the object LSI+65°010, a massive X-ray binary, using data that cover a ten-years period (1995–2005), observed at the Xinglong station, Beijing Astronomical Observatory. First suggested by Liu and Hang (1999), we here find further evidence to confirm the existence of an H II region around the neutron star.

Key words: astrophysics – X-ray binaries – neutron stars – accretion disks.

1. INTRODUCTION

An X-ray binary is a system composed of a compact object, neutron star or black hole, sometimes even a white dwarf accreting from a companion. Depending on the mass of the companion we have high-mass X-ray binaries and low mass X-ray binaries. A massive X-ray binary is a system in which the companion is a supergiant. Although once a very controversial matter, nowadays it is agreed that LSI+65°010 is such a system (Reig and Chakrabarty 1996).

The source LSI+65°010, also known as 2S 0114+650 was first reported in the SAS 3 galactic survey by Dower et al. (1977). Its optical counterpart was identified as LSI+65°010 to be an 11 magnitude B0.5 III star, which presents a broad Hα emission line in its spectrum.

The system optically resembles to a supergiant X-ray system, whereas its X-ray radiation is similar to Be X-ray binaries. Its rotational velocity of ~100 km/s is too low for a Be star. It is unlike the Be X ray binaries, which have lower luminosity and very high rotational velocity. X-ray emission due to high rotation while mass loss from the stellar wind/lobe overflow powers the supergiant X-ray binary. The accretion rate is reduced by the relatively wide separation of the two stars. The primary has a mass of ~18 $M_{\odot}$ if the central source is a typical neutron star. This mass is nearly normal for this type of star and indicates that significant mass loss has not taken place, unlike the case of most supergiant X-ray binaries, in which the primary has lost about half its mass.

The spectra show a broad Hα emission, He I is in absorption, strong interstellar lines, and a large number of metallic lines. In two spectra, obtained in September 1984, at a four-days interval, strong absorptions are first present and then disappear, while at the same time Hα emission increases. This "shell" effect may be caused by a density enhancement of the star envelope.

A long term variation (Minarini et al. 1994), anticorrelation between emission and absorption lines equivalent width, could be indicative of a long-term modulation in the non radial pulsations (NRP), resulting in a long-term modulation of mass loss.

Interesting enough, this source shows episodes of Be-like activity, like "shell" effects, but the envelope is probably quasi-spherical, as we can infer from the lack of secular variation of luminosity. Due to the instabilities in the stellar wind the disc is in permanent rapid formation or dissipation. The particles would leave the star because of some instability and radiation pressure, but not passing enough angular momentum to form a disc.

Interesting as well is the origin and evolution of this object. If the 2.78-hours pulse period indeed represents the rotation period of the neutron star, 2S 0114+650 would be by far the slowest known X-ray pulsar. Li and Van den Heuvel (1999) explain the long rotation period by considering 2S 0114+650 to be a magnetar.

2. DATA. ORIGIN AND ANALYSIS METHODS

Beginning with the autumn of 1992, a set of mostly Be/X-ray binaries observable in the Northern Hemisphere have been selected to be monitored spectroscopically. LSI +65°010 has been regarded as one of the subjects of the group also because at that time it was still believed to be a Be/X-ray binary (Van den Heuvel and Rappaport 1987). The optical spectroscopic observations were undertaken at Xinglong station in the National Astronomical Observatory complex, with a CCD grating spectrograph detector at the Cassegrain focus of the 216-cm diameter telescope. The data were collected over a ten-years period, starting in October 1995 until October 2005. We have calculated the corresponding Julian date using the Universal Time value. We have as well calculated the equivalent width, the radial velocity inferred from the Hα line variation, and the orbital period; all data being used for the figures throughout this article. For data analysis the software IRAF was used for extraction and calibration. Also, the data have been normalized, so that the continuum level is unity, by fitting a smooth function through the continuum and dividing the spectrum by this fit.

3. DATA ANALYSIS. RESULTS

In the first two figures we present the orbital phase versus the Hα line width or the radial velocity. In Figs. 1 and 2 we notice that the values tend to concentrate into a horizontal line between 350 km/s and 550 km/s. The values in Fig. 2 seem to be less dispersed than those in Fig. 1. Fig. 2 clearly shows a relation between the line profile variations and the orbital phase.

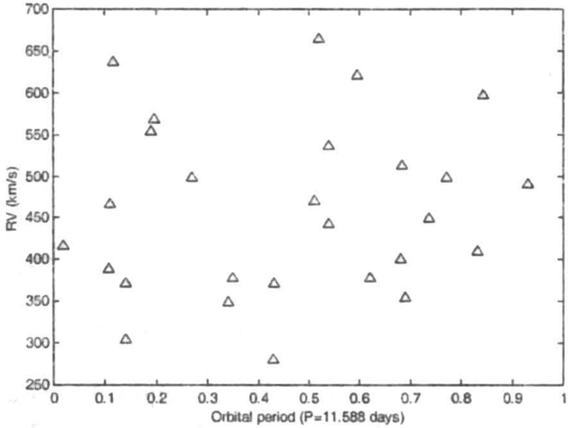

Fig. 1 – Radial velocity versus orbital period element for each observation for the orbital period P = 11.588 days.

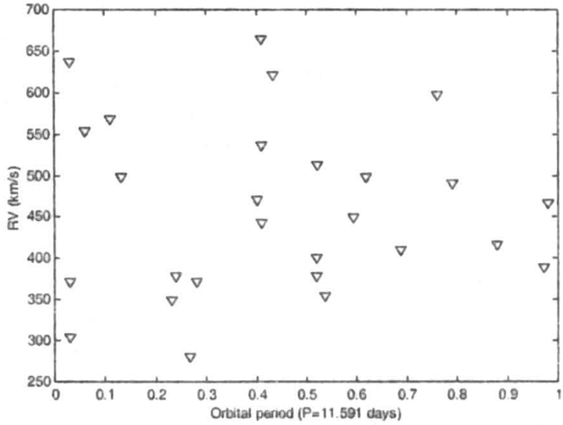

Fig. 2 – Radial velocity versus orbital period element for each observation for the orbital period P = 11.591 days.

Koenigsberger et al. (2003) computed the radial velocity versus the orbital period. Due to the limited number of orbital phases covered by their data, and because they did not repeat the observations at the same phases, they were unable to conclude that the line profile variations are phase-locked. However, Barziv et al. (2001) observed a distortion of the RV curve obtained from the Hγ line in the optical counterpart of the Vela X-1 that can be traced to line-profile variability. That is, they also detected the appearance of a blue wing on the photospheric absorption.

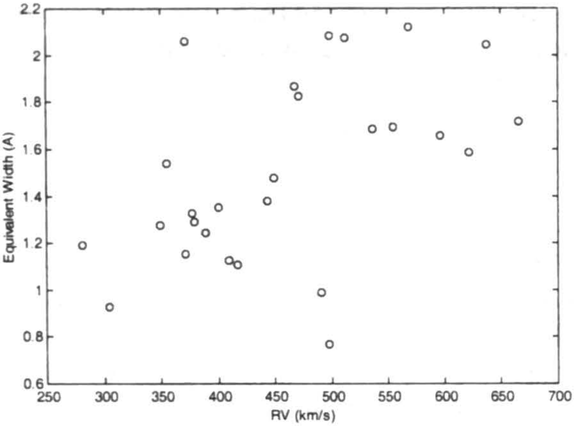

Fig. 3 – Equivalent width versus radial velocity.

In Fig. 3 we plot the radial velocity versus the equivalent width, and we notice the almost linear ascending trend of the values, suggesting a relationship between the two elements. The same trend has been observed by other authors as well, as, e.g., Koenigsberger et al. (2003). They found a Spearsman's rank correlation coefficient between RV and EW to be $r = 0.79$ with a two-sided significance of 0.001 of its deviation from zero (small value means a significant correlation). Unlike Koenigsberger et al. (2003), who plotted Hα and He I line profile in the same diagram, we have only represented the correlation between radial velocity and equivalent width for Hα. Aab and Bychkova (1983) and Crampton et al. (1985) noted that in LSI+65°010 there is a correlation between radial velocity and the excitation of the atomic transition responsible for the line and this is, generally speaking, the same effect we are seeing in our data.

Variations mainly on the blue wing of the line profile of Hα have been reported by Liu and Hang (1999), who favor contamination by emission, due to the presence of an ionized bubble around the neutron star. This ionized region is expected to partake in the orbital motion of the neutron star. Hence the extra-emission will tend to fill in the blue wing of the photospheric absorption line only when it is approaching the observer. In the discussion of Fig. 3 we have already pointed out how at certain phases the absorption element disappears completely, implying that it is completely filled in by the emission. Thus, Hα line does provide support for the hypothesis of an H II region surrounding the neutron star.

To better support the hypothesis of an H II region around the neutron star, we are going to look deeper into the physics of this phenomenon, trying to understand better before any further discussion.

The Hα emission in supergiants is caused by a spherical shell whose origin is in the powerful super-wind from the primary ,which is heated by absorption of the UV radiation of the supergiant. Theoretical modeling of HMXB stellar winds has shown that the presence of the X-ray source affects the wind structure in a complicated and interactive way. The non-spherical shape of the primary, and of the effective gravitational potential around it (including rotation and radiation pressure), leads to a directional dependence of the flow rate in the wind with an enhancement into the direction of the compact star (wind "focusing"; this occurs when the primary does not fill its Roche lobe). X-ray heating and ionization of the wind have, as primary effects, the formation of an ionization bubble around the X-ray source leading to an increase rate of mass accretion and a higher level of X-ray emission. Coriolis force allows interaction of this focused part of the wind with undisturbed (fast-moving) parts, thereby producing strong density enhancements which trail the X-ray source. These enhancements may explain the above mentioned orbital variations of Hα profiles and of the low-energy cut-off in X-ray spectra of HMXBs. Time dependence of the flow is expected when radiative feedback on the wind acceleration is included; in particular at high mass transfer rates the flow in the trailing wake is expected to be unstable.

Another interesting fact about HMXBs, Be/X-ray binaries in particular, which we believe is worth mentioning here, is that the emission lines in Be stars are typically double-peaked, with the peak separation correlated to the observed line width. The most common lines in emission are H I, He I, Fe II and sometimes also Si II and Mg II. In a given Be star, the strength of the emission can be highly variable. It may disappear completely only to return decades later. Shell-line Be stars are characterized by narrow absorption cores in addition to the broad photospheric absorption lines. In the majority of Be stars, both peaks of the emission lines are of equal height. The ultraviolet spectral energy distribution of a B emission line star does not differ significantly from that of a non-Be star, but the Paschen continuum can be brighter than expected. Shell stars, on the other hand, show highly-veiled ultraviolet spectra, and their Paschen continua are typically dimmer. Depending on the amount of circumstellar matter, the spectra of both types of Be stars becomes dominated by free-free and free-bound emission from the disc in the near-to-middle infrared region. Almost all Be stars emit polarized light. Polarization strength may vary also with other quantities, such as the V/R ratio, while the polarization angles are constant. A classical Be star is a rapidly rotating B star that produces a disc in its equatorial plane. This disc is not related to the natal disc the star had during its accreting phases. A well-known problem in all census studies is that Be stars are highly variable and may lose the disc completely, thus be classified as B-type stars.

The reason we insisted in talking about Be stars and Be shell stars is to show once again the dazzling peculiarity of the LSI +65°010 object. It does not rotate fast enough to be a Be star, but yet its spectrum shows many similarities with a star in this class. Some of the data collected show in the spectra of this object double-peaked emission lines, similar to a Be star, but yet different: our object shows an enhanced blue peak unlike Be stars, which theoretically should show peaks of equal height. The double peak cannot be accounted for by the circumstellar shell of the primary star and that because of the low rotational velocity.

Before providing an explanation for the double peak in the spectrum, let us first take a closer look at our data. In Fig. 4 we have the same spectra of LSI+65°010 shown in comparison with the spectra of the B1Ia supergiant Kap Cas. As one can see, some lines are similar, although a bit shifted; there are also lines which differ substantially, like He I 4713.

In Fig. 5 we have a comparison of the different Hα lines over the years. Their variation is obvious, as well as the existence of the double-peak phenomena. The

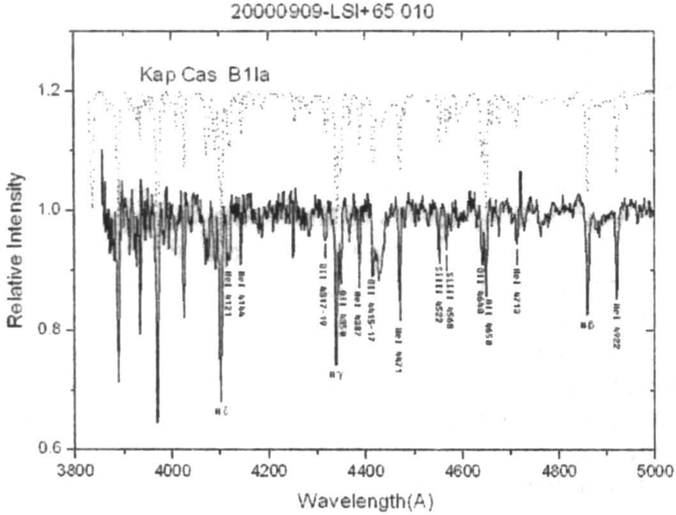

Fig. 4 – Spectra of LSI +65°010 in comparison with the spectra of the B1Ia supergiant Kap Cas.

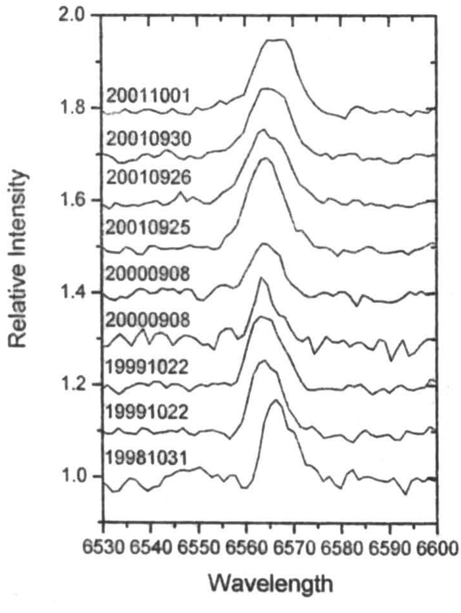

Fig. 5 – Relative intensity versus wavelength for observations over a period of four years.

observations performed in October 2001 show clearly the extra-peak. In the sequel we attempt an explanation of the phenomena.

It has been suggested that the red peak of the Hα line in LSI+65°010 is the usual one, due to the shell around the primary star, while the other one, the violet one, is from an H II region, a gas shell formed around the neutron star. According to Liu and Hang (1999), this H II region has an orbital motion induced by X-ray emission around the neutron star in the massive X-ray binary, or may be due to a blob of gas moving to and from the supergiant.

4. CONCLUDING REMARKS

This paper presents the spectra variability of the massive X-ray binary LSI+65°010 from 1995 to 2005. The majority of the spectra show a single-peaked Hα emission line, but there are a series of spectra that show a great enhancement in EW of Hα lines, which we believe to be due to the H II region around the neutron star and to its orbital motion together with the neutron star. The splitting of the Hα, which was first reported by Liu and Hang (1999), which could not be explained by the rotating circumstellar shell due to the low rotational velocity of the star and the to fact that only the shorter line is shifted. They explained it to be due to the superposition of two emission lines, one from the shell of the primary star, another from an H II region around the neutron star. This article comes to support and confirm their findings through the analysis of a new set of observations done over a period of time of ten years, from 1995 to 2005.

Acknowledgments. The first author is profoundly grateful to her thesis coordinator, Qing-Zhong Liu, for the extremely useful suggestions and comments, as well as for providing all the assistance necessary for obtaining the results presented in this paper. She is also indebted to Jing-Zhi Yan for valuable advices and for his great help as regards data processing. The assistance in observations of the Beijing Astronomical Observatory is duly acknowledged.

REFERENCES

Aab, O. E., Bychkova, L. V.: 1983, *Soviet. Astron. Lett.*, **9**, 313.

Barziv, O., Kaper, L., Van Kerkwijk, M.,Telting, J. H., Van Paradijs, J.: 2001, *Astron. Astrophys.*, 377, 925.

Crampton, D., Hutchings, J. B., Cowley, A. P.: 1985, *Astrophys. J.*, **299**, 839.

Dower, R., Kelley, R., Margon, B., Bradt, H.: 1977, *IAU Circ.* 3144.

Koenigsberger, G., Canalizo, G., Arrieta, A., Richer, M. G., Georgiev, L.: 2003, *Rev. Mex. Astron. Astrofis.*, **39**, 17.

Li, X.-D., Van den Heuvel, E. P. J.: 1999, *Astrophys. J.*, **513**, L45.

Liu, Q.-Z., Hang, H.-R.: 1999, *Astron. Astrophys.*, **350**, 855.

Minarini, R., Teodorani, M., Bartolini, C., Guarnieri, A., Piccioni, A.: 1994, in S. S. Holt, C. S. Day (eds), *The Evolution of X-Ray Binaries*, AIP Conf. Proc. Vol. **308**, October 1993, AIP Press, p. 275.

Reig, P., Chakrabarty, D., Coe, M. J., Fabregat, J., Negueruela, I., Prince, T. A., Roche, P., Steele, I. A.: 1996, *Astron. Astrophys.*, **311**, 879.

Van den Heuvel, E. P. T., Rappaport, S. A.: 1987, in *Physics of Be Stars*, Proc. 92nd IAU Coll., Boulder, CO, August 18–22, 1986, Cambridge University Press, Cambridge, New York, 1987, p. 291.

Received on 30 August 2006

LIGHT-CURVE VARIABILITY OF RZ CEPHEI. III. OBSERVATIONS 1984–1985 PERFORMED IN CLUJ-NAPOCA

IOAN TODORAN, ALEXANDRU POP, RODICA ROMAN

Astronomical Institute of the Romanian Academy
Astronomical Observatory Cluj-Napoca
Str. Cireşilor 19, 400487 Cluj-Napoca, Romania
E-mail: apop@academie.cj.edu.ro, rroman@math.ubbcluj.ro

Abstract. Two observational data sets on the RRc star RZ Cephei obtained between November 1984 and October 1985 are presented and analyzed through Fourier decomposition technique, and the Fourier-type structural parameters are computed. The variability of the light-curve shape is confirmed.

Key words: variable stars – RR Lyrae stars – light curve variability.

1. INTRODUCTION

The third part of our preliminary investigation of the light-curve variability of RZ Cephei is dedicated to the analysis of the last observations performed on this star by one of us (I.T.), which we present in this paper. The data, consisting in 617 photoelectric observations in *V*, performed between November 1984 and October 1985, were obtained using the 50-cm Newton telescope equipped with an unrefrigerated EMI 9558QB photomultiplier and a Tesla EZ-8 chart recorder. As in the case of the previously published data of Todoran (1976), the considered comparison star was BD +64°1699, the observations being given in the instrumental system, without extinction correction (see Table 1 below). We have to mention that, unlike the above mentioned data, these ones have been performed from the new location of the Astronomical Observatory, i.e., in the Southern part of the town, on the Feleacu Hill, at 750 m altitude above sea level.

2. THE OBSERVATIONAL DATA AND DATA ANALYSIS

As in our previous paper (Pop and Roman 2006b), we split the whole data set in two shorter ones, in order to be able to emphasize possible changes of the light-curve

Rom. Astron. J., Vol. **16**, No. 2, p. 141–149, Bucharest, 2006

shape. The observational data are given in Tables 1 and 2, while the corresponding light curves are displayed in Figs. 1 and 2.

The analysis methods were those described in the first paper of this series (Pop and Roman, 2006a). During the preliminary tests performed by us, we rejected the following data (2440000.0 + ...): 6291.3739, 6291.3746, 6291.3760, 6291.3788, 6291.3732, 6034.3624, 6034.3714, 6346.2630, 6346.2627, 6346.2759, 6346.3453, 6346.5329, their corresponding residuals having deviations larger than 3σ.

Unfortunately, no data set does display suitable phase coverage due to the presence of gaps of about tenth of a pulsation cycle (see Pop et al. 2004) in order to take into account all the significant terms in the truncated Fourier series. Therefore, the fitted models are not able to describe the fine details of the light curve.

The results of the application of the Fourier decomposition technique as well as the values of the light-curve amplitude and residuals' standard deviation, are given in Table 3. The values of the corresponding Fourier structural parameters are displayed in Table 4.

The statistical analysis of the residuals obtained after subtraction of the fitted model reveals their non-randomness and their close-to-Gaussian character.

3. CONCLUDING REMARKS

The analysis of these two new observational data sets on RZ Cephei and the examination of the obtained results lead us to the following preliminary conclusions:

3.1. The present data confirm the variability of the light curve shape (Cester and Todoran 1976; Todoran 1976; Pop and Roman, 2006a, b), not only during the maximum brightness, but also in minimum light.

3.2. The residuals corresponding to both analyzed data sets are featured by a non-random character already reported by us in other data (Pop and Roman 2006a, b).

3.3. The first analyzed data set displayed a significant variation of the zeropoint Δm_0, which needed a third-order-polynomial trend to be taken into account. Such a behaviour could be understood having in view the long time-base of these data. We mention that three data-sets analyzed in our previous paper (Pop and Roman 2006 b) were find to present linear trends of the zeropoint. New observations are thus needed to establish the real cause of this behaviour: does it belong to RZ Cephei, or to the lack of the complete data reduction (extinction correction, standardization) together with weather variability, or is it a consequence of the possible variability of the comparison star BD+64°1699?

3.4. The above conclusions, together with those of our above quoted studies, constitute arguments for searching a microvariability phenomenon in RZ Cep and/or BD +64°1699.

Table 1

Observations November 1984 – August 1985 (t given in HJD–2440000, ΔV in magnitudes)

t	ΔV	t	ΔV	t	ΔV
6019.2089	0.596	6019.2568	0.213	6019.3019	0.175
6019.2095	0.574	6019.2573	0.228	6019.3026	0.182
6019.2102	0.596	6019.2595	0.208	6019.3058	0.237
6019.2106	0.619	6019.2606	0.241	6019.3065	0.247
6019.2113	0.596	6019.2613	0.247	6019.3072	0.192
6019.2123	0.596	6019.2637	0.212	6019.3106	0.205
6019.2150	0.585	6019.2648	0.221	6019.3116	0.207
6019.2176	0.574	6019.2665	0.215	6019.3123	0.207
6019.2183	0.585	6019.2679	0.228	6019.3144	0.205
6019.2190	0.574	6019.2690	0.220	6019.3153	0.213
6019.2197	0.563	6019.2697	0.226	6019.3172	0.234
6019.2204	0.563	6019.2704	0.244	6019.3179	0.228
6019.2210	0.563	6019.2727	0.218	6019.3186	0.238
6019.2217	0.563	6019.2741	0.239	6019.3193	0.221
6019.2224	0.541	6019.2748	0.217	6019.3200	0.223
6019.2231	0.521	6019.2780	0.224	6019.3207	0.207
6019.2238	0.521	6019.2803	0.197	6019.3221	0.223
6019.2245	0.510	6019.2815	0.211	6019.3241	0.234
6019.2252	0.521	6019.2828	0.197	6019.3266	0.266
6019.2259	0.500	6019.2849	0.182	6019.3273	0.275
6019.2266	0.510	6019.2863	0.169	6019.3280	0.266
6019.2325	0.472	6019.2873	0.192	6019.3308	0.275
6019.2345	0.430	6019.2905	0.215	6019.3318	0.266
6019.2370	0.365	6019.2915	0.212	6019.3356	0.273
6019.2377	0.359	6019.2921	0.197	6019.3363	0.285
6019.2394	0.374	6019.2942	0.143	6019.3370	0.285
6019.2401	0.332	6019.2950	0.161	6019.3377	0.279
6019.2419	0.351	6019.2955	0.161	6019.3398	0.302
6019.2429	0.336	6019.2963	0.175	6019.3404	0.310
6019.2450	0.299	6019.2970	0.169	6019.3415	0.304
6019.2460	0.283	6019.2977	0.151	6019.3440	0.308
6019.2483	0.285	6019.2984	0.182	6019.3450	0.311
6019.2491	0.275	6019.2991	0.182	6019.3474	0.315
6019.2519	0.237	6019.2998	0.169	6019.3481	0.304
6019.2526	0.237	6019.3005	0.176	6019.3488	0.319
6019.2545	0.212	6019.3012	0.182	6019.3495	0.302
6019.3502	0.312	6034.3357	0.535	6284.3260	0.609
6019.3509	0.319	6034.3364	0.539	6284.3267	0.609
6034.2968	0.628	6034.3371	0.519	6284.3274	0.604
6034.2975	0.634	6034.3378	0.516	6284.3295	0.573
6034.2999	0.636	6034.3385	0.504	6284.3302	0.554
6034.3003	0.647	6034.3392	0.516	6284.3357	0.547
6034.3010	0.625	6034.3399	0.504	6284.3364	0.542
6034.3017	0.636	6034.3413	0.508	6284.3371	0.549
6034.3024	0.670	6034.3438	0.499	6284.3399	0.521
6034.3062	0.653	6034.3448	0.445	6284.3419	0.533
6034.3069	0.653	6034.3468	0.390	6284.3427	0.507

6034.3073	0.635	6034.3489	0.402	6284.3457	0.499
6034.3096	0.605	6034.3503	0.457	6284.3478	0.440
6034.3107	0.631	6034.3538	0.404	6284.3496	0.422
6034.3131	0.651	6034.3562	0.380	6284.3510	0.432
6034.3148	0.631	6034.3583	0.361	6284.3517	0.420
6034.3152	0.610	6034.3603	0.301	6284.3541	0.432
6034.3177	0.629	6034.3610	0.263	6284.3548	0.385
6034.3184	0.608	6034.3624	0.228	6284.3569	0.341
6034.3190	0.608	6034.3631	0.234	6284.3582	0.341
6034.3198	0.596	6034.3652	0.240	6284.3610	0.338
6034.3205	0.592	6034.3687	0.230	6284.3617	0.338
6034.3211	0.592	6034.3714	0.163	6284.3624	0.336
6034.3218	0.580	6034.3749	0.222	6284.3659	0.282
6034.3246	0.567	6034.3770	0.257	6284.3684	0.270
6034.3253	0.551	6034.3780	0.136	6284.3691	0.249
6034.3267	0.572	6034.3802	0.223	6284.3700	0.259
6034.3274	0.564	6034.3816	0.231	6284.3707	0.259
6034.3301	0.570	6034.3836	0.169	6284.3714	0.251
6034.3308	0.570	6284.3138	0.702	6284.3721	0.251
6034.3316	0.574	6284.3145	0.647	6284.3753	0.255
6034.3323	0.574	6284.3159	0.682	6284.376	0.263
6034.3330	0.535	6284.3194	0.616	6284.3767	0.246
6034.3336	0.539	6284.3214	0.647	6284.3777	0.268
6034.3343	0.539	6284.3228	0.613	6284.3784	0.268
6034.3350	0.535	6284.3253	0.622	6284.3805	0.239
6284.3811	0.242	6291.3350	0.581	6291.3853	0.666
6284.3816	0.242	6291.3367	0.623	6291.3860	0.672
6284.3823	0.251	6291.3374	0.677	6291.3867	0.679
6284.3829	0.251	6291.3381	0.677	6291.3871	0.647
6284.3860	0.256	6291.3388	0.621	6291.3881	0.666
6284.3867	0.265	6291.3395	0.607	6291.3888	0.679
6284.3881	0.265	6291.3402	0.626	6291.3895	0.679
6284.3909	0.259	6291.3408	0.614	6291.3904	0.685
6284.3916	0.251	6291.3414	0.589	6291.3911	0.685
6284.3923	0.242	6291.3430	0.631	6291.3918	0.679
6284.3944	0.249	6291.3441	0.637	6291.3925	0.699
6284.3950	0.249	6291.3457	0.656	6291.3931	0.692
6284.3964	0.236	6291.3468	0.631	6291.3936	0.692
6284.3971	0.245	6291.3475	0.636	6291.3944	0.705
6284.3996	0.253	6291.3496	0.648	6291.3954	0.699
6284.4006	0.238	6291.3503	0.648	6291.3961	0.679
6291.3003	0.461	6291.3517	0.649	6293.3096	0.400
6291.3027	0.421	6291.3524	0.649	6293.3107	0.355
6291.3073	0.440	6291.3590	0.674	6293.3138	0.339
6291.3078	0.433	6291.3593	0.668	6293.3156	0.276
6291.3100	0.470	6291.3600	0.661	6293.3201	0.261
6291.3112	0.502	6291.3617	0.655	6293.3230	0.262
6291.3128	0.522	6291.3623	0.654	6293.3239	0.235
6291.3135	0.518	6291.3635	0.672	6293.3249	0.232
6291.3156	0.535	6291.3656	0.649	6293.3281	0.251

6291.3163	0.525	6291.3668	0.649	6293.3290	0.225
6291.3173	0.518	6291.3704	0.671	6293.3316	0.255
6291.3225	0.522	6291.3732	0.583	6293.3329	0.290
6291.3235	0.528	6291.3739	0.564	6293.3353	0.239
6291.3258	0.544	6291.3746	0.564	6293.3367	0.265
6291.3263	0.518	6291.3760	0.548	6293.3392	0.247
6291.3281	0.583	6291.3788	0.564	6293.3405	0.272
6291.3291	0.557	6291.3807	0.698	6293.3429	0.244
6291.3309	0.541	6291.3812	0.698	6293.3444	0.244
6291.3332	0.613	6291.3834	0.668	6293.3450	0.227
6291.3343	0.588	6291.3843	0.673	6293.3492	0.284
6293.3503	0.197	6293.3659	0.230	6293.3800	0.259
6293.3503	0.223	6293.3666	0.223	6293.3864	0.268
6293.3503	0.214	6293.3711	0.265	6293.3871	0.249
6293.3503	0.198	6293.3718	0.290	6293.3906	0.297
6293.3503	0.208	6293.3725	0.239	6293.3920	0.306
6293.3503	0.230	6293.3739	0.258	6293.3930	0.315
6293.3503	0.230	6293.3749	0.259	6293.3941	0.297
6293.3503	0.215	6293.3753	0.242	6293.3954	0.312
6293.3503	0.211	6293.3777	0.262	6293.3989	0.337
6293.3503	0.234	6293.3781	0.268	6293.3996	0.310
6293.3503	0.230	6293.3788	0.268		

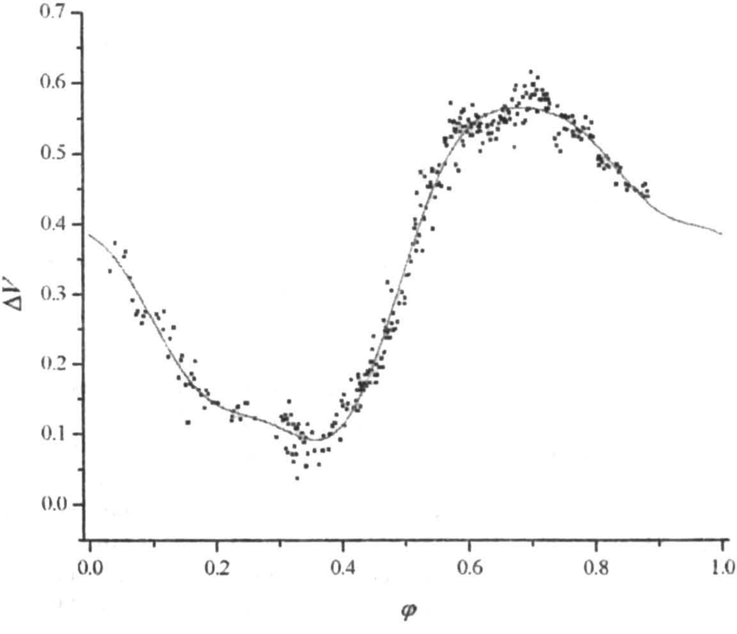

Fig. 1 – Light curve of RZ Cep based on the data given in Table 1.

Table 2

Observations September–October 1985
(t given in HJD–2440000, ΔV in magnitudes)

t	ΔV	t	ΔV	t	ΔV
6328.2714	0.319	6346.2724	0.597	6346.3148	0.698
6328.2728	0.332	6346.2734	0.616	6346.3165	0.695
6328.2735	0.332	6346.2749	0.627	6346.3171	0.698
6328.2742	0.321	6346.2759	0.691	6346.3189	0.711
6328.2753	0.366	6346.2766	0.645	6346.3207	0.672
6328.2781	0.351	6346.2773	0.623	6346.3214	0.698
6328.2795	0.319	6346.2780	0.633	6346.3220	0.725
6328.2819	0.332	6346.2787	0.645	6346.3227	0.705
6328.2895	0.366	6346.2808	0.671	6346.3234	0.678
6328.2916	0.382	6346.2822	0.652	6346.3255	0.672
6328.2937	0.356	6346.2829	0.640	6346.3261	0.698
6328.2954	0.369	6346.2836	0.652	6346.3269	0.712
6328.2964	0.406	6346.2842	0.640	6346.3276	0.705
6328.2971	0.406	6346.2863	0.652	6346.3283	0.691
6328.2988	0.361	6346.2870	0.674	6346.3311	0.684
6328.2995	0.388	6346.2877	0.674	6346.3318	0.671
6328.3013	0.402	6346.2891	0.684	6346.3325	0.671
6328.3020	0.396	6346.2919	0.678	6346.3332	0.667
6328.3034	0.421	6346.2940	0.674	6346.3349	0.664
6328.3041	0.430	6346.2947	0.677	6346.3356	0.664
6328.3058	0.406	6346.2967	0.677	6346.3363	0.671
6328.3065	0.406	6346.2974	0.651	6346.3373	0.652
6328.3072	0.406	6346.2981	0.651	6346.3398	0.647
6328.3079	0.424	6346.2988	0.664	6346.3404	0.659
6328.3086	0.424	6346.2995	0.684	6346.3412	0.652
6328.3092	0.415	6346.3002	0.677	6346.3422	0.652
6328.3099	0.424	6346.3016	0.698	6346.3453	0.732
6328.3106	0.443	6346.3023	0.698	6346.3460	0.656
6328.3113	0.453	6346.3030	0.684	6346.3467	0.669
6346.2627	0.457	6346.3061	0.698	6346.3491	0.669
6346.2630	0.440	6346.3082	0.718	6346.3498	0.669
6346.2655	0.573	6346.3086	0.705	6346.3505	0.664
6346.2683	0.601	6346.3092	0.705	6346.3512	0.651
6346.2690	0.601	6346.3106	0.718	6346.3519	0.638
6346.2714	0.616	6346.3113	0.691	6346.3530	0.664
6346.2720	0.629	6346.3137	0.691	6346.3537	0.656
6346.3558	0.636	6346.4002	0.313	6346.4435	0.226
6346.3565	0.630	6346.4012	0.300	6346.4470	0.250
6346.3572	0.630	6346.4033	0.303	6346.4477	0.241
6346.3586	0.628	6346.404	0.293	6346.4484	0.241
6346.3620	0.638	6346.4047	0.293	6346.4498	0.234

6346.3627	0.651	6346.4054	0.284	6346.4509	0.231
6346.3634	0.651	6346.4061	0.265	6346.4516	0.231
6346.3644	0.633	6346.4123	0.245	6346.4523	0.222
6346.3686	0.601	6346.4130	0.248	6346.4530	0.213
6346.3693	0.584	6346.4137	0.248	6346.4537	0.222
6346.3700	0.568	6346.4144	0.238	6346.4558	0.227
6346.3707	0.584	6346.4151	0.229	6346.4565	0.244
6346.3714	0.576	6346.4158	0.246	6346.4575	0.244
6346.3741	0.576	6346.4162	0.248	6346.4609	0.250
6346.3748	0.568	6346.4183	0.257	6346.4630	0.269
6346.3780	0.554	6346.4190	0.265	6346.4651	0.263
6346.3787	0.549	6346.4197	0.248	6346.4665	0.252
6346.3794	0.537	6346.4220	0.257	6346.4679	0.262
6346.3801	0.547	6346.4234	0.256	6346.4693	0.271
6346.3808	0.526	6346.4269	0.293	6346.4700	0.281
6346.3815	0.514	6346.4276	0.284	6346.4707	0.271
6346.3856	0.477	6346.4283	0.265	6346.4714	0.271
6346.3863	0.459	6346.4290	0.284	6346.4727	0.300
6346.3870	0.459	6346.4297	0.257	6346.4734	0.300
6346.3877	0.448	6346.4304	0.256	6346.4741	0.310
6346.3884	0.437	6346.4310	0.238	6346.4780	0.310
6346.3908	0.404	6346.4342	0.262	6346.4794	0.302
6346.3922	0.401	6346.4345	0.225	6346.4808	0.343
6346.3926	0.391	6346.4352	0.243	6346.4815	0.343
6346.3933	0.384	6346.4359	0.226	6346.4821	0.341
6346.3940	0.363	6346.4377	0.262	6346.4839	0.349
6346.3947	0.352	6346.4384	0.243	6346.4845	0.346
6346.3954	0.349	6346.4394	0.243	6346.4852	0.339
6346.3961	0.352	6346.4415	0.215	6346.4863	0.328
6346.3967	0.349	6346.4424	0.243	6346.4870	0.346
6346.3995	0.313	6346.4429	0.224	6346.4891	0.349
6346.4898	0.349	6346.5032	0.384	6346.5238	0.461
6346.4904	0.339	6346.5044	0.392	6346.5252	0.427
6346.4912	0.339	6346.5058	0.403	6346.5262	0.427
6346.4919	0.339	6346.5064	0.381	6346.5269	0.427
6346.4926	0.339	6346.5072	0.381	6346.5276	0.452
6346.4940	0.354	6346.5079	0.381	6346.5297	0.429
6346.4947	0.335	6346.5086	0.403	6346.5315	0.445
6346.4954	0.346	6346.5106	0.369	6346.5322	0.449
6346.4957	0.356	6346.5113	0.432	6346.5329	0.409
6346.4960	0.366	6346.5120	0.432	6346.5342	0.495
6346.4967	0.366	6346.5137	0.440	6346.5387	0.513
6346.4988	0.349	6346.5151	0.406	6346.5394	0.532
6346.4991	0.349	6346.5179	0.398	6346.5401	0.513
6346.5005	0.359	6346.5220	0.449	6346.5419	0.495
6346.5012	0.359	6346.5227	0.449	6346.5433	0.479

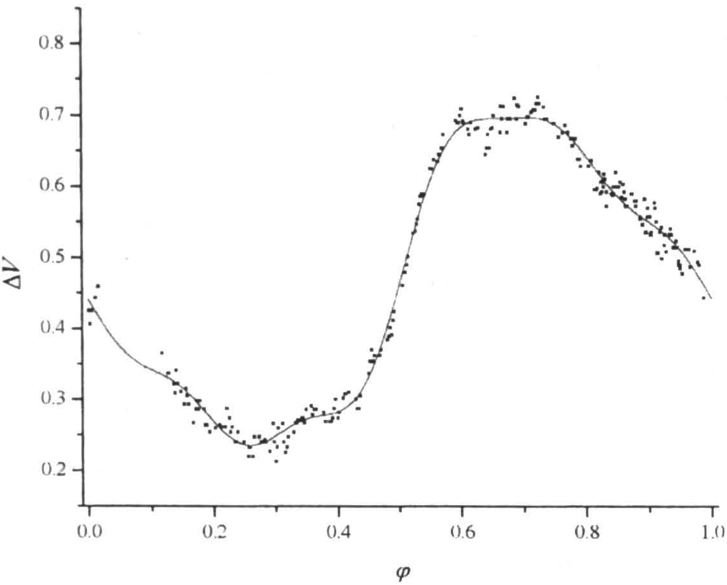

Fig. 2 – Light curve of RZ Cep based on the data given in Table 2.

Table 3

The values of the fitted light-curve parameters

t_0 (HJD−2400000) Δt N	f (c/d)	M_0(mag)	A (mag)	σ (mmag)	
	A_1 (mag) Φ_1 (rad)	A_2 (mag) Φ_2 (rad)	A_3 (mag) Φ_3 (rad)	A_4 (mag) Φ_4 (rad)	A_5 (mag) Φ_5 (rad)
46156.3043 274.1970 349	3.240126 ±0.00001 1	$0.315 + 1.21\cdot10^{-3}\cdot t +$ $\pm0.025\ \ \pm0.18\cdot10^{-3}$ $6.5\cdot10^{-6}\cdot t^2 - 5.7\cdot10^{-8}\cdot t^3$ $\pm1.4\cdot10^{-6}\ \ \pm1.0\cdot10^{-8}$	0.4725 ±0.0047	23.3	
	0.2255 ±0.0026 2.323 ±0.018	0.0618 ±0.0025 3.385 ±0.058	0.0165 ±0.0033 3.35 ±0.14	0.0195 ±0.0020 5.45 ±0.14	
46337.4074 18.2719 256	3.23971 ±0.00024	0.4767 ±0.0013	0.4615 ±0.0040	16.7	
	0.2285 ±0.0017 1.138 ±0.015	0.0457 ±0.0018 0.439 ±0.050	0.0201 ±0.0018 5.998 ±0.099	0.0102 ±0.0018 5.28 ±0.16	0.0171 ±0.0017 5.17 ±0.11

Table 4

The values of the Fourier parameters of the two analyzed light curves

t_0 (HJD–2400000)	R_{21} Φ_{21} (rad)	R_{31} Φ_{31} (rad)	R_{41} Φ_{41} (rad)	R_{51} Φ_{51} (rad)
46156.3043	0.274 ±0.013 5.021 ±0.069	0.073 ±0.014 2.66 ±0.15	0.0864 ±0.0090 2.44 ±0.15	
46337.4074	0.2001 ±0.0083 4.446 ±0.058	0.0879 ±0.0078 2.58 ±0.11	0.0447 ±0.0078 0.73 ±0.17	0.0747 ±0.0074 5.76 ±0.14

REFERENCES

Cester, B., Todoran, I.: 1976, *Mem. Soc. Astron. Italiana*, **47**, 217.
Pop, A. Roman, R.: 2006a, *Rom. Astron. J.*, **16**, 49.
Pop, A. Roman, R.: 2006b, *Rom. Astron. J.*, **16**, 59.
Pop, A., Turcu, V., Codreanu, S.: 2004, *Astrophys. Space Sci.*, **293**, 393.
Todoran, I.: 1976, *Contrib. Astron. Obs.*, Univ. "Babeş-Bolyai" Cluj-Napoca.

Received on 16 June 2006

LIGHT-CURVE VARIABILITY OF RZ CEPHEI. IV. FEATURING THE LIGHT-CURVE SHAPE

ALEXANDRU POP, RODICA ROMAN

Astronomical Institute of the Romanian Academy
Astronomical Observatory Cluj-Napoca
Str. Cireşilor 19, 400487 Cluj-Napoca, Romania
E-mail: apop@academie.cj.edu.ro, rroman@math.ubbcluj.ro

Abstract. The aim of this paper is to give an accurate description of the light-curve shape of RZ Cephei, which proved to be featured by some variability. Thus, we introduced a new class of structural parameters quantifying the skewness and the acuteness of the light curve. They are defined as the relative length of given sections of the light curve. Their application to the case of RZ Cephei reveals their ability to correctly detect those light curves that display strong distortions of their shape.

Key words: variable stars – RR Lyrae stars – light-curve shape variability.

1. INTRODUCTION

Along the previous three papers on the study of the light curve of RZ Cephei (Pop and Roman 2006a, b; Todoran et al. 2006 (hereafter Papers I–III); see also references therein), we supplied new evidences for the existence of a quite important variability phenomenon of the light curve shape, as well as one of amplitude variability. We also emphasized the alternate behaviour of the light-curve profile during the maximum brightness. For the twenty two analyzed data sets we gave the Fourier amplitudes and phases, as well as the corresponding Fourier structural parameters, i.e. amplitude ratios and phase lags.

An important goal in the study of the variability of RZ Cephei would be the analysis of the temporal behaviour of its amplitude and Fourier structural parameters. Unfortunately, there are two problems: (i) only five data sets were performed in the Johnson standard photometric system, Ponsen and Oosterhoff using a yellow GG7 filter and a blue BG12 + GG13 one, while Todoran's observations (Todoran 1976; Paper III), obtained through a Johnson V filter, were given in the instrumental system; (ii) the interplay between the quite different precision of the different observations and the corresponding data sampling led to the use of a different number of periodic terms in the respective Fourier decompositions. Therefore, we decided to use the structural parameters considered by Stellingwerf and Donohoe (1986, 1987): skewness (Sk) and acuteness (Ac) (see also Andreasen and Petersen 1987; Andreasen 1988; Petersen 1994). The skewness of a light curve is defined as the ratio between the phase duration of the descending branch ($\Delta\varphi_{rb}$) and that of the rising branch, while the acuteness is defined as the ratio between the phase duration of fainter than average (median) light m_m (see below), and that of brighter than average light ($\Delta\varphi_{mp}$). According to their definitions, these structural parameters are dimensionless, and thus they might be less influenced by the lack of standardization in some data. In addition, the values of these parameters are very easy to estimate, even in a graphical way. On the other hand, taking into account the strong variability of the maximum light profile of RZ Cephei, one could expect that the above mentioned phase durations be insensible to the local changes of the light curve shape. Andreasen (1988) mentioned a situation (stars with periods between 12 days and 18 days) in which the presence of a second "bump", when passing from the ascending to the descending branch, incorrectly determines a decrease of the light-curve skewness.

The aim of this paper is to introduce and to study new types of structural parameters able to describe more accurately the shape of the light curve of pulsating stars, possibly featured by the presence of some distortions like "bumps", "dips", "humps", "shoulders", "standstills" (e.g., Christy 1966; Simon 1981, 1985; Gillet and Crowe 1988). We tested the behaviour of these structural parameters using the light curves of RZ Cephei analyzed in Papers I–III.

2. NEW STRUCTURAL PARAMETERS OF THE LIGHT CURVE

In the following we shall introduce two types of parameters defined as the relative length of some characteristic sections of the light curve (considered in the phase diagram) (see Figs. 1a and 1b):

1.a. The relative length of the rising branch:

$$l_{rb} = l_{rb}^{0} / l_{0} , \tag{1}$$

1.b. The relative length of the light curve situated over a given brightness level m_x (e.g. m_m – the median (average) magnitude, $m_m = (m_{\min} + m_{\max})/2 \equiv m_{\max} + A/2$, with $A = m_{\min} - m_{\max}$, m_0 – the "zero" or "DC" level (see eq. (4) below), $m_{P/2}$ – the level corresponding to a $P/2$ width of the light curve, or 0.5 in phase):

$$l_{m_x p} = l^0_{m_x p} / l_0 \,. \tag{2}$$

In the above equations l^0_{rb}, $l^0_{m_x p}$, and l_0 are, respectively, the length of the rising branch, the length of the light curve situated over the brightness level m_x (i.e. brighter than m_x), and the length of the whole light curve. As it is well-known, the length of the light curve between two different points of phases φ_1 and φ_2 is given by

$$l_{12} = \int_{\varphi_1}^{\varphi_2} \sqrt{1 + \left(\mathrm{d}m(\varphi)/\mathrm{d}\varphi\right)^2}\, \mathrm{d}\varphi \,. \tag{3}$$

where $m(\varphi)$ may be expressed analytically using the Fourier decomposition of the light curve considered in the phase diagram

$$m(\varphi) = m_0 + \sum_{k=1}^{K} A_k \cos\left(2\pi k \varphi + \Phi_k\right). \tag{4}$$

In this way, and considering the above mentioned magnitude levels (m_0, m_m, $m_{P/2}$) we can define the following parameters: l_{0p}, l_{mp}, and $l_{P/2p}$.

For a better understanding of the behaviour of these parameters with respect to the corresponding old ones, we shall introduce similar parameters defined on the basis of the relative area of the surface delimited by the light curve between some given points (minimum and maximum light) or some given magnitude levels (the same as above) (see Figs. 1a and 1b). Thus we get:

2.a. The relative area of the surface delimited by the rising branch of the light curve

$$a_{rb} = a^0_{rb} / a_0 \,, \tag{5}$$

2.b. The relative area of the surface delimited by the light curve above the magnitude level m_x (m_0, m_m, $m_{P/2}$)

$$a_{m_x p} = a^0_{m_x p} / a_0 \,, \tag{6}$$

where a^0_{rb}, $a^0_{m_x p}$, and a_0 are, respectively, the area of the surface delimited by the light curve rising branch and a given magnitude level, e.g., the m_0 level, the area of the surface delimited by the light curve over the brightness level m_x (i.e. brighter than m_x), and the area of the surface delimited by the whole light curve. The area of the surface delimited by the light curve between two different points of phases φ_1 and φ_2, and a given magnitude level, m_0 say, is

$$a_{12} = \int_{\varphi_1}^{\varphi_2} m(\varphi)\mathrm{d}\varphi \ , \qquad (2.7)$$

where $m(\varphi)$ is given by (3). Thus, we can define the parameters a_{0p}, a_{mp} and $a_{P/2p}$.

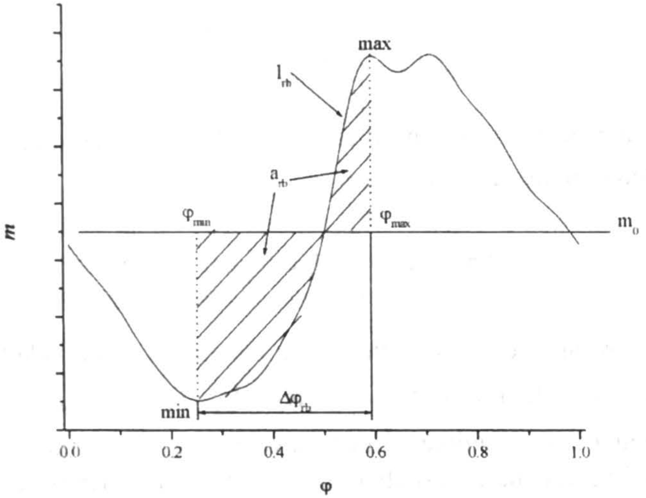

Fig. 1a – Structural parameters defined with respect to the rising branch of the light curve.

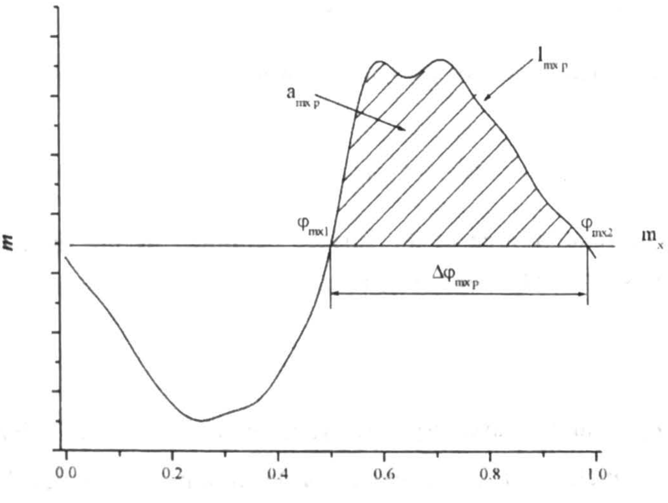

Fig. 1b – Structural parameters defined with respect to a given magnitude level of the light curve.

Table 1 lists the values of the "old" structural parameters of the light curve of RZ Cephei, defined as phase duration, and Table 2 those of the "new" ones, defined as relative lengths and areas of some sections of the light curve or surfaces delimited by the light curve and some given magnitude levels. They were determined on the basis of the synthetic light curves described by the Fourier coefficients listed in Papers I–III. We mention that for the data set No. 8, i.e., HJD 2441625.3738, we estimated the values $l_{P/2P}$ and $a_{P/2P}$ using a Fourier decomposition of the observed light curve with only 5 periodic terms.

Table 1

Values of structural parameters defined as phase duration between specific points of the light curve

Data set number	t (*HJD*–2400000)	$\Delta\varphi_{rb}$	$\Delta\varphi_{0p}$	$\Delta\varphi_{3mp}$	$\Delta\varphi_{mp}$	$\Delta\varphi_{3Mp}$
1	35762.5196(1)	0.4729	0.4517	0.5629	0.4263	0.3476
2	36424.8372(2)	0.3266	0.4817	0.5909	0.4655	0.3587
3	38258.3619(3)	0.3977	0.4887	0.5831	0.4757	0.3710
4	41484.8800(4)	0.3620	0.4892	0.5725	0.4789	0.3467
5	41537.9477(4)	0.3967	0.4674	0.5920	0.4635	0.3804
6	41605.4393(4)	0.4102	0.4918	0.6112	0.4969	0.4088
7	41608.4031(4)	0.3095	0.5190	0.6300	0.5224	0.3221
8	41625.3738(4)	0.2760	0.5660	0.6288	0.5732	0.4322
9	41896.0333(4)	0.2580	0.4371	0.5573	0.4083	0.3295
10	41904.9441(4)	0.4528	0.5386	0.6168	0.5385	0.3639
11	41942.3987(4)	0.3805	0.5074	0.5985	0.5049	0.3555
12	41969.3550(4)	0.4248	0.5307	0.6107	0.5165	0.3942
13	41984.8280(4)	0.4947	0.5270	0.6510	0.5654	0.3942
14	41998.8319(4)	0.4295	0.4944	0.5704	0.4793	0.3843
15	42324.8868(4)	0.3600	0.5548	0.6823	0.5893	0.3784
16	42685.8612(5)	0.4536	0.4848	0.5925	0.4749	0.3558
17	42693.3154(4)	0.3880	0.4695	0.7144	0.4967	0.3959
18	42718.3313(4)	0.3182	0.4727	0.5982	0.4756	0.3880
19	44900.8741(6)	0.4140	0.4906	0.5818	0.4781	0.3535
20	46156.3043(7)	0.3238	0.5516	0.6392	0.5624	0.3968
21	46337.4074(7)	0.4476	0.4869	0.5622	0.4828	0.3843
22	48441.5166(8)	0.4525	0.4978	0.5801	0.4911	0.3615

References for the considered data sets and their Fourier parameters: (1) Ponsen and Oosterhoff (1966), Paper I; (2) Spinrad (1959), Paper I; (3) Paczyński (1965), Paper I; (4) Todoran (1976), Paper II; (5) Cester and Todoran (1976), Paper I; (6) Alania and Abuladze (1986), Paper I; (7) Paper III; (8) ESA (1997) (t is expressed in *BJD*, i.e., Barycentric Julian Date), Paper I.

Note that according to the considered magnitude level m_τ, we have to adjust the value of m_0 in (4) in order to get the correct $m(\varphi)$ values with respect to m_τ.

Thus, the skewness or asymmetry of a light curve will be featured by the parameters defined with respect to the rising branch ($\Delta\varphi_{rb}$, l_{rb}, a_{rb}), and its acuteness by those related to the above magnitude levels ($\Delta\varphi_{mp}$, l_{0p}, l_{mp}, $l_{P/2p}$, a_{0p}, a_{mp}, $a_{P/2p}$). In addition we shall consider the widths of the light curve at the magnitude levels m_0, $m_{\min} - A/3$, $m_{\max} + A/3$, and denote them $\Delta\varphi_{0p}$, $\Delta\varphi_{3mp}$, and $\Delta\varphi_{3Mp}$.

Table 2

Values of the structural parameters defined either as relative lengths of different branches of the light curve, or as relative surfaces' areas delimited by different sections of the light curve. The references for the observational data and the corresponding Fourier parameters are the same as in Table 1.

t (*HJD*–2400000)	l_{rb}	l_{0p}	l_{mp}	$l_{P/2p}$	a_{rb}	a_{mp}	$a_{P/2p}$
35762.5196(1)	0.5144	0.5029	0.4695	0.5533	0.5682	0.4371	0.5844
36424.8372(2)	0.4389	0.5105	0.4897	0.5327	0.3587	0.4609	0.5408
38258.3619(3)	0.4792	0.5146	0.4978	0.5291	0.4645	0.4683	0.5271
41484.8800(4)	0.4422	0.5142	0.5011	0.5286	0.3893	0.4753	0.5279
41537.9477(4)	0.4755	0.5068	0.5022	0.5415	0.4660	0.4911	0.5638
41605.4393(4)	0.4743	0.4925	0.4998	0.5042	0.4550	0.5142	0.5229
41608.4031(4)	0.4170	0.5193	0.5233	0.4969	0.3341	0.5078	0.4555
41625.3738(4)	0.3749	0.5168	0.5308	0.4296	0.2816	0.5317	0.3229
41896.0333(4)	0.3806	0.4569	0.4240	0.5085	0.3174	0.4344	0.5751
41904.9441(4)	0.4992	0.5273	0.5273	0.4746	0.5593	0.4999	0.3929
41942.3987(4)	0.4567	0.5123	0.5084	0.5008	0.4379	0.4918	0.4758
41969.3550(4)	0.4827	0.5147	0.4999	0.4835	0.4998	0.4759	0.4501
41984.8280(4)	0.5237	0.5084	0.5412	0.4885	0.6132	0.5450	0.4804
41998.8319(4)	0.4865	0.5136	0.4938	0.5211	0.4940	0.4626	0.5141
42324.8868(4)	0.4378	0.4922	0.5310	0.4417	0.4400	0.5870	0.3969
42685.8612(5)	0.5133	0.5196	0.5068	0.5395	0.5415	0.4758	0.5384
42693.3154(4)	0.4614	0.4637	0.4989	0.5028	0.4419	0.5713	0.5792
42718.3313(4)	0.4246	0.4976	0.5015	0.5337	0.3345	0.5076	0.5692
44900.8741(6)	0.4850	0.5172	0.5013	0.5288	0.4818	0.4697	0.5220
46156.3043(7)	0.4138	0.5168	0.5324	0.4523	0.3518	0.5332	0.3692
46337.4074(7)	0.4928	0.5018	0.4955	0.5225	0.5147	0.4864	0.5442
48441.5166(8)	0.5069	0.5190	0.5097	0.5222	0.5364	0.4820	0.5061

For a strictly sinusoidal light curve, we have the following obvious results:

$\Delta\varphi_{rh} = 0.5$, $\Delta\varphi_{0p} = \Delta\varphi_{mp} = 0.5$, $l_{rh} = 0.5$, $l_{0p} = l_{mp} = l_{P/2p} = 0.5$, $a_{rh} = 0.5$, $a_{0p} = a_{mp} = a_{P/2p} = 0.5$. For any arbitrary periodic light curve we have $a_{0p} = 0.5$.

3. "NEW" VERSUS "OLD" STRUCTURAL PARAMETERS OF THE LIGHT CURVE

In this Section we will investigate the degree of correlation between the different structural parameters of the light curve defined in the previous one. Thus we have in view three types of parameter pairs:

(i) relative length versus phase duration type parameters;

(ii) relative surface area versus phase duration type parameters;

(iii) relative surface area versus relative length type parameters.

The analysis of the first set of parameter pairs should reveal whether the relative length type parameters bring some new information in comparison with the phase duration type ones. The aim of the analysis of the two other sets of parameters pairs is to emphasize the effect of using different quantities in order to feature specific sections of a pulsating star light curve.

In Table 3 we list the values of the correlation coefficient r, its standard deviation σ_r, those of the statistic t_r, which allows us to test the significance of r through the Student two-tailed test (e.g., Wackerly et al. 1996), and the corresponding confidence level P. Figs. 2–9 display the graphs of the different pairs of structural parameters of the 22 analyzed light curves of RZ Cephei.

Table 3

The analysis of the correlation between different pairs of structural parameters

Parameters	$r \pm \sigma_r$	t_r	P (%)
$(\Delta\varphi_{rh}, l_{rh})$	0.9846 ±0.0067	25.165	> 99.99
$(\Delta\varphi_{rh}, a_{rh})$	0.9819 ±0.0078	23.193	> 99.99
(l_{rh}, a_{rh})	0.967 ±0.014	17.009	> 99.99
$(\Delta\varphi_{0p}, l_{0p})$	**0.51 ±0.16**	**2.619**	**> 98.00**
$(\Delta\varphi_{mp}, l_{mp})$	0.887 ±0.047	8.592	> 99.99
$(\Delta\varphi_{mp}, a_{mp})$	0.807 ±0.076	6.110	> 99.99
(l_{mp}, a_{mp})	0.70 ±0.11	4.426	> 99.90
$(l_{P/2p}, a_{P/2p})$	0.899 ±0.042	9.205	> 99.99

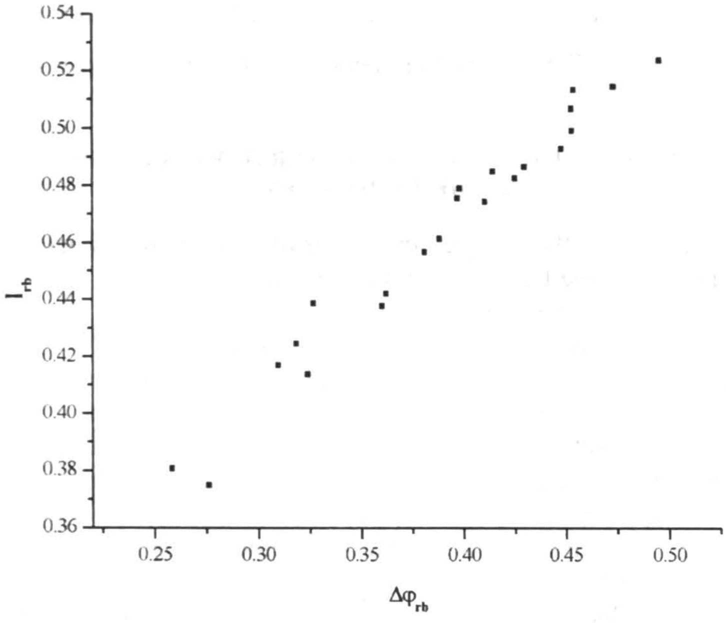

Fig. 2 – RZ Cephei data in the ($\Delta\varphi_{rb}$, l_{rb})-plane.

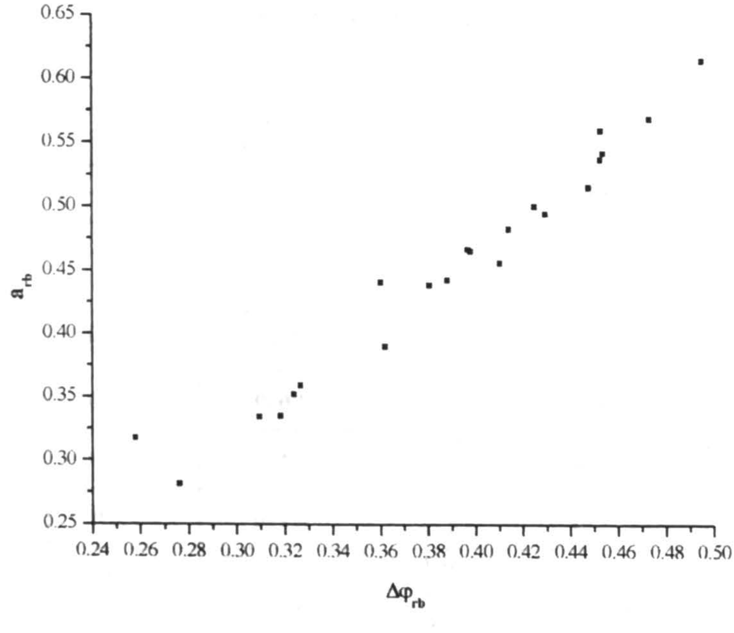

Fig. 3 – RZ Cephei data in the ($\Delta\varphi_{rb}$, a_{rb})-plane.

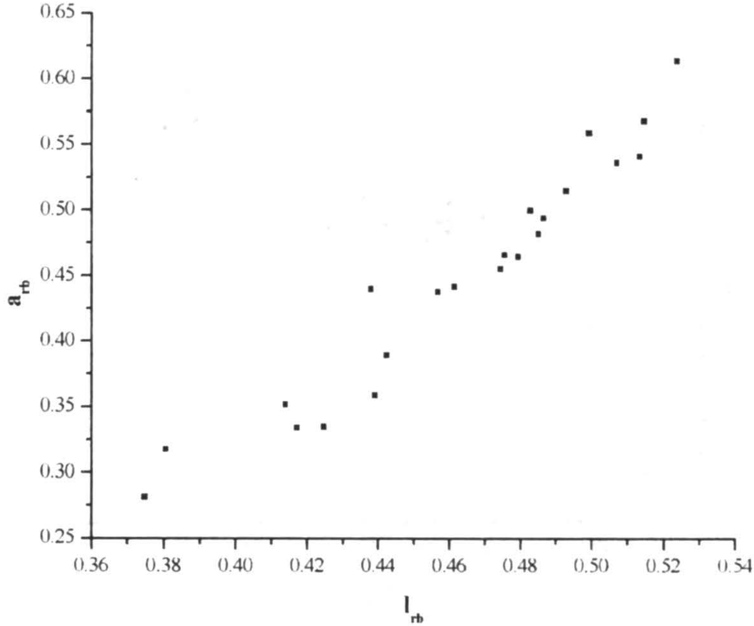

Fig. 4 – RZ Cephei data in the (l_{rb}, a_{rb})-plane.

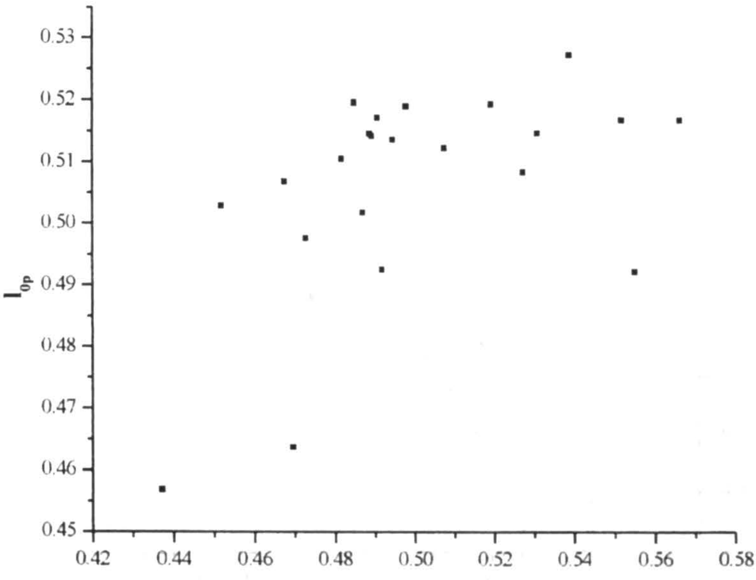

Fig. 5 – RZ Cephei data in the ($\Delta\varphi_{0p}$, l_{0p})-plane.

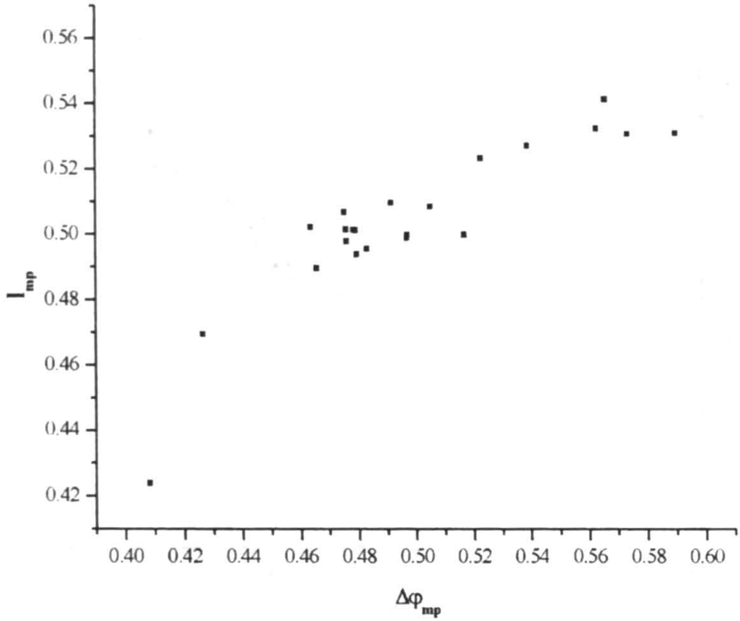

Fig. 6 – RZ Cephei data in the ($\Delta\varphi_{mp}$, l_{mp})-plane.

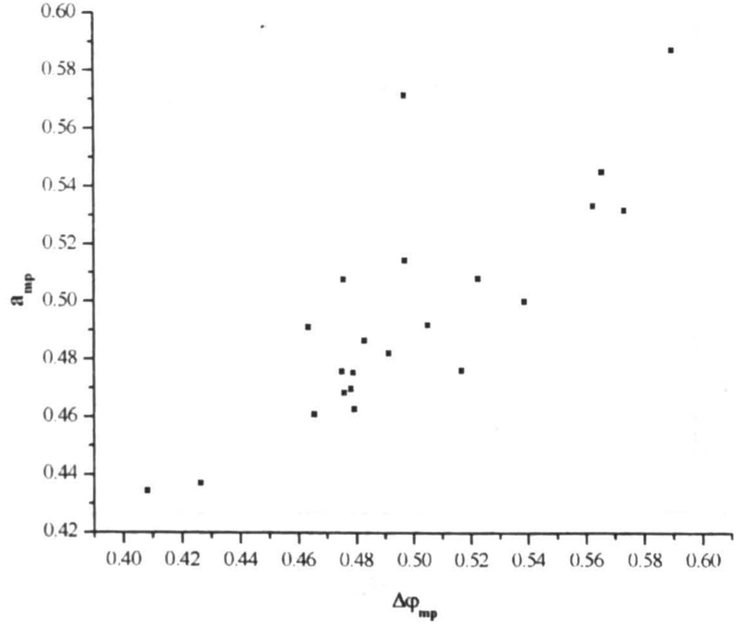

Fig. 7 – RZ Cephei data in the ($\Delta\varphi_{mp}$, a_{mp})-plane.

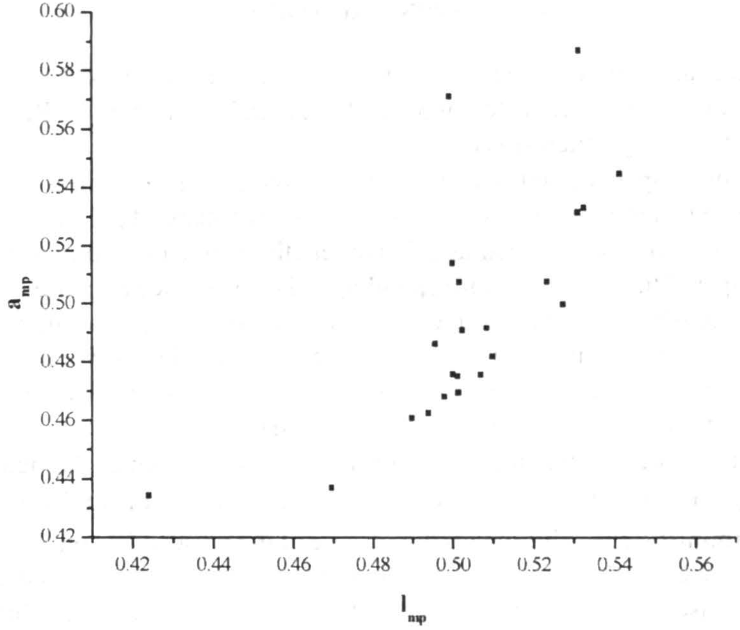

Fig. 8 – RZ Cephei data in the (l_{mp}, a_{mp})-plane.

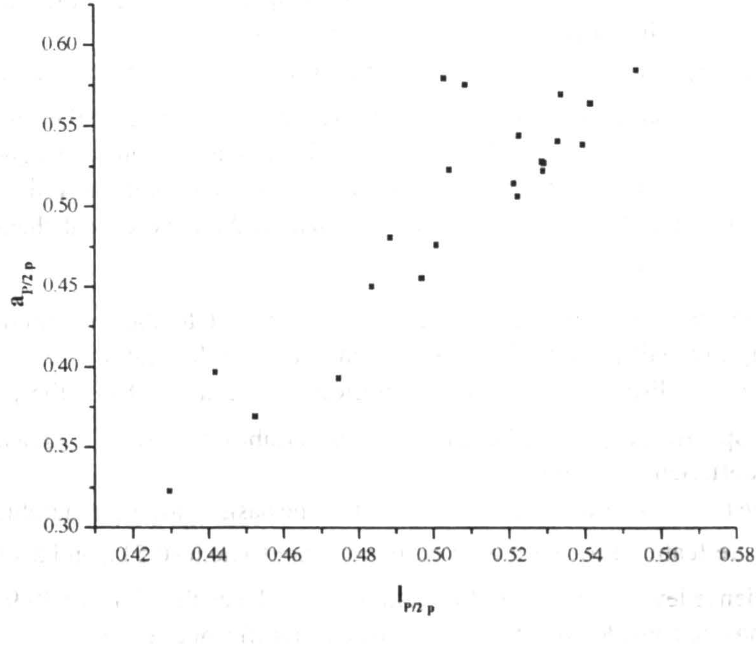

Fig. 9 – RZ Cephei data in the ($l_{P/2\,p}$, $a_{P/2\,p}$)-plane.

4. CONCLUDING REMARKS

A careful examination of the results listed in Table 3, as well as of the Figs. 2–9, displaying the relation between different pairs of structural parameters for RZ Cephei, leads us to the following conclusions:

4.1. In this paper we introduced a new class of dimensionless structural parameters meant to describe quantitatively the light-curve shape of pulsating stars in a more natural way. They are defined as relative length of given sections of the light curve. We compared them with the corresponding old ones defined as phase durations and, also, with auxiliary new ones, defined as relative area of the surfaces delimited by given sections of the light curve and some reference magnitude levels. We investigated the behaviour of these new structural parameters by computing them for 22 observational data sets on RZ Cephei (see Papers I–III).

4.2. All the structural parameters featuring the rising branch of the light curve ($\Delta\varphi_{rb}$, l_{rb}, a_{rb}) are strongly correlated at high confidence levels, their relation being a relatively deterministic one. This means that in case of the present data on RZ Cephei, this light curve section does not display important distortions which could cause a significant decrease in the correlation between the three types of parameters. In spite of the very strong correlation between these parameters, we are of the opinion that l_{rb} is a more suitable estimator of the light curve asymmetry.

4.3. As it was expected, taking into account the specific profile of the maximum light of RZ Cephei, the structural parameters defined with respect to the light curve median level ($\Delta\varphi_{mp}$, l_{mp}, a_{mp}) displayed quite strong, highly significant correlation ($P > 99.9$ %). The decrease of the correlation intensity with respect to the case of the rising branch from 0.967 ÷ 0.9846 % to 0.70 ÷ 0.887 % is an obvious consequence of the presence of a secondary maximum as well as of the temporal variability of the maximum light shape: $\Delta\varphi_{mp}$ cannot contain information about these local phenomena, as l_{mp} and a_{mp} are able to do.

4.4. The structural parameters defined with respect to the magnitude level corresponding to a half-period width (i.e., 0.5 in phase) of the light curve maximum ($l_{P/2p}$ and $a_{P/2p}$) display a strong and significant correlation. As in the previous situation, the specific shape of RZ Cephei, and its variability caused a decrease in the correlation coefficient to 0.899.

4.5. The two structural parameters defined on the basis of the m_0 magnitude level ($\Delta\varphi_{0p}$, l_{0p}) are featured by the lowest correlation coefficient (0.51), and also by the lowest confidence level (> 98.0 %). If we admit a confidence threshold of 99.9 %, this correlation may be considered to have no statistical significance. The reason for such a behaviour is the same as in the above conclusions 4.3 and 4.4. Thus, l_{0p} proved to be able to describe more accurately the shape variability of the light-curve maximum than $\Delta\varphi_{0p}$ does.

4.6. Taking into account the above conclusions 4.3 and 4.5, it is natural to ask ourselves: which is the parameter able to describe most accurately the acuteness of the light curve. On the other hand, on the basis of the data given in Table 1, we estimated for $\Delta\varphi_{mp}$ and $\Delta\varphi_{0p}$: $r = 0.948 \pm 0.022$, with $t_r = 13.307$, which means a strong correlation between these parameters, significant at a confidence level $P > 99.99\%$. Moreover, by virtue of (4), one may consider that m_0 has a more rigorous meaning than m_m when choosing a reference level in order to feature the light curve acuteness. Therefore, having in view all these considerations, we concluded that l_{0p} could be a better estimator of the light curve acuteness.

4.7. As a result of the above conclusions, we have to compare the two pairs of structural parameters quantifying the light curve shape: ($\Delta\varphi_{rb}$, $\Delta\varphi_{0p}$) and (l_{rb}, l_{0p}). Figs. 10a and 10b display the plots of these parameters using the data on RZ Cephei given in Tables 1 and 2. Examining the distribution of the data corresponding to the different light curves, we note that in each of these figures appear three outlying points as follows: in Fig. 10a: 1 (see Fig. 1 in Paper I), 8, and 9 (see Figs. 5 and 6 in Paper II), and in Fig. 10b: 8, 9, and 17 (see Fig. 13 in Paper II).

Let us examine each of these cases. Data set 1 corresponds to the light curve of Ponsen and Oosterhoff (1966), which seems to be a common one, i.e., without significant distortions. In Fig. 10a, it is incorrectly placed in an outlying position, while in Fig. 10b its position is in agreement with its shape. Both data sets 8 and 9 come from Todoran's (1976) paper and display important distortions of the light curve. They correctly appear in outlying positions in both figures. Data set 17 comes from the same paper and displays strong distortions in both minimum and maximum light. In spite of this appearance, in Fig. 10a, it is not placed in an outlying position, although it has a peripheral one with respect to the other data, excepting data sets 1, 8, and 9. The peculiar shape of this light curve is correctly emphasized by the outlying position of data set 17 in Fig. 10b. A final remark on the distribution of the data points in these two plots is that Fig. 10a (based on phase duration type parameters), is featured by an obvious spread, while Fig. 10b displays a lower spread excepting the three outliers, which appear very distinctly discriminated against the other data. The identification of the actual cause of the emphasized deviation of the data sets 8, 9, and 17 needs special care and will be approached in a future paper.

4.8. Although the new structural parameters featuring the skewness and the acuteness of the pulsating star light curves seem to work very well, their behaviour needs to be tested on different data sets on various pulsating stars.

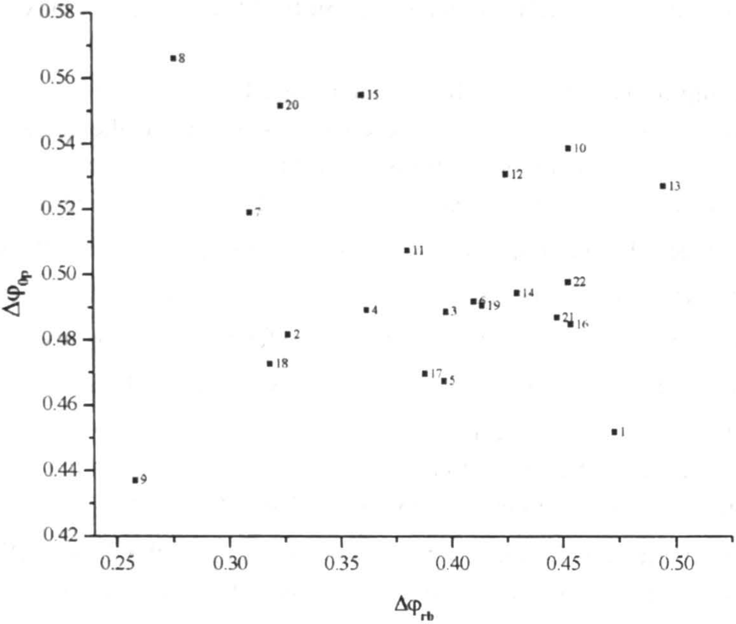

Fig. 10a – RZ Cephei data in the (skewness, acuteness) diagram, through phase duration type parameters.

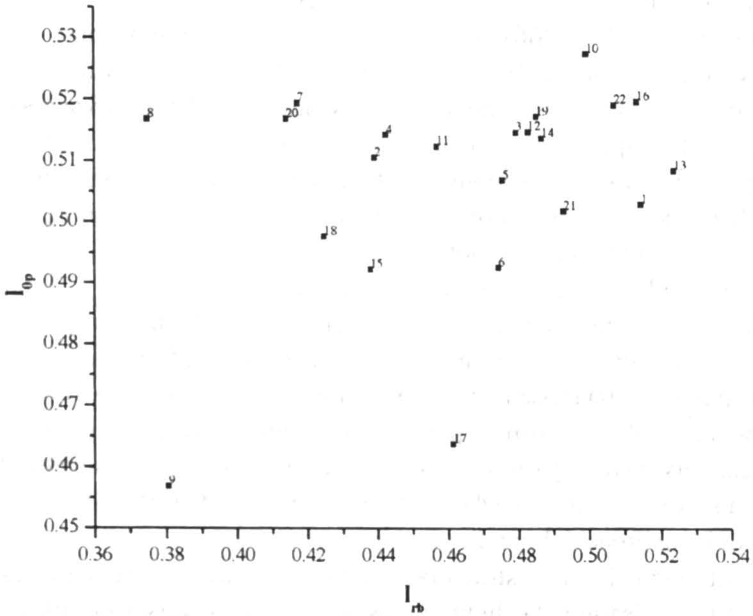

Fig. 10b – RZ Cephei data in the (skewness, acuteness) diagram, through relative light curve length type parameters.

REFERENCES

Alania, I. F., Abuladze, O. P.: 1986, *Bull. Abastumani Astrophys. Obs.*, **61**, 15.
Andreasen, G. K.: 1988, *Astron. Astrophys.*, **196**, 159.
Andreasen, G. K., Petersen, J. O.: 1987, *Astron. Astrophys.*, **180**, 129.
Cester, B., Todoran, I.: 1976, *Mem. Soc. Astron. Italiana*, **47**, 217.
Christy, R. F.: 1966, *Astrophys. J.*, **144**, 108.
ESA: 1997, *The Hipparcos and Tycho Catalogues*, ESA SP-1200.
Gillet, D., Crowe, R. A.: 1988, *Astron. Astrophys.*, **199**, 242.
Paczyński, B.: 1965, *Acta Astron.*, **15**, 115.
Petersen, J. O.: 1994, *Astron. Astrophys. Suppl. Ser.*, **105**, 145.
Ponsen, J., Oosterhoff, P. T.: 1966, *Bull. Astron. Inst. Netherlands*, **18**, 459.
Pop, A. Roman, R.: 2006a, *Rom. Astron. J.*, **16**, 49 (Paper I).
Pop, A. Roman, R.: 2006b, *Rom. Astron. J.*, **16**, 59 (Paper II).
Simon, N. R.: 1981, *Astrophys. J.*, **248**, 291.
Simon, N. R.: 1985, *Astrophys. J.*, **299**, 723.
Spinrad, H.: 1959, *Astrophys. J.*, **130**, 539.
Stellingwerf, R. F., Donohoe, M.: 1986, *Astrophys. J.*, **306**, 183.
Stellingwerf, R. F., Donohoe, M.: 1987, *Astrophys. J.*, **314**, 252.
Todoran, I.: 1976, *Contrib. Astron. Obs.*, "Babeş-Bolyai"Univ., Cluj-Napoca, 1.
Todoran, I., Pop, A. Roman, R.: 2006, in this issue.
Wackerly, D. D., Mendenhall III, W., Scheaffer, R. L.: 1996, *Mathematical Statistics with Applications*, 5th ed., Duxbury Press, Wadsworth Publ. Comp., Belmont, MA.

Received on 1 September 2006

ON HOMOGRAPHIC SOLUTIONS AND CENTRAL CONFIGURATIONS OF THE *n*-BODY PROBLEM

FERENC SZENKOVITS, VASILE URECHE

Babeş-Bolyai University, Faculty of Mathematics and Computer Science
Astronomical Observatory Cluj-Napoca
Str. Cireşilor 19, 400487 Cluj-Napoca, Romania
E-mail: fszenko@math.ubbcluj.ro

Abstract. The concept of central configuration is important in the study of total collisions, in the relative equilibrium state of a rotating system or in the variation of the topological type of the energy and angular momentum invariant manifolds in the *n*-body problem, in close connections with homographic motions. In this paper, by using the variation of the moment of inertia, we characterize those particular solutions of the *n*-body problem, in which the bodies form a central configuration at any moment of the motion, which are not necessary supposed to be homographic solutions.

Key words: *n*-body problem – central configurations – homographic solutions.

1. INTRODUCTION

This paper concerns an old problem: the n-body problem and connections with homographic motions. The n barycentric position vectors x_i of the n bodies with masses m_i form a *central configuration* if the force of gravitation acting on m_i at the moment of the given configuration is proportional to the mass m_i and to the barycentric position vector x_i. The notion of central configuration was introduced by Laplace (1789).

There are several reasons why central configurations are of interest in celestial mechanics. If the masses are released from a central configuration with zero initial velocity, then all particles accelerate toward the origin in such a way that the configuration collapses homothetically. The result is a collision singularity. Simple collision orbits of this kind were the first explicitly known solutions of the three-body problem (Euler 1767). These ones are not the only possible orbits that end in collision of all n particles, but it can be shown that for any such an orbit, the configuration is very close to central configurations. The homothetical collapse plays an essential role in the stellar evolution (the initial collapse of a cloud of dust particles, the final collapse of the star), where the number of particles (molecules, then atoms, or nuclei and electrons) is so large and the particles are so tiny that the configuration usually is approximated with a continuum.

A planar central configuration also gives rise to a family of periodic solutions. The particles are released from the central configuration with initial velocities normal to their position vectors and with magnitudes proportional to their distances from the origin. Each particle will traverse an elliptic orbit, as in the Kepler problem; moreover, the configuration remains similar to the initial configuration throughout the motion, varying only in size, i.e., the solutions are homographic. If the velocities are just large enough, the orbits will be circular. As the velocities tend to zero, the ellipses become more and more eccentric and the periodic solutions approach the collision solutions.

The central configurations also play a role in the study of the topology of the energy and angular-momentum invariant manifolds of the n-body problem. It is known that in the three-body problem bifurcations in the topological type of invariant manifold occur at the levels that contain the circular periodic orbits mentioned above (Smale 1970a, b; McCord et al. 1998).

Finding all central configurations for an arbitrary number n of points is a difficult problem, which is still open. In the trivial case $n = 2$, all configurations of the two bodies are central configurations. We list the most important results known presently in this direction, for $n \geq 3$.

For $n = 3$, the only noncollinear central configuration is formed by the vertices of an equilateral triangle, solution discovered by Lagrange in 1773 (see Lagrange 1873). For $n = 4$, the unique noncoplanar configuration is given by the vertices of a regular tetrahedron (Dziobek 1900). The general approach to central configurations is also due to Dziobek (1900).

The collinear central configurations are described by the following theorem of Moulton (1910): each enumeration of the points determines uniquely a central configuration in which the points lie collinearly in the given order. Therefore, there are exactly $n!/2$ distinct collinear central configurations. For $n = 3$ there are exactly three such configurations, discovered by Euler (1767).

In the last years, many authors studied different aspects related to the central configurations (e.g. Moeckel 1990; Llibre 1991; Meyer and Schmidt 1993; Casasayas et al. 1994; Albouy 1995; Moeckel and Simó 1995).

A given solution of the problem of n bodies is called *homographic* if the configuration formed by the n bodies moves in the inertial barycentric coordinate system in such a way as to remain similar to itself when the time varies.

The basic result connecting homographic solutions and central configurations can be formulated as follows (see Wintner 1941): A solution of the n-body problem with given values m_i of the masses is homographic if and only if the point masses form the same central configuration for every moment t. As also Wintner (1941) mentioned, if there exists a continuum of distinct central configurations for n given masses, it may occur that these point masses form a central configuration for every moment t in a suitable solution, which is not homographic, since the central configuration might then vary with t.

In this study we investigate the variation of the moment of inertia, if only those particular solutions of the n-body problem, in which the bodies form a central configuration at any moment of time, are considered. The solutions we study are not necessarily homographic.

2. CENTRAL CONFIGURATIONS AND HOMOGRAPHIC SOLUTIONS

The Newtonian n-body problem concerns the motion of n point-particles with masses $m_1,\ldots, m_n$ ($m_i > 0$, $i = \overline{1,n}$), in the Euclidean space R^3, subjected to the mutual Newtonian attractions.

The *configuration space* is the $3n$-dimensional manifold

$$M' = \{x = (x_1, x_2, \ldots, x_n) \in (\mathbf{R}^3)^n \mid x \notin \Delta\} = (\mathbf{R}^3)^n \setminus \Delta, \tag{1}$$

where

$$\Delta = \bigcup_{1\le i<j\le n} \Delta_{ij} = \{x \in (\mathbf{R}^3)^n \mid x_i = x_j\} \tag{2}$$

is the collision-ejection set. The *potential energy* $V \in C^\infty(M'; \mathbf{R})$ of the problem is given by

$$V(x) = -\sum_{1\le i<j\le n} \frac{m_i m_j}{\|x_i - x_j\|}, \tag{3}$$

Δ being the set of singularities of V.

The equations of the motion of the n-body problem are:

$$m_i \ddot{x}_i = -\operatorname{grad}_i V(x), \quad i = \overline{1,n}, \tag{4}$$

where grad_i is taken with respect to the usual Euclidean metric on R^3 in the i-th factor of $(\mathbf{R}^3)^n$.

In order to simplify the problem, we fix the center of mass of the system at origin. In other words, we want to consider the linear manifold

$$M = \{x \in M' \mid \sum_{i=1}^{n} m_i x_i = 0\}. \tag{5}$$

In the n-body problem, the *moment of inertia* of the system

$$I(x) = \sum_{i=1}^{n} m_i \|x_i\|^2 \tag{6}$$

and the force function $U=-V$ are connected within the Lagrange–Jacobi equation

$$\ddot{I}=2U+4h, \tag{7}$$

where $h\in\mathbf{R}$ is the *energy constant* in the n-body problem (e.g., Wintner 1947).

A configuration $x\in M$ is called *central configuration* in the n-body problem, if there is some $\lambda\in\mathbf{R}$ such that

$$\text{grad}_i U(x)=\lambda m_i x_i. \tag{8}$$

An immediate result says that the configuration $x\in M$ is a central configuration if and only if x is a critical point of the map $x\mapsto I(x)U^2(x): M\to\mathbf{R}$, that is

$$\text{d}(IU^2)(x)=0 \tag{9}$$

(e.g., Wintner 1947).

A given solution $x_i=x_i(t)$ of the problem of n bodies is called *homographic* if the configuration formed by the n bodies at a given t_0 moves in the barycentric coordinate system in such a way as to remain similar to itself when t varies. By this is meant that there exists a scalar $r=r(t)$ and an orthogonal 3-matrix $\Omega=\Omega(t)$ such that for every i and t one has $x_i(t)=r(t)\Omega(t)x_i^0$, where x_i^0 denotes x_i at some initial instant $t=t^0$.

The more important result connecting homographic motions and central configurations can be formulated as follows (Wintner 1947): A solution $x_i=x_i(t)$ of the problem of n bodies, with given values m_i of the masses, is homographic if and only if there exist two functions $r(t)$, $\phi(t)$, and n initial position vectors x_i^0 by means of which $x_1(t),\ldots,x_n(t)$ can be represented in the form

$$x_i=r\,\Omega\,x_i^0,\ \text{where}\ r=r(t),\ \Omega=\Omega(t)=\begin{pmatrix}\cos\phi & -\sin\phi & 0\\ \sin\phi & \cos\phi & 0\\ 0 & 0 & 1\end{pmatrix}, \tag{10}$$

with

$$r(t^0)=r^0=1,\quad (r=r(t)>0),\quad \phi(t^0)=\phi^0=0, \tag{11}$$

where $r=r(t), \phi=\phi(t)$ may be chosen as any solution of the Lagrangian equations

$$\begin{aligned}\ddot{r}-r\dot{\phi}^2&=-m^0/r^2,\\ r\ddot{\phi}+2\dot{r}\dot{\phi}&=0,\end{aligned} \tag{12}$$

belonging to

$$L=\tfrac{1}{2}(\dot{r}^2+r^2\dot{\phi}^2)+m^0/r, \tag{13}$$

and satisfying (11), while $(x_1^0,\ldots,x_n^0)$ is any central configuration belonging to $m_1,\ldots,m_n$, and

$$m^0=U^0/I^0,\quad I^0=\sum m_i\left|x_i^0\right|^2,\quad U^0=\sum_{j\neq k}\frac{m_j m_k}{\left|x_j^0-x_k^0\right|}. \tag{14}$$

The conservation of energy and angular momentum of the system (12) tells us that

$$\begin{aligned}&\tfrac{1}{2}(\dot{r}^2+r^2\dot{\phi}^2)-m^0/r=h^0,\\ &r^2\dot{\phi}=\left|C^0\right|,\end{aligned} \tag{15}$$

with $h^0=h/I^0$ and , where h is the total energy constant and C is the total angular momentum constant of the system. Eliminating $\dot{\phi}$ from equations (15), we have

$$\dot{r}^2=2h^0+2m^0/r-\left|C^0\right|/r^2. \tag{16}$$

Introducing the moment of inertia I, and using $I=r^2I^0$, equation (16) is equivalent to

$$\dot{I}^2=8hI+8\sqrt{I^0}U^0\sqrt{I}-4|C|^2. \tag{17}$$

3. VARIATION OF THE MOMENT OF INERTIA

Let now consider those solutions $x=x(t)$ of the equation (4) of the n-body problem, in which the configuration $x(t)$ is a central configuration at any moment t. These are not necessarily homographic solutions (see Wintner 1947, p. 298). For these solutions, condition (9) implies that IU^2 is constant, i.e.

$$IU^2=I^0(U^0)^2. \tag{18}$$

Substituting U from (18) in the Lagrange-Jacobi equation (7), one obtains

$$\ddot{I}-2\frac{U^0\sqrt{I^0}}{\sqrt{I}}=4h. \tag{19}$$

Multiplying equation (19) by IU^2 and integrating, we obtain the equivalent form

$$\dot{I}^2 = 8hI + 8\sqrt{I^0}U^0\sqrt{I} + 8cI^0, \tag{20}$$

where c is a constant.

We can observe that equation (20), describing the variation of the moment of inertia of solutions supposed to form a central configuration for any moment, is the same as equation (17), which describes the variation of the moment of inertia in homographic solutions, a subset of the solutions we have been considered here.

Introducing the new variable r, connected with I by $I = r^2 I^0$, equation (20) leads to

$$\dot{r}^2 = \frac{2hr^2 + 2U^0 r + 2c}{I^0 r^2}, \tag{21}$$

or

$$\frac{r\,\mathrm{d}r}{\sqrt{hr^2 + U^0 r + c}} = \pm\sqrt{2}\,\mathrm{d}t. \tag{22}$$

This equation can be integrated, and, according to the sign of the total energy constant, h, we have different cases:

(i) If $h < 0$ and $2I^0(U^0)^2 \le h[(\dot{I}^0)^2 - 8U^0I^0 - 8hI^0]$, then the motion is not possible.

(ii) If $h < 0$ and $2I^0(U^0)^2 > h[(\dot{I}^0)^2 - 8U^0I^0 - 8hI^0]$, then the variation of the moment of inertia is described by

$$\sqrt{hI + U^0\sqrt{I} + c} + \frac{U^0}{2\sqrt{-h}}\arccos\frac{c - 4h\sqrt{I}}{\sqrt{(U^0)^2 - 4ch}} = \pm\sqrt{2}h(t - \tau_1), \tag{23}$$

where τ_1 is the moment, when the left-hand side expression is zero. The variation of the moment of inertia is periodic (see Fig. 1). The whole system has an "elliptical"-type motion.

(iii) If $h = 0$, then

$$\sqrt{U^0\sqrt{I} + c}\,(U^0\sqrt{I} - 2c) = \pm\frac{3\sqrt{2}}{2}(U^0)^2(t - \tau_2), \tag{24}$$

where τ_2 is the moment when the left-hand side expression is zero. The variation of the moment of inertia is unbounded (see Fig. 2). The whole system has a motion of "parabolic" type.

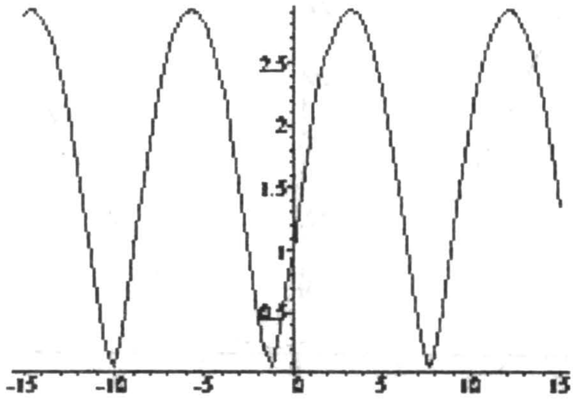

Fig. 1 – The moment of inertia for $h < 0$, ($I^0 = 1$, $\dot{I}^0 = 1$).

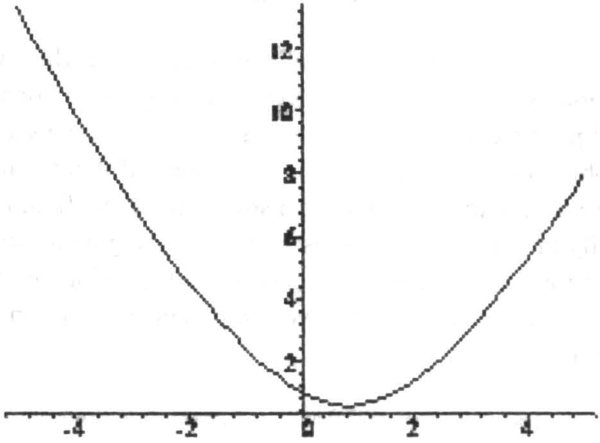

Fig. 2 – The moment of inertia for $h = 0$, ($I^0 = 1$, $\dot{I}^0 = -1$).

(iv) If $h > 0$, then

$$\sqrt{hI + U^0\sqrt{I} + c} - \frac{U^0}{2\sqrt{h}} \ln\left|\sqrt{I} + \frac{U^0}{2h} + \frac{1}{\sqrt{h}}\sqrt{hI + U^0\sqrt{I} + c}\right| = \pm 2h(t - \tau_3), \quad (25)$$

where τ_3 is the instant when the left-hand side expression is zero. The variation of the moment of inertia is unbounded (fig. 3). The system has a motion of "hyperbolic" type.

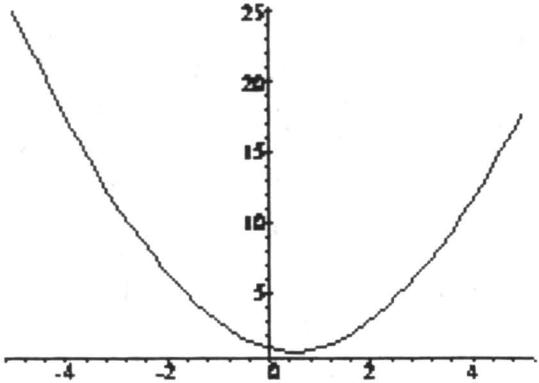

Fig. 3 – The moment of inertia for $h > 0$, ($I^0 = 1$, $\dot{I}^0 = -1$).

4. CONCLUSIONS

Our results show that in this larger family of solutions, in which we suppose only that the configuration of the n bodies form a central configuration for all time, there are only three types of possible motions, the same families of solutions as in the classical case of homographic motions. This result is immediate, if there is no continuum of families of central configurations, including distinct central configurations, because in that case our family of solutions coincides with the homographic solutions. But the inexistence of a continuum of families of central configurations is still a conjecture (Wintner 1947, p. 282). Our result could be a supplementary argument in favour of Wintner's conjecture.

Acknowledgments. The authors express thanks and gratitude to Professor Florin Diacu for his suggestions intended to improve the paper.

REFERENCES

Albouy, A.: 1995, *C. R. Acad. Sci. Paris*, **320**, 217.

Casasayas, J., Llibre, J., Nunes, A.: 1994, *Celest. Mech. Dyn. Astron.*, **60**, 273.

Dziobek, O.: 1900, *Astron. Nachr.*, **152**, 33.

Euler, L.: 1767, *Novi Comm. Acad. Sci. Imp. Petropolis*, **11**, 144.

Lagrange, J. L.: 1873, *Essai sur le problème des trois corps*, *Œuvres*, Vol. **6**, Gauthier-Villars, Paris, 272.

Laplace P. S.: 1789, *Euvres 11*, 553; **4**, 307.

Llibre, J.: *Celest. Mech.*, **50**, 89.

McCord, C. K., Meyer, K. R., Wang, Q.: 1998, *Mem. Amer. Math. Soc.*, **132**, 628.

Meyer K. R., Schmidt D. S.: 1993, *Celest. Mech.*, **55**, 289.

Moeckel, R.: 1990, *Math. Z.*, **205**, 499.
Moeckel, R., Simó, C.: 1995, *SIAM J. Math. Anal.*, **26**, 978.
Moulton, F. R.: 1910, *Ann. Math.*, **12**, 1.
Smale, S.: 1970a, *Invent. Math.*, **10**, 305.
Smale, S.: 1970b, *Invent. Math.*, **11**, 45.
Wintner, A.: 1947, *The Analytical Foundations of Celestial Mechanics*, Princeton University Press, Princeton, NJ.

Received on 11 August 2005

SEELIGER'S TWO-BODY PROBLEM: COLLISION, ESCAPE, SYMMETRIES

VASILE MIOC[1], MIRCEA RUSU[2]

[1] *Astronomical Institute of the Romanian Academy*
Str. Cuţitul de Argint 5, 040557 Bucharest, Romania
E-mail: vmioc@aira.astro.ro

[2] *University of Bucharest, Faculty of Physics*
Str. Atomiştilor 1, CP MG-11, Bucharest-Măgurele, Romania
E-mail: mrusu@dnt.ro

Abstract. We offer a first insight into the two-body problem associated to the potential proposed by Hugo Seeliger at the end of 1800s. Our goal is twofold: to describe two limit situations (collision and escape), and to emphasize the symmetries of the problem. First, we resort to McGehee transformations to blow up the collision singularity and the (artificial) escape singularity, and to replace them by manifolds pasted on the phase space. Then we describe the flows on these manifolds, which are useful to understand the behaviour of nearby orbits. An important issue is that collision solutions are regularizable, whereas escape solutions are not regularizable. Finally, we point out the symmetries that characterize the vector field in various coordinates. These symmetries form isomorphic Abelian groups endowed with an idempotent structure, owing proper subgroups isomorphic to Klein's group.

Key words: celestial mechanics – two-body problem – Seeliger's theory of gravitation – collision – escape – symmetries.

1. INTRODUCTION

At the end of the 19th century, the German astronomer Hugo von Seeliger formulated a "philosophical astonishment" concerning the stability of the whole Universe: "Why are we not crashed under the infinite pressure yielded by the infinite number of stars of the Universe, as predicted by the Newtonian Mechanics?" (Ionescu-Pallas 2003). Such an "astonishment" comes from the fact that, for a uniform distribution of masses, Laplace-Poisson's equation has no finite solution for a nonempty Universe (see the so-called Newtonian cosmology).

In the realm of classical mechanics, the only possibility to overcome this difficulty is to generalize Laplace-Poisson's equation by adding a term analogous to the

Rom. Astron. J., Vol. 16, No. 2, p. 177–191, Bucharest, 2006

cosmological constant from relativity. This ensures the existence of a static Newtonian solution. (Of course, the simplest such generalization is the linear one).

Following this way, Seeliger (1895, 1896) proposed a new theory of gravitation that obviously entailed a revision of the classical (Newtonian) mechanics. The Special Relativity Theory (Einstein 1905) and the General Relativity Theory (Einstein 1916) applied to celestial mechanics made Seeliger's model (also called Seeliger-Neumann's theory) fall into oblivion. Nevertheless, connections between Seeliger's and Einstein's theories, especially as regards fundamental constants, have been emphasized (Pauli 1921; Hubble 1936; Jones et al. 1956; Tifft 1995; Ionescu-Pallas 2003).

We shall not go deeper into the gravitational implications of Seeliger's model, directing the reader to the extensive and detailed discussion done by Ionescu-Pallas (2003). All we want to retain is the gravitational potential characteristic to this theory:

$$U(\mathbf{r}) = (A/r)\exp(-Kr), \tag{1}$$

where $r = |\mathbf{r}|$ is the distance between two pointlike masses m_1 and m_2, $A = Gm_1m_2 > 0$ (G = Newtonian constant of gravitation), while K is a positive constant of order 10^{-28} cm^{-1} (see Ionescu-Pallas 2003 and the references therein).

As a brief digression, we have to mention that a field featured by a (1)-like potential has much larger physical implications than in celestial mechanics (via gravitation). London's theory of superconductivity involves an electromagnetic potential of this form. Debye-Hückel's theory of screening in electrolytes leads to a similar screened potential. As regards nuclear physics, the potential of a mesonic field also joins this model (see Pauli and Weisskopf 1934).

In this paper we intend to perform a first insight into the two-body problem associated to the Seeliger-type model. We use the term "type" because we let A run along the whole real line. More general models (which include repulsive forces, as, e.g., the radiative ones) can also be studied in this way. In Section 2 we establish the equations of motion and the first integrals of energy and angular momentum in configuration-momentum coordinates.

Section 3 tackles the collision dynamics. The potential, the motion equations, and the energy integral, all present an isolated singularity at the origin, which corresponds to a collision. Applying a sequence of McGehee-type transformations, we regularize all these equations. In this way, the collision singularity is replaced by a manifold M_0 pasted on the phase space. This collision manifold is homeomorphic to a 2D torus. We describe the flow on M_0 (a flow deprived of physical significance, but – due to the continuity of solutions with respect to initial data – a good provider of information about orbits that neighbour collision). The flow on M_0 is fairly simple: two circles of degenerate equilibria (UC = upper circle, LC = lower circle) and heteroclinic orbits that move from LC to UC.

In Section 4 we approach the escape dynamics. We bring infinity at the origin, making it turn to a singularity, then we desingularize the equations that characterize this situation. Exactly as in the previous limit case, we define the manifold M_{∞} (that replaces the artificial singularity) and describe the flow on it. The flow on M_{∞} has the same look (except the slope of the homoclinic orbits) as that on M_0.

Here we have to remark that we use, by abuse, the term *collision* for both collision ($r \to 0$ in the future) and ejection ($r \to 0$ in the past). It is the same for *escape*, which means both escape ($r \to \infty$ in the future) and capture ($r \to \infty$ in the past).

Section 5 tackles a quite different aspect of the problem: symmetries. The vector fields corresponding to various coordinates present symmetries that form eight-element Abelian groups endowed with an idempotent structure. All these groups are isomorphic, and this is not trivial, given the structure of the corresponding phase spaces. Every such a group has seven four-element proper subgroups isomorphic to Klein's group.

Section 6 surveys the main results of the paper concerning the characteristics of collision dynamics, escape dynamics, and symmetries of the motion equations.

Our endeavours provide only a first insight into this problem. However, on the one hand, we prove once again how strong and useful the qualitative tools of the theory of dynamical systems are. On the other hand, our present results join the investigations of dynamics in post-Newtonian fields, contributing to a better understanding of such models.

2. BASIC EQUATIONS

Seeliger's potential is central, therefore the associated two-body problem can be reduced to a central-force problem. The motion is confined to a plane, and is described by the equations

$$\begin{aligned} \dot{\mathbf{q}} &= \frac{\partial H(\mathbf{q},\mathbf{p})}{\partial \mathbf{p}}, \\ \dot{\mathbf{p}} &= -\frac{\partial H(\mathbf{q},\mathbf{p})}{\partial \mathbf{q}}, \end{aligned} \tag{2}$$

with the Hamiltonian

$$H(\mathbf{q},\mathbf{p}) = \frac{|\mathbf{p}|^2}{2} - \frac{A}{|\mathbf{q}|\exp(K|\mathbf{q}|)}. \tag{3}$$

Here $\mathbf{q} = (q_1, q_2) \in \mathbf{R}^2 \setminus \{0,0\}$ and $\mathbf{p}(=\dot{\mathbf{q}}) = (p_1, p_2) \in \mathbf{R}^2$ are the position (configuration) vector and the momentum vector of a unit-mass particle with respect to the field source (centre), respectively.

The Hamiltonian (3) provides the first integral of energy

$$H(\mathbf{q},\mathbf{p}) = T(\mathbf{p}) - U(\mathbf{q}) = h, \tag{4}$$

where h stands for the energy constant, and $T(\mathbf{p}) = |\mathbf{p}|^2 / 2$ is the kinetic energy of the particle.

Besides the energy integral, the motion equations also admit the first integral of angular momentum

$$L(\mathbf{q},\mathbf{p}) = q_1 p_2 - q_2 p_1 = C, \tag{5}$$

in which C denotes the angular momentum constant.

Explicitly, the equations of motion read

$$\begin{aligned} &\dot{\mathbf{q}} = \mathbf{p}, \\ &\dot{\mathbf{p}} = -A\exp(-K|\mathbf{q}|)(K/|\mathbf{q}|^2 + 1/|\mathbf{q}|^3)\mathbf{q}. \end{aligned} \tag{6}$$

They will constitute the basis for our next endeavours.

3. COLLISION DYNAMICS

The potential (1), the motion equations (6) and the energy integral (4) have an isolated singularity at the origin $\mathbf{q} = (0,0)$. It is easy to prove, via a Painlevé-type criterion (e.g., Mioc and Stavinschi 2000b, 2001, 2002), that this singularity corresponds to a collision particle-centre. To remove it and to regularize eqs. (6), we resort to the powerful tool of McGehee-type transformations of the second kind (McGehee 1974). In our case they are:

$$\begin{aligned} &r = |\mathbf{q}|, \\ &\theta = \arctan(q_2 / q_1), \\ &u = \dot{r} = (q_1 p_1 + q_2 p_2)/|\mathbf{q}|, \\ &v = r\dot{\theta} = (q_1 p_2 - q_2 p_1)/|\mathbf{q}|, \end{aligned} \tag{7}$$

which introduce standard polar coordinates and polar components of the velocity;

$$x = r^{1/2}u,$$
$$y = r^{1/2}v, \tag{8}$$

which scale down the velocity components;

$$ds = r^{-3/2}dt, \tag{9}$$

which rescales the time.

Under these transformations, which all are real analytic diffeomorphisms, the equations of motion (6) become

$$\begin{aligned} r' &= rx, \\ \theta' &= y, \\ x' &= x^2/2 + y^2 - A\exp(-Kr)(Kr+1), \\ y' &= -xy/2, \end{aligned} \tag{10}$$

where $(\cdot)' = d(\cdot)/ds$ and we kept, by abuse, the same notation for the new functions of the timelike variable s.

Using (3)–(5), (7) and (8), a straightforward computation leads to the new expressions of the integrals of energy and angular momentum, respectively:

$$x^2 + y^2 - 2A\exp(-Kr) = 2hr; \tag{11}$$

$$r^{1/2}y = C. \tag{12}$$

Remark that, by virtue of (11), eqs. (10) can also be written in the form

$$\begin{aligned} r' &= rx, \\ \theta' &= y, \\ x' &= y^2/2 + hr - AKr\exp(-Kr), \\ y' &= -xy/2. \end{aligned} \tag{13}$$

At this moment, both motion equations and first integrals are well defined for the boundary $r = 0$. This means that the phase space of the McGehee-type coordinates can be extended analytically to contain the manifold $M_{\text{col}} = \{(r,\theta,x,y) \mid r = 0\}$, which is invariant to the flow because, by (10) or (13), $r' = 0$ for $r = 0$. The integrals (11) and (12) also extend smoothly to this boundary.

Let us consider h to be a parameter, and define the constant-energy manifold $E_h = \{(r,\theta,x,y) \mid (11) \text{ holds}\}$. The intersection

$$M_0 = M_{col} \cap E_h = \{(r, \theta, x, y) \mid r = 0, \theta \in S^1, x^2 + y^2 = 2A\} \tag{14}$$

will be called the *collision manifold*.

In this way, we have blown the collision singularity up, and we replaced it by the manifold M_0 pasted on the phase space. Although the flow on M_0 seemingly has no physical significance, the continuity of solutions with respect to initial data allows us to understand the near-collisional orbits.

By (14), for $A > 0$, M_0 is homeomorphic to a 2D cylinder in the 3D space of the coordinates $(\theta, x, y) \in S^1 \times \mathbf{R}^2$. But, since S^1 is the segment $[0, 2\pi]$ with the end points pasted together, the M_0 cylinder may also be considered homeomorphic to a 2D torus, both actually imbedded in the 4D full phase space of the coordinates (r, θ, x, y).

For $A = 0$, the torus M_0 restricts to a circle. For $A < 0$, M_0 is the empty set (a result that matches those of Saari 1974, or Mioc and Stavinschi 2001, 2002).

To depict the flow on M_0 (for $A > 0$), we put $r = 0$ in eqs. (13). The corresponding vector field will be

$$\begin{aligned} \theta' &= y, \\ x' &= y^2/2, \\ y' &= -xy/2. \end{aligned} \tag{15}$$

By (15), we see that the flow on the M_0 torus is fairly simple. There are two circles of degenerate equilibria: the upper circle $\mathrm{UC} = \{(\theta_0, x, y) \mid x = \sqrt{2A}, y = 0\}$ and the lower circle $\mathrm{LC} = \{(\theta_0, x, y) \mid x = -\sqrt{2A}, y = 0\}$, with arbitrary $\theta_0 \in S^1$. By the second equation (15), it is obvious that the flow on M_0 is gradientlike with respect to the x-coordinate. This means that all other orbits on M_0 are heteroclinic and move from LC to UC. The slope of these trajectories can be deduced by putting $x = \sqrt{2A}\sin\alpha$, $y = -\sqrt{2A}\cos\alpha$. This leads to $\mathrm{d}\alpha/\mathrm{d}\theta = -1/2$, hence every heteroclinic curve runs a θ-interval of length 2π from LC to UC. Fig. 1 illustrates the flow on M_0.

By (12), we observe easily that collisions occur for $C = 0$ (rectilinear, radial motion). By (13), we observe that collisions correspond to the halfplane $(x < 0, y = 0)$, whereas ejections correspond to the halfplane $(x > 0, y = 0)$. This means that the collisions solutions are regularizable.

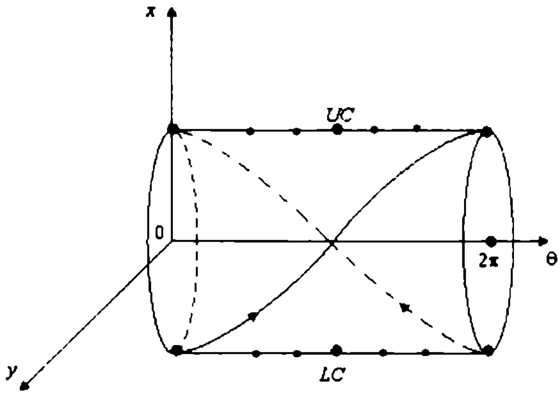

Fig. 1 – The collision manifold as a cylinder and the flow on it.

Another important issue: M_0 does not depend on h. This entails the fact that every energy levels shares this boundary manifold.

Lastly, having in view the transformation (9), it is easy to see that the particle needs an infinite amount of fictitious time s to reach the collision manifold. In other words, M_0 is a manifold of equilibria for the global flow in the McGehee-type coordinates (r, θ, x, y).

4. ESCAPE DYNAMICS

Another limit situation for the motion is escape. We shall treat it in the same way as we treated the collision. To this end, we use a new sequence of McGehee-type transformations, starting from eqs. (11)–(13). The first step is

$$\rho = r^{-1}. \tag{16}$$

This McGehee-type transformation of the first kind (McGehee 1973) brings the infinity at origin making it turn to the singularity $\rho = 0$. The next two steps are standard (cf. Section 3):

$$\begin{aligned} \xi &= \rho^{1/2} x, \\ \eta &= \rho^{1/2} y, \end{aligned} \tag{17}$$

which scale down the velocity components;

$$\mathrm{d}\tau = \rho^{-1/2} \mathrm{d}s, \tag{18}$$

Under these transformations, which all are real analytic diffeomorphisms, the equations of motion (13) become

$$\begin{aligned}
\frac{d\rho}{d\tau} &= -\rho\xi, \\
\frac{d\theta}{d\tau} &= \eta, \\
\frac{d\xi}{d\tau} &= -\xi^2/2 + \eta^2/2 + h - AK\exp(-K/\rho), \\
\frac{d\eta}{d\tau} &= -\xi\eta,
\end{aligned} \tag{19}$$

whereas the first integrals (11) and (12) respectively read

$$\xi^2 + \eta^2 = 2A\rho \exp\left(\frac{-K}{\rho}\right) + 2h; \tag{20}$$

$$\eta = C\rho. \tag{21}$$

In (19), we kept, by abuse, the same notation for the new functions of the timelike variable τ.

Observe that, by virtue of (20), eqs. (19) can also be written in the form

$$\begin{aligned}
\frac{d\rho}{d\tau} &= -\rho\xi, \\
\frac{d\theta}{d\tau} &= \eta, \\
\frac{d\xi}{d\tau} &= \eta^2 - A(K+\rho)\exp(-K/\rho), \\
\frac{d\eta}{d\tau} &= -\xi\eta.
\end{aligned} \tag{22}$$

Now, both motion equations and first integrals are well defined for the boundary $\rho = 0$. So, the phase space of the McGehee-type coordinates $(\rho, \theta, \xi, \eta)$ can be extended analytically to contain the manifold $M_{esc} = \{(\rho, \theta, \xi, \eta) \mid \rho = 0\}$, which is invariant to the flow because, by the first equation (19) or (22), $d\rho/d\tau = 0$ for $\rho = 0$. The integrals (20) and (21) also extend smoothly to this boundary.

As in Section 3, we consider h to be a parameter, and define the constant-energy manifold $\widetilde{E}_h = \{(\rho, \theta, \xi, \eta) \mid (20) \text{ holds}\}$. The intersection

$$M_\infty = M_{\text{esc}} \cap \widetilde{E}_h = \{(\rho,\theta,\xi,\eta) \mid \rho = 0, \theta \in S^1, \xi^2 + \eta^2 = 2h\} \qquad (23)$$

will be called the *infinity manifold.*

In this way, we have blown the escape singularity (created via (16)) up, and we replaced it by the manifold M_∞ pasted on the phase space. The flow on M_∞ has no more physical significance than that on M_0, but – due to the same continuity of solutions with respect to initial conditions – it provides valuable information about near-escape orbits.

By (23), for $h > 0$, M_∞ is homeomorphic to a 2D cylinder in the 3D space of the coordinates $(\theta,\xi,\eta) \in S^1 \times \mathbf{R}^2$. This cylinder may also be considered homeomorphic to a 2D torus (see Section 3), both actually imbedded in the 4D full phase space of the coordinates (ρ,θ,ξ,η).

For $h = 0$, the torus M_∞ restricts to a circle. For $h < 0$, M_∞ is the empty set (in other words, for negative energy levels, the particle cannot escape).

To describe the flow on M_∞ (for $h > 0$), we put $\rho = 0$ in eqs. (22). The corresponding vector field will be

$$\begin{aligned} \frac{d\theta}{d\tau} &= \eta, \\ \frac{d\xi}{d\tau} &= \eta^2, \\ \frac{d\eta}{d\tau} &= -\xi\eta. \end{aligned} \qquad (24)$$

As in the case of M_0, the flow on M_∞ is fairly simple, too. There are two circles of degenerate equilibria: the upper circle $\mathrm{UC} = \{(\theta_0,\xi,\eta) \mid \xi = \sqrt{2h}, \eta = 0\}$ and the lower circle $\mathrm{LC} = \{(\theta_0,\xi,\eta) \mid \xi = -\sqrt{2h}, \eta = 0\}$, with arbitrary $\theta_0 \in S^1$. By the second equation (24), it is obvious that the flow on M_∞ is gradientlike with respect to the ξ-coordinate. This means that all other orbits on M_∞ are heteroclinic and move from LC to UC. The slope of these trajectories can be deduced by putting $\xi = \sqrt{2h}\sin\alpha$, $\eta = -\sqrt{2h}\cos\alpha$. This leads to $d\alpha / d\theta = -1$, hence every heteroclinic curve runs a θ-interval of length π from LC to UC. Fig. 2 illustrates the flow on M_∞.

By (21), we observe that escapes occur for both zero and nonzero values of C (radial and spiral motion, respectively). By (22), we observe that escapes correspond to the halfplane $(\xi > 0, \eta = 0)$, whereas captures correspond to the halfplane $(\xi < 0, \eta = 0)$. This means that escape solutions are not regularizable.

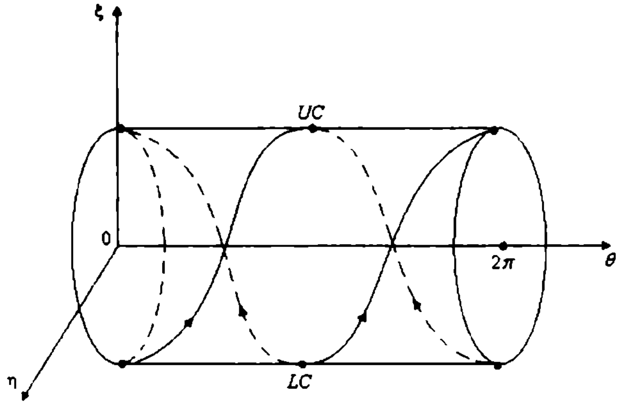

Fig. 2 – The infinity manifold as a cylinder and the flow on it.

Lastly, having in view the transformation (18), it is easy to see that the particle needs an infinite amount of fictitious time τ to reach the infinity manifold. In other words, M_∞ is a manifold of equilibria for the global flow in the McGehee-type coordinates $(\rho, \theta, \xi, \eta)$. By (20), an escape solution with $h > 0$ has positive asymptotic velocity at infinity, while an escape solution with $h = 0$ has zero asymptotic velocity at infinity.

5. SYMMETRIES

As we have done in many other cases, for various fields (see, e.g., Mioc 2002a, b, 2003; Mioc et al. 2003a, b), we shall examine the symmetries pointed out by the vector field written in different coordinates.

Let us start with the vector field (6) corresponding to Cartesian coordinates. Explicitly, it reads

$$
\begin{aligned}
\dot{q}_1 &= p_1, \\
\dot{q}_2 &= p_2, \\
\dot{p}_1 &= -A\exp(-K\sqrt{q_1^2+q_2^2})[K/(q_1^2+q_2^2)+1/(q_1^2+q_2^2)^{3/2}]q_1, \\
\dot{p}_2 &= -A\exp(-K\sqrt{q_1^2+q_2^2})[K/(q_1^2+q_2^2)+1/(q_1^2+q_2^2)^{3/2}]q_2.
\end{aligned}
\tag{25}
$$

Eqs. (25) benefit of eight symmetries $S_i = S_i(q_1, q_2, p_1, p_2, t)$, $i = \overline{0,7}$, as follows:

$$\begin{aligned}
S_0 &= (q_1, q_2, p_1, p_2, t) = I \quad \text{(identity)},\\
S_1 &= (q_1, q_2, -p_1, -p_2, -t),\\
S_2 &= (q_1, -q_2, p_1, -p_2, t),\\
S_3 &= (q_1, -q_2, p_1, -p_2, t),\\
S_4 &= (q_1, -q_2, -p_1, p_2, -t),\\
S_5 &= (-q_1, q_2, p_1, -p_2, -t),\\
S_6 &= (-q_1, -q_2, -p_1, -p_2, t),\\
S_7 &= (-q_1, -q_2, p_1, p_2, -t).
\end{aligned} \tag{26}$$

Indeed, one sees immediately that eqs. (25) are invariant to the transformations described by (26). Moreover, out of the symmetries S_i, $i = \overline{1,7}$, only three are independent. Let these ones be S_1, S_2, S_3. One observes that

$$\begin{aligned}
S_4 &= S_1 \circ S_2,\\
S_5 &= S_1 \circ S_3,\\
S_6 &= S_2 \circ S_3,\\
S_7 &= S_1 \circ S_2 \circ S_3.
\end{aligned} \tag{27}$$

Choosing arbitrarily three symmetries in $\{S_i \mid i = \overline{1,7}\}$ that are mutually independent, a structure similar to (27) is recovered.

As in other cases, the set $G = \{S_i \mid i = \overline{0,7}\}$, endowed with the composition law "$\circ$", forms a symmetric Abelian group with an idempotent structure. To prove this, it is sufficient to construct the composition table

$\circ$	S_0	S_1	S_2	S_3	S_4	S_5	S_6	S_7
S_0	S_0	S_1	S_2	S_3	S_4	S_5	S_6	S_7
S_1	S_1	S_0	S_4	S_5	S_2	S_3	S_7	S_6
S_2	S_2	S_4	S_0	S_6	S_1	S_7	S_3	S_5
S_3	S_3	S_5	S_6	S_0	S_7	S_1	S_2	S_4
S_4	S_4	S_2	S_1	S_7	S_0	S_6	S_5	S_3
S_5	S_5	S_3	S_7	S_1	S_6	S_0	S_4	S_2
S_6	S_6	S_7	S_3	S_2	S_5	S_4	S_0	S_1
S_7	S_7	S_6	S_5	S_4	S_3	S_2	S_1	S_0

The Abelian character is obvious. In addition, every element is its own inverse, which proves the idempotent structure.

Given these results, G is an Abelian group of order 8 with three generators of order 2. According to the Fundamental Theorem of Abelian Groups, it is isomorphic to $\mathbf{Z}_2 \oplus \mathbf{Z}_2 \oplus \mathbf{Z}_2$.

Let us now pass to polar coordinates via the transformations (7). The corresponding vector field reads

$$\begin{aligned} \dot{r} &= u, \\ \dot{\theta} &= \frac{v}{r}, \\ \dot{u} &= \frac{v^2}{2} - A\exp(-Kr)\left(\frac{K}{r} + \frac{1}{r^2}\right), \\ \dot{v} &= -\frac{uv}{r}. \end{aligned} \tag{28}$$

The results obtained for Cartesian coordinates can be transposed within this new framework under the issues below.

The vector field (28) has eight symmetries $\widetilde{S}_i = \widetilde{S}_i(r,\theta,u,v,t)$, $i = \overline{0,7}$, as follows:

$$\begin{aligned} \widetilde{S}_0 &= (r,\theta,u,v,t) = I, \\ \widetilde{S}_1 &= (r,\theta,-u,-v,-t), \\ \widetilde{S}_2 &= (r,-\theta,u,-v,t), \\ \widetilde{S}_3 &= (r,\pi-\theta,u,-v,t), \\ \widetilde{S}_4 &= (r,-\theta,-u,v,-t), \\ \widetilde{S}_5 &= (r,\pi-\theta,-u,v,-t), \\ \widetilde{S}_6 &= (r,\pi+\theta,u,v,t), \\ \widetilde{S}_7 &= (r,\pi+\theta,-u,-v,-t). \end{aligned} \tag{29}$$

The invariance of (28) to (29) can be easily checked.

Imitating the proofs given above for Cartesian coordinates, we obtain immediately that the set $\widetilde{G} = \{\widetilde{S}_i \mid i = \overline{0,7}\}$ is isomorphic to $\mathbf{Z}_2 \oplus \mathbf{Z}_2 \oplus \mathbf{Z}_2$. Moreover, given the phase spaces corresponding to G and $\widetilde{G}$, these two groups are diffeomorphic.

As to collision-blow-up coordinates (r,θ,x,y,s), the vector field generates the symmetries obtained by formally writing $\hat{S}_i(r,\theta,x,y,s)=\tilde{S}_i(r,\theta,u,v,t)$, $i=\overline{0,7}$. Following the above arguments, the symmetries $\hat{S}_i$ also form a group G_0 isomorphic to $\mathbf{Z}_2\oplus\mathbf{Z}_2\oplus\mathbf{Z}_2$, with the same properties as $\tilde{G}$.

As to infinity-blow-up coordinates $(\rho,\theta,\xi,\eta,\tau)$, the vector field (19) has similar symmetries obtained by formally writing $S_i'(\rho,\theta,\xi,\eta,\tau)=\hat{S}_i(r,\theta,x,y,s)$, $i=\overline{0,7}$. One immediately obtains the group G_∞', endowed with the same properties as G_0.

Observe that we could regularize the motion equations for $r\to\infty$ starting from the vector field (28). The equations obtained in this way also present eight symmetries, S_i'' ($i=\overline{0,7}$) say, which form a group G_∞'' which exactly the same properties as G_∞'. Given the phase spaces corresponding to G_∞' and G_∞'', these two groups are diffeomorphic.

To end, we show another interesting property of the symmetries exhibited by our vector fields expressed in different coordinates. Consider the group G. Perusing its composition table, we see that G has seven four-element proper subgroups:

$$G_{ijk}=\{S_0\}\cup\{S_i\in G\mid S_i\circ S_j=S_k,\ S_i\circ S_k=S_j,\ S_j\circ S_k=S_j\}, \tag{30}$$

with $(i,j,k)\in\{(1,2,4),(1,3,5),(1,6,7),(2,3,6),(2,5,7),(3,4,7),(4,5,6)\}$ (examine (27), too). As one can immediately check, these subgroups also are Abelian and endowed with an idempotent structure. They all of order 4 with two generators of order 2, hence they are isomorphic to $\mathbf{Z}_2\oplus\mathbf{Z}_2$ (or to Klein's group).

As regards the groups of symmetries $\tilde{G}$, G_0, G_∞', G_∞'', one can easily verify that each of them has seven four-element proper subgroups, with the same indices and with the same properties as G_{ijk}.

6. CONCLUSIONS

Surveying the results obtained in this paper, we can formulate some conclusions:

6.1. At collision/ejection and escape/capture, the two-body problem associated to Seeliger's potential behaves like the classical Kepler problem. There also are similarities with problems associated to different potentials. For instance, M_0 has exactly the same structure as in the case of the point-mass approximation (gravito-elastic) field (Mioc and Stavinschi 1999). As regards M_∞, its structure is the same as in the case of the fields of Schwarzschild (Stoica and Mioc 1997a), Manev (Stoica and Mioc 1997b), Fock (Mioc and Stavinschi 2000a), in the zonal-satellite problem (Mioc and Stavinschi 1998), or in the much more general situation of quasihomogeneous fields (Mioc and Stavinschi 2000c).

6.2. The collision manifold does not depend on the energy constant h, so every energy level shares this manifold. But it depends on the field parameter A, such that collisions are possible only for nonnegative values of A. The infinity manifold essentially depends on h; escape is possible only for nonnegative energy levels.

6.3. By (9) and (18), it is clear that the flows on M_0 and M_∞ have different time scales: $ds = r^{-1/2}d\tau = r^{-3/2}dt$. Moreover, these time scales differ from the "physical time" used in classical celestial mechanics.

6.4. Both M_0 and M_∞ constitute manifolds of equilibria for the global flow in full phase space (of course, each one on its own time scale).

6.5. Collisions occur only for zero angular momentum (radial motion), whereas escape is also possible for nonzero angular momentum (spiral motion).

6.6. Collision/ejection orbits tend to LC/UC of M_0; escape/capture orbits tend to UC/LC of M_∞. Taking into account Figs. 1 and 2, this means that collision solutions are regularizable, while escape solutions are nonregularizable.

6.7. The motion equations of our problem, expressed in Cartesian or polar coordinates, or in (collision-blow-up or infinity-blow-up) McGehee-type coordinates, present symmetries that form eight-element Abelian groups endowed with an idempotent structure. All these groups are isomorphic. This is not a trivial result, because the phase space corresponding to G_0 contains the supplementary boundary manifold M_0, whereas the one corresponding to G'_∞ (G''_∞) contains the supplementary boundary manifold M_∞. Every such an eight-element group of symmetries has seven four-element proper subgroups isomorphic to Klein's group.

All these results constitute only a first part of a long-term study intended to understand the dynamics corresponding to Seeliger's model. They also join many previous issues in post-Newtonian celestial mechanics.

REFERENCES

Einstein, A: 1905, *Ann. Physik*, **17**, 891.

Einstein, A.: 1916, *Ann. Physik*, **49**, 769.

Hubble, E.: 1936, *The Realm of Nebulae*, Yale University Press, New Haven.

Ionescu-Pallas, N.: 2003, *Rom. Rep. Phys.*, **55**, 7.

Jones, G. O., Rotblatt, J., Whithrow, G. J.: 1956, *Atoms and the Universe*, Eyre and Spottiswoode, London.

McGehee, R.: 1973, *J. Diff. Eq.*, **14**, 70.

McGehee, R.: 1974, *Invent. Math.*, **27**, 191.

Mioc, V.: 2002a, *Phys. Lett A*, **301**, 429.
Mioc, V.: 2002b, *Spacetime Subst.*, **3**, 104.
Mioc, V.: 2002c, *Rom. Astron. J.*, **12**, 193.
Mioc, V.: 2003, *Astron. Nachr.*, **324**, 271.
Mioc, V., Stavinschi, M.: 1998, *Serb. Astron. J.*, **158**, 37.
Mioc, V., Stavinschi, M.: 1999, *Rom. Astron. J.*, **9**, 21.
Mioc, V., Stavinschi, M.: 2000a, *Rom. Astron. J.*, **10**, 71.
Mioc, V., Stavinschi, M.: 2000b, *Rom. Astron. J.*, **10**, 95.
Mioc, V., Stavinschi, M.: 2000c, *Rom. Astron. J.*, **10**, 151.
Mioc, V., Stavinschi, M.: 2001, *Phys. Lett A*, **279**, 223.
Mioc, V., Stavinschi, M.: 2002, *Phys. Scripta*, **65**, 193.
Mioc, V., Pérez-Chavela, E., Stavinschi, M.: 2003a, *Celest. Mech. Dyn. Astron.*, **86**, 81.
Mioc, V., Rusu, M. V., Stavinschi, M.: 2003b, *Rom. Astron. J.*, **13**, 67.
Pauli, W.: 1921, *Relativitätstheorie*, Handbuch Math. Wiss., Leipzig, Berlin.
Pauli, W., Weisskopf, V.: 1934, *Helvetica Phys. Acta*, **7**, 809.
Saari, D. G.: 1974, *Celest. Mech.*, **9**, 55.
Seeliger, H.: 1895, *Astron. Nachr.*, **137**, 129.
Seeliger, H.: 1896, *Münch. Akad. Ber.*, **26** 373.
Stoica, C., Mioc, V.: 1997a, *Astrophys. Space Sci.*, **249**, 161.
Stoica, C., Mioc, V.: 1997b, *Rom. Astron. J.*, **7**, 183.
Tifft, W.: 1995, *Astrophys. Space Sci.*, **227**, 25.

Received on 13 December 2005

ASSOCIATED LEGENDRE FUNCTIONS: SYMBOLIC COMPUTATION

MOHAMED ADEL SHARAF [1], HADIA HASSAN SELIM [2], ESSAM AHMED ELKHOLY [2]

[1] *Department of Astronomy, Faculty of Science, King Abdul Aziz University*
Jeddah, Saudi Arabia
E-mail: sharaf_adel@hotmail.com

[2] *Department of Astronomy, National Research Institute of Astronomy and Geophysics*
Cairo, Egypt
E-mail: hadia@nriag.sci.eg, es_ah_el@yahoo.com

Abstract. In this paper we provide symbolic expressions for the associated Legendre functions $P_{l,m}(\sin\varphi)$ for any l and m, and for any φ belonging to the interval $(-90^\circ, 90^\circ)$. Numerical evolutions that use these expressions prove their extreme efficiency.

Key words: potential theory – Earth's gravity – symbolic algebra.

1. INTRODUCTION

The study of the computation of artificial satellite orbits has wide application in mission planning, satellite geodesy, spacecraft navigation, etc. Via very accurate satellite tracking systems, the precision in the orbit computation has become necessary. Three mathematical solution techniques, analytical, semi analytical and numerical, are used for generating the ephemeris of a satellite. The numerical integration methods provide the most accurate ephemeris of a satellite with respect to any type of perturbing forces.

By utilizing the recursive formulas of Legendre polynomials, we are able to include any number of zonal harmonics of the geopotential (J_n) in the package, and also to economize the computations (Sharma et al. 1998).

Sharaf et al. (1989) proposed economical recursive formulae for the Earth's gravitational potential and its partial derivatives with respect to the Cartesian coordinates. They presented the necessary computational time for any number and any type of harmonic coefficients.

Fourier coefficients are expressed in terms of the associated Legendre functions (Garfinkel 1964). The interest in the artificial satellite problem (ASP) has been renewed thanks to space programs like NEAR and ROSETTA, which consider orbiting (and even landing on) an asteroid and a comet, respectively. As a result, much effort has been devoted to the computation of periodic and frozen orbits about different types of bodies: from models of small asteroids (massive straight segment, triaxial ellipsoids (Scheeres 1994)) to real asteroids (the famous Earth-cruiser 4179 Toutatis, or 4769 Castalia (Scheeres 1996; Scheeres et al. 1998)), or to "Earth-like planets" (Coffey et al. 1994; Lara 1997). In all these reference papers the approach relied heavily on numerical computations. Only Langbort (2002) took an opposite direction and tried to be as analytical as possible, using tools from the theory of dynamical systems. He considered the main ASP, where the first and second dominant terms of the gravitational potential of the body constitute the hope that a correct qualitative understanding of the general properties of periodic orbits can be gained in this way. His main problem was the potential function of an axially symmetric celestial body, written in terms of Legendre polynomials.

In this paper, considering the importance of Legendre's polynomials and associated functions in the ASP through the model of the Earth's gravitational field, we provide symbolic expressions for the associated Legendre functions $P_{l,m}(\sin\varphi)$ for any l, m and any $\varphi\in(-90°, 90°)$. Recent numerical evaluations that used these expressions proved their extreme efficiency.

2. SYMBOLIC TRIGONOMETRIC REPRESENTATION OF $P_{l,m}(\sin\varphi)$

In what follows the trigonometric series representation of $P_{l,m}(\sin\varphi)$ will be obtained. It is defined as (Kaula 1966):

$$P_{l,m}(\sin\varphi) = (-1)^m \cos^m\varphi \sum_{l=0}^{k} T_{l,m,t} \sin^{l-m-2t}\varphi\,, \tag{1}$$

where

$$T_{l,m,t} = \frac{(-1)^t (2l-2t)!}{2^l t!(l-t)!(l-m-2t)!}, \quad k = \left[\frac{l-m}{2}\right]. \tag{2}$$

Note that for the zeroth order ($m = 0$) the associated Legendre functions are simply called Legendre polynomials.

Since

$$\sin^p\theta\cos^q\theta = \frac{(-J)^p}{2^{p+q}}(\Phi-\Phi^{-1})^p(\Phi+\Phi^{-1})^q\,, \tag{3}$$

where $J=\sqrt{-1}$; $\Phi=\exp(J\theta)$, using the binomial theorem we get:

$$\sin^{p}\theta\cos^{q}\theta=\frac{(-J)^{p}}{2^{p+q}}\sum_{c=0}^{p+q}Q_{c}^{(p,q)}\Phi^{p+q-2c} \tag{4}$$

where

$$Q_{c}^{(p,q)}=\sum_{l=l_1}^{l_2}(-1)^{l}\binom{p}{l}\binom{q}{c-l} \tag{5}$$

$l_1=\max(0,c-q)$; $l_2=\min(c,p)$.
From Equation (5) we deduce that:

$$\sum_{c=0}^{p+q}Q_{c}^{(p,q)}=0 \tag{6}$$

$$Q_{(p+q)/2}^{(p,q)}=0 \text{ if } p \text{ and } q \text{ are positive odd integers} \tag{7.1}$$

$$Q_{2t-1}^{(p,p)}=0;\ t=1,2,\cdots,p \tag{7.2}$$

$$Q_{2t}^{(p,p)}=(-1)^{t}\binom{p}{t};\ t=0,1,\cdots,[p/2] \tag{7.3}$$

$$Q_{2t}^{(p,p)}=(-1)^{p}Q_{2p-2t}^{(p,p)};\ t=[p/2]+1\ ,\ [p/2]+2,\cdots,p \tag{7.4}$$

From Equations (4), (5) and(3) we have

$$\sin^{p}\theta\cos^{q}\theta=\frac{(-J)^{p}}{2^{p+q}}\sum_{c=0}^{p+q}\sum_{l=l_1}^{l_2}(-1)^{l}\binom{p}{l}\binom{q}{c-l}\times \\ \times\{\cos(p+q-2c)\theta+J\sin(p+q-2c)\theta\}\ . \tag{8}$$

By making $(J)^{m}$ equal to zero when m odd, that is, by writing

$$(J)^{m}=\frac{1}{2}(-1)^{[m/2]}\{1+(-1)^{m}\},$$

we deduce by means of Equations (7) and (8) the trigonometric series representation of $P_{l,m}(\sin\varphi)$ as:

$$P_{l,m}(\sin\varphi)=\frac{1}{2}H_0^{(l,m)}+\sum_{s=1}^{(l/2)}H_s^{(l,m)}\cos 2s\varphi\,;\; l=\text{even};\; m=\text{even}; \tag{9.1}$$

$$P_{l,m}(\sin\varphi)=\sum_{s=1}^{(l/2)}H_s^{(l,m)}\sin 2s\varphi\,;\; l=\text{even};\; m=\text{odd}; \tag{9.2}$$

$$P_{l,m}(\sin\varphi)=\sum_{s=1}^{(\frac{l+1}{2})}H_s^{(l,m)}\sin(2s-1)\varphi\,;\; l=\text{odd};\; m=\text{even}; \tag{9.3}$$

$$P_{l,m}(\sin\varphi)=\sum_{s=1}^{(\frac{l+1}{2})}H_s^{(l,m)}\cos(2s-1)\varphi\,;\; l=\text{odd};\; m=\text{odd}; \tag{9.4}$$

where:

$$H_S^{(m,l)}=(-1)^m(-1)^{(l-m+3\eta)/2}2^{-2l+1};$$

$$\sum_{t=0}^{t_1}\frac{4^t(2l-2t)!}{t!(l-t)!(l-m-2t)!}\sum_{j=j_1}^{j_2}(-1)^j\binom{l-m-2t}{j}\times\binom{m}{\frac{2m-l-\delta}{2}+t+s+j}; \tag{10}$$

$$\delta=\begin{cases}0 \text{ if } l \text{ even}\\ 1 \text{ if } l \text{ odd}\end{cases};\; \eta=\begin{cases}0 \text{ if } l-m \text{ even}\\ 1 \text{ if } l-m \text{ odd}\end{cases}; \tag{11.1}$$

$$t_1=\min(k,\frac{l+\delta}{2}-s);$$
$$j_1=\max(0,\frac{l-2m+\delta}{2}-t-s); \tag{11.2}$$
$$j_2=\min(\frac{l+\delta}{2}-t-s,l-m-2t).$$

Applications of the above formulae for the symbolic trigonometric series representation of $P_{l,m}(\sin\varphi)$ are given in Appendix A in a simple example for

$l = 4,5$, $m = 0,1,\cdots l$ and in Appendix B numerical evaluations using the symbolic series given by Equations (9) are given for some values of l, m, and random values of φ between -90° to $+90^{\circ}$, where $S[x, y]$ denotes the value of the symbolic series for $x = l$, $y = m$ and for a given value of φ, a complete example under requisite via authors.

The numerical values of $P_{l,m}(\sin\varphi)$ for the x, y and φ as evaluated from Equation (1) are also given and denoted by $E[x, y]$. The S's and E's values are in full agreement, a result which proves the efficiency and the accuracy of our symbolic representations of the associated Legendre functions.

REFERENCES

Coffey, S., Deprit, A., Deprit, E.: 1994, *Celest. Mech. Dyn. Astron.*, **59**, 37.
Garfinkel, B.: 1964, *Astron. J.*, **9**, 699.
Kaula, W. M.: 1966, *Theory of Satellite Geodesy*, Blaisdell Publ. Co., Waltham, MA.
Langbort, C.: 2002, *Celest. Mech. Dyn. Astron.*, **84**, 369.
Lara, M. :1997, *J. Astron. Sci.*, **45**, 321.
Scheeres, D. J. :1994, *Proc. Roy. Soc. Edinburgh*, A **126**, 1035.
Scheeres, D. J., Ostro, S. J., Hudson, R. S., Werner, R. A.: 1996, *Icarus*, **121**, 67.
Scheeres, D. J. Ostro, S. J., Hudson, R. S., De Jong, E. H., Suzuki, S.:1998, *Icarus*, **132**, 53.
Sharaf, A., Awad, M., Banajah, M.: 1989, *Earth, Moon Planets*, **47**, 171.
Sharma, R. K., James, M. X.: 1988, *Earth, Moon Planets*, **42**, 163.

APPENDIX A

Examples of trigonometric series for $P_{l,m}(\sin\phi)$, at $l = 4,5$ and $m = 0,1,\ldots,l$.

$$P_{4,0} = \frac{9}{64} - \frac{5}{16}\cos 2\phi + \frac{35}{64}\cos 4\phi$$

$$P_{4,1} = -\frac{5}{8}\sin 2\phi + \frac{35}{16}\sin 4\phi$$

$$P_{4,2} = \frac{45}{16} - \frac{15}{4}\cos 2\phi - \frac{105}{16}\cos 4\phi$$

$$P_{4,3} = -\frac{105}{4}\sin 2\phi - \frac{105}{8}\sin 4\phi$$

$$P_{4,4} = \frac{315}{8} + \frac{105}{2}\cos 2\phi + \frac{105}{8}\cos 4\phi$$

$$P_{5,0} = \frac{15}{64}\sin\phi - \frac{35}{128}\sin 3\phi + \frac{63}{128}\sin 5\phi$$

$$P_{5,1} = -\frac{15}{64}\cos\phi - \frac{35}{128}\cos 3\phi - \frac{315}{128}\cos 5\phi$$

$$P_{5,2} = \frac{105}{16}\sin\phi - \frac{105}{32}\sin 3\phi - \frac{315}{32}\sin 5\phi$$

$$P_{5,3} = -\frac{315}{16}\cos\phi + \frac{1365}{32}\cos 3\phi + \frac{945}{32}\cos 5\phi$$

$$P_{5,4} = \frac{945}{8}\sin\phi + \frac{2835}{16}\sin 3\phi + \frac{945}{16}\sin 5\phi$$

$$P_{5,5} = -\frac{4725}{8}\cos\phi - \frac{4725}{16}\cos 3\phi - \frac{945}{16}\cos 5\phi$$

APPENDIX B

Comparison between the numerical evaluations of $P_{l,m}(\sin\phi)$

ϕ°	S[7,7]	E[7,7]	S[4,4]	E[4,4]
25.1075	−67457.5	−67457.5	70.594	70.594
80.0633	−0.61569	−0.615682	0.0931016	0.0931016
9.81228	−121890	−121890	98.9895	98.9895
21.7963	−80403.1	−80403.1	78.0432	78.0432
10.6077	−119775	−119775	98.0044	98.0044
80.7746	−0.367841	−0.36781	0.069363	0.069363
29.5446	−50969	−50969	60.1466	60.1466
85.2048	−0.00385511	−0.00383645	0.0051276	0.0051276
82.4468	−0.0916286	−0.0914753	0.0313471	0.0313471
66.9507	−190.576	−190.576	2.46728	2.46728
78.4382	−1.75558	−1.75558	0.16943	0.16943
60.4745	−953.949	−953.949	6.1931	6.1931
75.6262	−7.85148	−7.85149	0.39877	0.39877
38.8467	−23488.4	−23488.4	38.6325	38.6325
46.847	−9460.93	−9460.93	22.9765	22.9765
16.3352	−101275	−101275	89.045	89.045
84.9969	−0.0051847	−0.0046055	0.00607365	0.00607365
11.4313	−117451	−117451	96.9131	96.9131
60.8333	−882.397	−882.397	5.92323	5.92323
1.31966	−134884	−134884	104.889	104.889
64.3348	−386.334	−386.334	3.69476	3.69476
12.2894	−114893	−114893	95.7014	95.7014
63.8589	−435.479	−435.479	3.95643	3.95643
3.54235	−133338	−133338	104.2	104.2
50.7727	−5466.42	−5466.42	16.7939	16.7939
2.35269	−134340	−134340	104.646	104.646
35.9534	−30779.8	−30779.8	45.0864	45.0864
71.746	−39.9771	−39.9771	1.01075	1.01075

49.8349	−6275.48	−6275.48	18.1721	18.1721
6.87272	−128483	−128483	102.014	102.014
83.5912	−0.0291761	−0.0288536	0.0163003	0.0163003
76.5413	−4.99956	−4.99956	0.308114	0.308114
42.2817	−16396.7	−16396.7	31.4597	31.4597
29.922	−49644.1	−49644.1	59.2482	59.2482
84.8471	−0.00637069	−0.00502019	0.00683237	0.00683237
47.0158	−9254.47	−9254.47	22.6886	22.6886
27.9079	−56872.8	−56872.8	64.034	64.034
21.2313	−82621.1	−82621.1	79.2662	79.2662
41.6941	−17491.2	−17491.2	32.643	32.643
59.3194	−1216.92	−1216.92	7.11751	7.11751
32.911	−39716.2	−39716.2	52.1559	52.1559
80.2001	−0.559289	−0.559275	0.0881281	0.0881281
70.8607	−55.0351	−55.0351	1.21331	1.21331
29.361	−51618.7	−51618.7	60.5836	60.5836
58.5762	−1415	−1415	7.75808	7.75808

Received on 8 September 2006

PLANNING NEAR-EARTH ASTEROID OBSERVATIONS ON A 1-METER CLASS TELESCOPE

OVIDIU VĂDUVESCU[1,2,3], MIREL BIRLAN[2,3]

[1] *ACRU and SAAO, South Africa*
Astrophysics and Cosmology Research Unit
University of KwaZulu-Natal, School of Mathematics
Durban, South Africa
E-mail: ovidiuv@yahoo.com

[2] *IMCCE, Observatoire de Paris*
77, Avenue Denfert Rochereau, F-75014 Paris, France

[3] *Astronomical Institute of the Romanian Academy*
Str. Cuţitul de Argint 5, 040557Bucharest, Romania

Abstract. The number of known Near-Earth Asteroids (NEAs) and Potentially Hazardous Asteroids (PHAs) has continued to grow in the last decade. Follow-up and recovery of newly discovered objects, as well as new astrometry at second or third oppositions are necessary to improve their orbits and predict any potential collision with the Earth in the future. A project to follow-up and recovery PHAs and NEAs is proposed, using 1-meter class telescope in the next two years. Two incoming runs will take place first, at Pic du Midi (France) and SAAO (South Africa), both to use 1-meter telescopes. Other observing runs are sought in the future. Collaborators to extend this project are welcome.

Key words: astrometry – NEAs – PHAs – CCD observations – star catalogs.

1. INTRODUCTION

Follow-up observations of Near-Earth Asteroids are welcome by the astronomical community in order to recover newly discovered bodies, to secure and improve their orbits and to predict their future close encounters with the Earth, including any possible collision threat well in advance.

Near-Earth Asteroids (NEAs) are defined as the asteroids with a perihelion distance $q < 1.3$ AU. Potentially Hazardous Asteroids (PHAs) are the NEAs having a Minimum-Orbital-Intersection Distance (MOID) less than 0.05 AU and absolute magnitudes $H < 22$, which corresponds to objects larger than about 1 km. This limit in size represents asteroids large enough to potentially cause a global climate disaster and threaten the continuation of human civilization (e.g., Chapman and Morrison 1994).

Rom. Astron. J., Vol. **16**, No. 2, p. 201–206, Bucharest, 2006

According to ASTORB database (Bowell 2006), there are 329,654 catalogued asteroids known today (March 17, 2006). According to NEO website (NASA/JPL 2006), there are 3925 NEAs and 773 PHAs known today (March 17, 2006). During the last decade, these two numbers have increased dramatically.

There are about seven dedicated NEAs discovery programs in progress. Most of them have been funded and carried out in the US: LINEAR (MIT 2006, currently holding more than half of the NEAs discoveries), NEAT (NASA/JPL 2006), Spacewatch (LPL 2006), LONEOS (Lowell Observatory 1996), and Catalina. Three others have been carried out elsewhere, with some interruptions due to lack of funding: Catalina South in Australia, CINEOS in Italy, and BAO in Japan (JSA 2006).

Although the annual increase of the newly discovered NEAs/PHAs has declined in the last two years, suggesting that there are fewer unknown objects detectable in the range of the present facilities, the number of known NEAs continues to grow by 200–500 new NEAs and 50–90 new PHAs discovered each year (EARN 2006).

2. OBSERVING BRIGHT NEAs/PHAs

Only a small fraction of the NEAs and very few PHAs are accessible to small telescopes ($D < 1$ meter). About 24% of the NEAs and 22% of the PHAs have $H \leq 18.0$, with 57 NEAs and 8 PHAs reaching $H \leq 15$ (e.g., EARN 2006).

Between 2002 and 2004, we carried out a follow-up program to observe a few NEAs and PHAs using the 60-cm telescope at York University Observatory in Toronto, Ontario, Canada. Due to the very light-polluted sky of Toronto, the limit of this facility remained relatively modest ($V \leq 15$), which allowed minor planets to be observed only around opposition. Planning the observations in this case was simple, i.e., by searching the NEO Earth Close Approaches table maintained online by the NEO program (NASA/JPL 2006).

Following this program, an observatory code was assigned by MPC to York University Observatory (H79) and four batches have been included in the NEODyS database and MPC Circulars (Văduvescu 2004b, c). One paper addressed, planning the observations on a small telescope (Văduvescu 2004a), and another presented the program at York University Observatory (Văduvescu 2005a).

3. OBSERVING FAINT NEAs/PHAs

Most of the NEAs and PHAs are faint, having absolute magnitudes $H \geq 18.0$, corresponding to sizes smaller than ~1 km (EARN 2006). Using a 1-meter telescope, a good fraction of these objects are expected to be within the capabilities of a 1-meter class telescope (about $V \leq 19$) and can be followed at any time of the year.

In order to assert the number of objects with $V \leq 19$, we performed a database search using the MPC list *Dates of Last Observation of Unusual Minor Planets* (MPC 2006a) to find all NEAs/PHAs with $V \leq 19$ visible between April 1–7, 2006. We found 30 NEAs and 7 PHAs meeting this condition, with 15 NEAs and 4 PHAs listed as "urgent", "very desirable" or "desirable" for observations. Similar searches conducted in the last year confirmed similar results. Assuming a NEA/PHA population distributed homogenously around the ecliptic, we can conclude that at least about 30 NEAs and 5 PHAs are expected to be observable weekly, using a 1-meter telescope.

4. INCOMING OBSERVING RUNS

Using 1-meter class telescopes, we propose a few observing runs during the next two years, depending on the available telescope and observer time.

The first observing run took place between 15 and 29 May, 2006, at Pic du Midi Observatory, France.

A second application was submitted in March 2006 to South African Astronomical Observatory (SAAO). We hope to collect more data using the 1-meter telescope at SAAO.

Additional observing runs on 1-meter class telescopes are sought in the next two years, given telescope time-availability in France, South Africa or elsewhere. Also, additional observers on other 1-meter class telescopes are welcome.

5. OBSERVING STRATEGY

The main goals of the runs will be oriented toward astrometry and photometry. The reduced data will allow the improvement of the orbital elements and magnitudes. A 1-meter telescope located at a dark site can observe a larger number of asteroids, thus the observers have to prioritize and optimize their observing time available.

The first aim will be to recover bright newly discovered NEAs/PHAs at their first opposition. In this sense, we plan to consult, on a nightly base, the following online lists: *The NEO Confirmation Page* (MPC 2006c), *Bright Recovery Opportunities* (MPC 2006b), and *NEAObs: NEA Observation Planning Aid* (MPC 2006d). PHAs and NEAs, flagged as "Urgent" and "Desirable" will be preferred in this order.

The second aim will be to follow-up very desirable objects based on the list of *Dates of Last Observation of Unusual Minor Planets* (MPC 2006a). VIs (very important), PHAs, and NEAs (Amors, Apollo, Athens) with One-Opposition and Multi-Opposition will be preferred in this order. The MPC servers allow user to customize the lists, based on right ascension and declination limits, elongation range, V magnitude range, and observatory code.

An alternative server which can be used for double checking will be the new *HOP – Hierarchical Observing Protocol for Asteroids* (Lowell Observatory 2006). To produce a list including all NEAs visible from a given place at present time given a limiting magnitude, the Inner-Planet Crossers flag must be set to 9, and all Other Selection Criteria must be given also the highest priority (9). Another list including NEAs at opposition is maintained by JPL (NASA/JPL 2006).

Based on the effective observing time and number of observable objects, the third aim will be oriented toward photometry, i.e., lightcurves from which to derive rotational periods of NEAs/PHAs. A list with all known asteroids rotation periods is *Minor Planet Lightcurve Parameters* (MPC 2006e).

6. EPHEMERIDES AND FINDING CHARTS

We plan to use Celestial Maps 10 (Văduvescu et al. 2005) to produce the finding charts for the asteroids selected. Besides a few compressed catalogs available on the CD (SAO, PPM, GSC 1, Tycho-2), Celestial Maps 10 produces maps by querying online the largest stellar catalogs available today (GSC 2, USNO-A2, USNO-B1, 2MASS), via VizieR. The software includes an embedded integrator for the asteroids ephemerides, which ensures arcsecond accuracy for most minor planets, using up-to-date orbital elements derived from the ASTORB database (Bowell 2006).

Alternatively to the embedded ephemerides, one can check major online ephemerides servers, such as HORIZONS (JPL 2006) or IMCCE (IMCCE 2006). Both take into account planetary perturbations based on modern planetary theories (DE405/406 of JPL or VSOP87 of BdL), generating accurate NEAs ephemerides to less than 1″ for most orbits.

Some NEAs/PHAs will be observed at their first or second oppositions, having large uncertainties in their orbits and consequently their ephemerides. In this case, objects having large 1-sigma uncertainty values are preferred first, although these targets are more difficult to find around their predicted positions.

7. EXPOSURE TIMES

Most of the NEAs/PHAs are relatively faint ($V \geq 18$), requiring longer exposure times to be able to reach a good signal to noise, necessary for accurate astrometry. Most of the brightest NEAs/PHAs are expected to be observed close to opposition, thus their proper motion will be high.

The exposure times will be constraint by two variables: the apparent magnitude (which requires longer exposure times for faint targets), and the proper motion (which requires shorter exposures times in order to “freeze” the asteroid’s apparent motion). Simply, for one image, the maximum exposure time in seconds is given by the ratio between the seeing, expressed in arc-seconds, to the proper motion of the asteroid, expressed in arc-seconds per second.

8. DATA REDUCTION

We plan to use IRAF or MIDAS to reduce astrometry and relative photometry for the observed NEAs/PHAs. Tycho-2, 2MASS, and USNO-A2 catalogs will be preferred in this order for astrometry. Data will be reduced and sent to Minor Planet Centre within a few weeks after completion of the runs.

9. CONCLUSIONS

The number of known NEAs and PHAs has continued to grow in the last decade. Follow-up and recovery of newly discovered objects, as well as new data at second or third oppositions, are necessary to improve their orbits and to predict any potential collision with the Earth in the future.

Some experience in NEAs/PHAs observations has been gathered by the first author in the last few years using a 60-cm telescope at York University Observatory in Toronto, Canada. More observations are proposed using 1-meter class telescopes in the next two years. Two incoming runs were and will be at Pic du Midi Observatory (France) and SAAO (South Africa), both to use 1-meter telescopes. Other observing runs in the future will be sought, depending on the available 1-meter class facilities and observer times. Collaborators to extend this project are welcome.

REFERENCES

Bowell, T.: 2006, *ASTORB Database*, online at ftp://ftp.lowell.edu/pub/elgb/astorb.html.

Chapman, C. R., Morrison, D.: 1994, *Nature*, **367**, 33.

EARN: 2006, *The Near-Earth Asteroids Database*, online at http://earn.dlr.de/nea/.

IMCCE: 2006, *Serveur d'éphémérides de l'Institut de Mécanique Céleste et de Calcul des Éphémérides*, http://www.imcce.fr/ephemeride.html.

JPL: 2006, *JPL's HORIZONS System*, http://ssd.jpl.nasa.gov/?horizons.

Lowell Observatory: 2006, *HOP - Hierarchical Observing Protocol for Asteroids*, http://asteroid.lowell.edu/cgi-bin/koehn/hop.

MPC: 2006a, *Dates of Last Observation of Unusual Minor Planets*, http://cfa-www.harvard.edu/iau/lists/LastUnusual.html.

MPC: 2006b, *Bright Recovery Opportunities*, http://cfa-www.harvard.edu/iau/NEO/BrightRecovery.html.

MPC: 2006c, *The NEO Confirmation Page*, http://cfa-www.harvard.edu/iau/NEO/ToConfirmRA.html.

MPC: 2006d, *NEAObs: NEA Observation Planning Aid*, http://scully.cfa.harvard.edu/~cgi/NEAObs.COM.

MPC: 2006c, *Minor Planet Lightcurve Parameters*, `http://cfa-www.harvard.edu/iau/lists/LightcurveDat.html`.
NASA/JPL: 2006, *Near-Earth Object Program*, `http://neo.jpl.nasa.gov/`.
Văduvescu, O.: 2004a, *Rom. Astron. J.*, **14**, 199.
Văduvescu, O.: 2004b, M.P.C. 52511 (August 30, 2004).
Văduvescu, O.: 2004c: M.P.C. 52903 (October 28, 2004).
Văduvescu, O.: 2005a, *Rom. Astron. J.*, **15**, 171.
Văduvescu, O.: 2005b, Seminaires "Temps et Espace" (IMCCE - SYRTE), Observatoire de Paris, 7 mars 2005, Celestial Maps v.10 (abstract online).
Văduvescu O., Birlan M., Curelaru, L.: 2005, Celestial Maps Software, `http://www.geocities.com/ovidiuv/maps.html`.

Received on 2 May 2006

ÁRPÁD PÁL
(1929–2006)

One of the most prominent Romanian scientists, Professor Árpád Pál, astronomer and mathematician, left us on July 21, 2006.

He was born on 25 June 1929, in the village Hoghia, Harghita county, Romania. After the elementary school in his natal village, the gymnasium in Gheorgheni city, and the high school in Odorheiul Secuiesc, he graduated from the Department of Mathematics and Physics at the "Bolyai" University of Cluj in 1952. In 1957 he obtained the doctoral degree at the "Sternberg" Astronomical Institute of the "Lomonosov" University in Moscow, with a thesis of celestial mechanics: *Analytical Interpolation Theory of the Motion of Astraea*, under the supervision of professors N. D. Moiseev (1902–1955) and B. M. Shchigolev.

Back in Romania, he started to teach astronomy at the Department of Mathematics at "Babeş-Bolyai" University, where he was full professor from 1972. He was the Scientific Secretary of the University Council (1968–1972), Dean of the Department of Mathematics (1976–1984), Vice-Rector of the University (1984–1990). He was Director of the Institute for Numerical Analysis from Cluj-Napoca (1976–1984, 1986–1990).

Since 1977 he was Director of the Astronomical Observatory of the "Babeş-Bolyai" University, for which he constructed a new building, inaugurated in 1982.

Outstanding astronomer, Professor Pál had a brilliant career in both education and research. Author of high-level handbooks and scientific advisor for Ph. D. theses, he provided a solid astronomical training to generations of students. Many of them are professional astronomers today.

His researches dealt primarily with celestial mechanics and space dynamics.

Professor Pál brought valuable contributions to the study of asteroid and artificial satellite dynamics, as well as to the theory of averaging. Of no little importance are the researches performed along with his students during the doctoral stages of these ones. More than twenty doctors in astronomy elaborated their theses under his direction and within a fruitful cooperation with him.

He was the author of different textbooks at the academic level, of about 150 scientific papers, 35 grants with different scientific forums, and he founded and edited the series of the *Babeş-Bolyai University Faculty of Mathematics Research Seminars* (1979–1992).

As Editor-in-Chief of the *Romanian Astronomical Journal*, Professor Pál amply contributed to increase its prestige. Its pages hosted papers submitted by outstanding astronomers from Canada, France, Germany, Japan, Poland, Russia, Spain, UK, etc. The results of the Romanian astronomical research are worldwide spread especially via this journal.

He was member of different editorial boards: *Seria Mathematica* of the journal *Studia Universitatis Babeş-Bolyai*, *Matematikai Lapok*, edited by the Romanian Society of Mathematical Sciences.

He was invited for different lectures in Budapest, Moscow, Ondrejov.

He was member of many national and international bodies: Romanian Society of Mathematical Sciences, Romanian Commission for Space Activity, International Astronomical Union (Commission 7), COSPAR, European Astronomical Society. He was the President of the Romanian National Astronomical Committee since 1994.

Professor Pál made appreciable efforts to make the national astronomy better known worldwide, in order to reintegrate it in the international scientific community.

Between 1973 and 1979 he was Vice-President of the National Council for Science and Technology, and between 1985 and 1989 Vice-President of the State Council of Romania. He was awarded with different medals.

Romanian research feels a deep poverty after one of its most active scientists and professors left us.

Selected publications

Chiş, G., Pál, Á., *Astronomie (Curs de inițiere)*, Vol. 1: *Astrometrie, Mecanică cerească și cosmonautică*, Universitatea Babeş-Bolyai, Cluj-Napoca, 1975.

Chiş, G., Pál, Á., *Astronomie (Curs de inițiere)*, Vol. 2: *Astrofizică, Astronomie stelară, Cosmologie și cosmogonie*, Universitatea Babeş-Bolyai, Cluj-Napoca, 1975.

Oproiu, T., Pál, Á., Pop, V., Ureche, V., *Astronomie. Culegere de exerciții, probleme și programe de calcul*, Universitatea Babeş-Bolyai, Cluj-Napoca, ed. I, 1985, ed. II, 1989.

Pál, Á., Ureche, V., *Astronomie*, Ed. Didactică şi Pedagogică, Bucureşti, 1983.

Pál, Á., Pop, V., Ureche, V. *Astronomie. Culegere de probleme (cu soluții)*, Presa Universitară Clujeană, Cluj-Napoca, 1998.

Anisiu, M.-C., Pál, Á., *Two-Dimensional Inverse Problem of Dynamics for Families in Parametric Form*, Inverse Problems **15** (1999), 135.

Burs, L., Pál, Á., *Drag perturbations of artificial satellite orbites in a Spherically Symmetrical Atmosphere*, Astron. Nachr. **302** (1981), 189.

Burs, L., Pál, Á., *The Artificial Earth Satellite Motion in an Oblate, Rotating Atmosphere with Symmetrical Diurnal Effect*, Astron. Nachr. **303** (1982), 269.

Chiş, G., Pál, Á., *Asupra instabilității binarei fotometrice Y Leonis*", St. Cerc. Astron. **9** (1964), 15.

Chiş, G., Pál, Á., *Observații vizuale ale sateliților artificiali ai Pământului, efectuate la stația 1132 de la Observatorul Astronomic al Universității "Babeş-Bolyai" din Cluj-Napoca în anul 1963*, St. Cerc. Astron. **10** (1965), 110.

Chiş, G., Pál, Á., Oproiu, T., *Opredelenie nekotorykh elementov orbity sputnikov Kosmos 44 iz nabliudenii, polucennykh v programme INTEROBS*, Nabl. ISZ **5** (1966), 85.

Chiş, G., Pál, Á., *Observații vizuale ale sateliților artificiali ai Pământului, efectuate la stația 1132 de la Observatorul Astronomic al Universității "Babeş-Bolyai" din Cluj-Napoca în anul 1964*, St. Cerc. Astron. **12** (1967), 93.

Chiş, G., Pál, Á., *Ob opredelenii kvazidrakonicekogo perioda iskusstvennykh sputnikov Zemli. Primenenie k Kosmosu 44 (1964-53-1)*, Nabl. ISZ, **8** (1968), 221.

Chiş, G., Pál, Á., Todoran, I., *Observații vizuale ale sateliților artificiali ai Pământului, efectuate la stația 1132 de la Observatorul Astronomic al Universității "Babeş-Bolyai" din Cluj-Napoca în anul 1962*, St. Cerc. Astron. **9** (1964), 113.

Grebenicov, E., Pál, Á., *General Formulation of Some Problems of Celestial Mechanics for Constructing Solutions Using Computers*, Rom. Astron. J. **6** (1996), 155.

Grebenicov, E., Pál, Á., *On the Mathematical Substantiation of Averaging Schemes for Some Problems of Celestial Mechanics*, Rom. Astron. J. **4** (1994), 105.

Mioc, V., Pál, Á., *Nodal Period Perturbations Due to the Fifth Zonal Harmonic of the Geopotential*, Studia Univ Babeş-Bolyai, Math, **30** (1985), No.1, 55.

Mioc, V., Pál, Á., Giurgiu, I., *Unstable Orbit Evolution around Pulsating Stars*, Studia Univ. Babeş-Bolyai, Phys., **33** (1988), No. 2, p. 85.

Mioc, V., Pál, Á., Giurgiu, I., *Orbital Motion with Periodically Changing Gravitational Parameter*, Studia Univ. Babeş-Bolyai, Math., **33** (1988), No. 4, 67.

Pál, Á., *Asupra comparării teoriei analitice de interpolare a mişcării micii planete Astraea cu observaţiile*, St. Cerc. Astron. **8** (1963), 159.

Pál, Á., *Variantele de mediere în problema celor 3 corpuri*, St. Cerc. Astron. **8** (1963), 247.

Pál, Á., *Ob odnom kriterii identificatsii iskusstvennykh sputnikov Zemli*, Nabl. ISZ **2** (1963), 115.

Pál, Á., *Un criteriu de identificare a sateliţilor artificiali ai Pământului*, Studia Univ. Babeş-Bolyai, Math.-Phys., **9** (1964), No. 2, 49.

Pál, Á., *Opredelenie izmenenii perioda iskusstvennykh sputnikov 63171 (Kosmos 17) i 64531 (Kosmos 44)*, Nabl. ISZ **7** (1967), 117.

Pál, Á., *Criterion for Identification of Man-Made Satellites of the Earth*, Astron. Papers Transl. Russ., **12** (1968), 189.

Pál, Á., *Promezhutochnaya orbita iskusstvennogo sputnika Zemli, postroenaya po metodu osredneniya. Vozmushcheniya pervogo poryadka*, St. Cerc. Astron. **18** (1973), 17.

Pál, Á., *In memoriam: Profesorul Gheorghe Chiş*, Studia Univ. Babeş-Bolyai, Math., **26** (1981), No. 4, 80.

Pál, Á., *Observatorul Astronomic al Universităţii*, Studia Univ. Babeş-Bolyai, Math., **31** (1986), No. 3, 67.

Pál, Á., *Mecanica newtoniană şi lansarea primului satelit artificial al Pămîntului*, Studia Univ. Babeş-Bolyai, Math., **32** (1987), No. 4, 73.

Pál, Á., *Spiru Haret's Theorem*, Rom. Astron. J. **1** (1991), 5.

Pál, Á., *Early Romanian Contributions to Celestial Mechanics*, Rom. Astron. J. **2** (1992), 205.

Pál, Á., *Nicolae Copernic (1473–1549)*, Studia Univ. Babeş-Bolyai, Math., **38** (1993), No. 1, 105.

Pál, Á., *János Bolyai (1802–1860)*, Studia Univ. Babeş-Bolyai, Math., **38** (1993), No. 4, 95.

Pál, Á., Anisiu, M.-C., *On the Legendre Transform and its Applications*, Studia Univ. Babeş-Bolyai, Math., **40** (1995), No. 2, 75.

Pál, Á., Anisiu, M.-C., *On the Two-Dimensional Inverse Problem of Dynamics*, Astron. Nachr. **317** (1996), 205.

Pál, Á., Oproiu, T., *Calcule de orbite instantanee ale sateliţilor artificiali ai Pămîntului în cadrul programului INTEROBS, efectuate cu maşina electronică DACICC-1*, St. Cerc. Astron. **12** (1967), 39.

Pál, Á., Oproiu, T., *On the Determination of Circular Orbits of Artificial Satellites from Optical Visual Observations*, Studia Univ. Babeş-Bolyai, Math., **26** (1981), No. 2, 76.

Pál, Á., Oproiu, T., *Determination of the Slopes of "Zero Relative Velocity" Curve from the Elliptic Restricted Three- Body Problem with an Averaging Method*, Rom. Astron. J. **1** (1991), 97.

Pál, Á., Pârv, B., *Formal Construction of the Generalized Krylov - Bogolyubov Equations*, Rom. Astron. J. **5** (1995), 29.

Pál, Á., Szenkovits, F., *Recurrent Power Series Solution of the n-Body Problem Associated to a Quasihomogeneous Potential*, Rom. Astron. J. **8** (1998), 37.

Pál, Á., Ţarină, M., *Topological Considerations on the Averaging Method with Application in Celestial Mechanics*, Rev. Roum. Math. Pures Appl. **32** (1982), 831.

Pál, Á., Ureche, V., *The Research Seminars of the Astronomical Observatory Cluj-Napoca*, Rom. Astron. J. **1** (1991), 116.

Pál, Á., Mioc, V., Stavinschi, M., *First-Order Effects of Lense-Thirring Precession in Quasi-Circular Satellite Orbits*, Studia Univ. Babeş-Bolyai, Math., **38** (1993), No. 1, 99.

Pál, Á., Mioc, V., Stavinschi, M., *Perturbations of Initially Circular Satellite Orbits Caused by the Zonal Harmonics of the Geopotential*, Acta Geod. Geoph. Hung. **29** (1994), 439.

Pál, Á., Oproiu, T., Radu, E., *Determinarea variației perioadei cvasinodale a satelitului artificial al Pământului. Aplicație la satelitul Explorer 19*, Studia Univ. Babeș-Bolyai, Math., **22** (1977), No. 2, 48.

Pál, Á., Şelaru, D., Mioc, V., Cucu-Dumitrescu, C., *The Gyldén-Type Problem Revisited: More Refined Analytical Solutions*, Astron. Nachr. **327** (2006), 304.

The Editorial Board

THE SECOND INTERNATIONAL SYMPOSIUM ON SPACE CLIMATE (ISSC-2) "LONG-TERM CHANGES IN THE SUN AND THEIR EFFECTS IN THE HELIOSPHERE AND PLANET EARTH"

Sinaia, Romania, 13–16 September 2006

The symposium topic belongs to a modern scientific field, which is based on the multidisciplinary scientific research in the fields of solar physics, heliospheric physics, magnetosphere, and terrestrial atmosphere. The concept of *space weather* was launched a decade ago in order to describe the short-term solar variations and their effects in the near-terrestrial space (magnetosphere, atmosphere, biological systems, technological systems). Analogously to the relationship meteorology-climate, at the terrestrial level, the concept of space weather extended to that of *space climate*, at the beginning of the first decade of the 21st century, in order to include long-term solar variations, as well as their long-term effects in the heliosphere, magnetosphere, terrestrial climate and many other systems. The scientific research in this multi- and interdisciplinary field approaches problems of major interest for terrestrial life, such as the global warming phenomenon. The clarification of the possible causes of solar and/or heliospheric origin which might be at the origin of the multiple climate anomalies of the last decade will have a strong impact on the world economy and on the national one implicitly.

ISSC-2 continues the series of symposia initiated in Oulu (Finland) in June 2004. The Astronomical Institute of the Romanian Academy (AIRA) was the main organizer. The Institute for Space Sciences (ISS) also supported the organization of this symposium.

The symposium was held in Sinaia. The proceedings were structured on three major topics from the research fields involved: Sun and Solar Activity; Heliosphere and Cosmic Rays; Terrestrial Effects.

During ten sessions, 34 invited papers, 15 oral contributions and 35 posters were presented. The eleventh session was a one-hour debates on two topics of major scientific interest: What Happened to the Sun during the Last 100 Years?; How Does the Sun Affect Climate and what Evidence We Have for that? A survey of the Symposium papers was presented in the same session.

The posters were exhibited throughout the whole duration of the symposium and there was an interval of an hour and a half dedicated especially to the posters in the fourth session (13 September).

The structure of the presentations was a particular one. The invited lectures were in a greater number than at other meetings of a similar scope, in order to introduce a new scientific field, to define and set up the field of interest of new concepts, as well as the specific research methods. It is worth mentioning that seven invited lecturers were young people under 35, who have distinguished themselves through their previous results, of a high scientific level.

Out of the total of 58 foreign specialists, 16 were young doctors or Ph.D. students, and all of them presented papers. Renowned specialists from the fields of solar physics, heliosphere, magnetosphere, and terrestrial climatology also presented invited papers. It is worth mentioning that among them there were directors of research intitutes (from Germany, Switzerland, Azerbaijan), and professors from Finland, Russia, and USA universities.

Rom. Astron. J., Vol. **16**, No. 2, p. 211–213, Bucharest, 2006

Romania was represented by 17 specialists from three institutes (AIRA, ISS, and the Institute of Geodynamics of the Romanian Academy), as well as two universities (Bucharest University and the University "Dunărea de Jos", Galați). From among them, six were young researchers under 35. The participants of the three institutes presented three invited papers, two oral contributions and nine posters. There also were two contributions made in cooperation by researchers from different institutes: AIRA and the Institute of Geodynamics, AIRA and ISS, respectively.

The scientific contributions presented at the ISSC-2 Symposium will be published in a special issue of the *Advances in Space Research* journal. The volume will be edited by three guest editors (G. Mariş, K. Mursula and I. Usoskin) and supervised by the Editor-in-chief M. Shea.

The Symposium in Sinaia made possible the meeting of the national representatives from most of the countries that participate in the Regional Collaboration "Balkan, Black Sea and Caspian Sea Regional Network on Space Weather Studies". On that occasion, at an ad-hoc round table (14 September), important problems concerning the journal *Sun and Geosphere* and the organization of a regional meeting in Baku (Azerbaijan), in September 2007, were discussed.

The Romanian participants from various institutes of apparently different profiles (astronomy, space research, geodynamics) had one more evidence about the importance of collaboration for the opening of new directions of modern research, which are also beneficial to the Romanian scientific research. Thus, the unification of the research efforts in order to explain and to evaluate quantitatively the energy and mass transfer of the solar wind in the magnetosphere and terrestrial atmosphere system will offer a scientific basis for the improvement of both geomagnetic prognoses and of climatic ones. The symposium gave the Romanian researchers the opportunity to present the newest original results in a meeting with world top specialists. Still unpublished results were submitted to the analysis and the debates with the other participants.

The organization in Romania of this Symposium on the eve of our European integration was a serious challenge. Although the Symposium had a great number of participants and a restricted budget of expenses, the opportunity was fully capitalized, becoming also an evidence for the international scientific community that Romania can integrate in the circuit of important meetings organizers.

We wish to thank the following sponsors for their contribution to the success of this symposium: European Office of Aerospace Research and Development, Air Force Office of Scientific Research, United States Air Force Research Laboratory, and the National Authority for Scientific Research of the Romanian Ministry for Education and Research.

Georgeta Mariş

THE INTERNATIONAL CONFERENCE "FIFTY YEARS OF ROMANIAN ASTROPHYSICS" Bucharest, Romania, 27–30 September 2006

In 2006 we celebrate fifty years from the appearance of the first issue of the solar bulletin *Observations Solaires*, a yearly publication of the Romanian Academy Publishing House (in French). Fifty years ago, on the occasion of the International Geophysical Year, two research teams were set up in Romania: the solar group and the artificial Earth satellite group. The conference emphasized this jubilee and constituted itself into an opportunity to bring together scientists from all over the world to exchange ideeas and to present their recent results in all fields of astrophysics. This event joined the International Heliophysical Year activities for IHY Romania, and was sponsored by the Romanian Ministry of Education and Research, under the national program Research of Excellence.

The conference was structured on nine sessions, each dedicated to a special topic. Besides the opening (anniversary session), every other session benefitted of an invited conference. I give the topics and the invited speakers below:

– Solar Atmosphere (Brigitte Schmieder, France);

– Magnetic Structures on the Sun (Jan Olof Stenflo, Switzerland);

– Solar and Stellar Winds (Christophe Sauty, France);

– Waves, Oscillations, Cyclicities (Jose Luis Ballester, Spain);

– From the International Geophysical Year to the International Heliophysical Year (Joseph M. Davila, USA);

– Asteroseismology (Annie Baglin, France);

– Stellar Astrophysics (Eleni Rovithis-Livaniou, Greece);

– Extragalactic Astronomy and Cosmology (Cristina Popescu, Germany).

A special guest (and also an invited speaker) was Dr. Zadig Mouradian, who began his carrier in the Bucharest Observatory of the Astronomical Institute of the Romanian Academy, and is one of the best collaborators of the Astronomical Institute of the Romanian Academy.

More than 60 specialists attended the conference. Besides the invited lectures, many dozens of authors presented contributions. It is enough to say that the contributions belonged to authors from 16 countries (Armenia, Belgium, Bulgaria, France, Germany, Greece, Italy, Mexico, Romania, Russia, Serbia and Montenegro, Spain, Switzerland, The Netherlands, UK, USA).

The conference was a good opportunity to establish bases for new common projects, for new joint papers co-authored by specialists from various countries, and for new exchange of scientists between the participant countries. It was also a good opportunity for Romanian scientists to revive their past personalities and the research evolution during these fifty years, and also to emphasize the results of their work in the last few years. We also notice the presence of the new generation of scientists from Romania and abroad. The solar group from Bucharest was present with a new team, which includes four young people, one of them being the first returned home with PhD title obtained abroad.

This conference was an anniversary event, but also an adequate moment for pointing out a change of generations in the Romanian astrophysics. We hope this is a good signal for the re-integration of the Romanian astronomy into the international astronomical community. The conference also constituted itself into a genuine prologue for the centenary of the Astronomical Institute of the Romanian Academy, to be celebrated in 2008.

The volume will be soon published in the AIP Conferences Series (editors: C. Dumitrache, N. A. Popescu, M. D. Şuran, V. Mioc).

Cristiana Dumitrache

CRISTIANA DUMITRACHE, NEDELIA ANTONIA POPESCU, *Fifty Years of Romanian Astrophysics*, Ed. Cartea Universitară, Bucharest, Romania, 2005, 100 pp., ISBN 973-731-236-8; 2nd revised edition, 2006, ISBN 973-731-397-6

This book is a first fruit of a project financed by the Romanian Ministry of Education and Research within the framework of the program Research of Excellence. Far from being an exhaustive analysis, it sheds some light on the scientists, researches and results that represented the Romanian astrophysics along the last fifty years (1956–2006).

The authors structured the book in four main parts, according to the main astrophysical research directions tackled in Romania: solar physics, variable stars, extragalactic astronomy and cosmology, space research. A list of 101 works quoted in the text ends the book.

As expected, since the starting point of this anniversary was considered to be the first publication (1956) of the systematic solar observations performed at the Bucharest Observatory, the solar physics constitutes the topic of about half of the book. The reader is provided with a general image (as well as with many details) of what meant the solar research in Romania during these years. The evolution of this research is surveyed: observations (from drawings of sunspots to observations required by the international data centers), processing (of both own data and data provided by specialized space missions), interpretation (leading sometimes to surprising issues), theoretical researches (based especially on the powerful tools of magnetohydrodynamics), numerical simulations of the processes that occur in the solar atmosphere.

The next main part is dedicated to variable stars, domain that benefitted of the most significant astrophysical instruments owned by the Romanian astrophysical research: the reflectors in Bucharest, Cluj-Napoca, and Timişoara. The photoelectric and CCD observations of binaries (Bucharest) and pulsating stars (Cluj-Napoca), with all their results, occupy a place of choice. No less important are the theoretical models of the variability of such stars. The authors also emphasize the fact that almost all these researches were done within the framework of wide international cooperation programs.

In the third part, the authors dwell upon a much less investigated branch of astrophysics in Romania: extragalactic astronomy and cosmology. There were and still are rather few Romanian researchers working in this field, however noticeable results were obtained. These ones deal mainly with the structure and evolution of clusters of galaxies, the formation of structures in an early Universe, the large-scale structure of the Universe.

A short part dedicated to space research ends the book. It surveys the evolution of this research from the first visual observations of artificial Earth satellites to the investigation of the most various influences of perturbing factors on the dynamics of space missions. One could think that such studies belong rather to celestial mechanics and space dynamics than to astrophysics. But we must not forget a reality: there is no clear frontier between the branches of astronomy. The space dynamics and many aspects belonging to astrophysics (arbitrarily: solar activity, luminosity-changing sources, photogravitational effects, stellar and planetary magnetic fields, planetary atmospheres, etc.) are closely interrelated.

Besides research and results, the authors sketched in few sentences the portraits of those scientists who contributed to the fifty years of Romanian systematic astrophysical research. Within this context, I

Rom. Astron. J., Vol. **16**, No. 2, p. 215–217, Bucharest, 2006

appreciate the way in which the book makes much better known the figure and the activity of the founder of the modern Romanian astrophysics: Academician Călin Popovici.

The book is rather a report than a historical treatise. But everyone who wants to have an idea about the astrophysics in a country with noticeable traditions in astronomy is provided with good information that can be considerably extended. I hope that the astrophysicists who read it will find new fields and topics for enlarging the scientific cooperation with the Romanian astronomical community.

Vasile Mioc

VLADIMIR GERDJIKOV, MILCHO TSVETKOV (editors), *Prof. Manev's Legacy in Contemporary Astronomy, Theoretical and Gravitational Physics*, Proceedings of the First Maneff Conference, May 20–22, 2004, Sofia, Bulgaria, Heron Press, Sofia, Bulgaria, 2005, 345 pp., ISBN 954-580-183-2

This volume includes the contributions presented at the First Maneff Conference, organized by twelve institutions from Bulgaria, France, and Romania.

Georgi Manev was one of the most outstanding Bulgarian physicists during the first half of the 20th century. His ideas on the problems of cosmology and mathematical physics offered a classical alternative to special relativity, on which he exchanged letters with Albert Einstein. After World War II, his work was interdicted and then forgotten, but starting from 1990s his ideas found new applications. Florin Diacu and Cristina Stoica (Canada), Vasile Mioc and Magda Stavinschi (Romania) revived the interest in this subject, which has been intensely studied since.

At least at the solar-system level, Manev's model provides the same good theoretical approximations as relativity, but without leaving the framework of classical mechanics. During the last decade, scientists from Bulgaria, Brazil, Canada, Chili, Ireland, Italy, Mexico, Portugal, Romania, Serbia and Montenegro, Spain, Switzerland, UK, USA and other countries studied this topic, aiming at the description of the dynamics of particle systems in Manev-type fields.

The volume is structured in four large parts.

Part 1, *Historical Aspects*, tackles mainly the academic life and the scientific work of Georgi Manev. The contributions cover various aspects: from the lectures given by the Bulgarian scientist at the University of Sofia to the correspondence between him and Albert Einstein; from Manev's academic career promotion to the very large perspective about the study of his work as a significant part of the Bulgarian-Romanian cooperation. Of a particular interest is the database containing a lot of papers, books, PhD theses that deal with Manev's model. I have to emphasize that this database is continuously increasing and updated. There also are some historical contributions unrelated to Georgi Manev. They concern: physics and politics, with a special regard to Werner Heisenberg; the centenary of Konkoly Observatory, Budapest, Hungary; the Serbs and astronomy in the 18th and 19th centuries.

Part 2, *Developments of the Manev Theory*, presents some applications of Manev's model to problems of astronomy, celestial mechanics, relativity, differential equations, theoretical physics, etc. Subtle mathematical aspects, as superintegrability or analogy with a forced harmonic oscillator, are pointed out. I also emphasize more general results concerning Manev's model in the light of the Inverse Problem Theory, or the exotic phase-space structure of this model. Results belonging to relativistic physics (relativistic Coulomb problem), or to astrophysics (Roche's model in Manev's photogravitational field), are to be mentioned, too. It is to be remarked how many concrete applications Manev's model and the Manev-type models can be found in very different branches of physics, mathematics and astronomy.

Part 3, *Astronomy, Astrophysics, and Gravitational Physics*, is dedicated to contributions having large astronomical connotations. The contributions belong to various domains: galactic and extragalactic astronomy, cosmology, relativity, string theory. Very interesting topics are approached: white dwarfs, dark matter, starburst galaxies, gravitational waves, neutrino oscillations, cosmic strings, etc. Among them, I remark the paper about the use of Manev's term in galactic astronomy and the one treating the field generated by a chargeless point mass in general relativity, both within the spirit of the conference.

Part 4, *Contemporary Theoretical Physics*, even it seems to be less related to Manev's model, constitutes itself into a homage brought to the legacy of the scientist who created the Bulgarian theoretical physics. Contributions treating (I quote arbitrarily): soliton theory, nonlinear Schrödinger-type equations, Minkowski spacetime, conformally invariant differential operators, nonlinear waves, and so forth, help us to have an idea about the level of today's theoretical physics in Bulgaria, whose bases were put by Georgi Manev.

This volume of proceedings emphasizes, as the conference did two years ago, some important aspects:

– the inter- and multidisciplinary character of astronomy;

– the many domains and problems in which the mathematics of the Manev model is applicable, useful, and fruitful;

– the role of the history of science and history of ideas in the advance of research.

I think that, besides the role of the two editors, Prof. Vladimir Gerdjikov and Dr. Milcho Tsvetkov, the efforts of Dr. Katya Tsvetkova, Prof. Plamen Fiziev, and especially the late Prof. Sawa Manoff made this volume become a reality.

To end, I have to greatly appreciate the excellent graphical conditions in which Heron Press published this book.

Vasile Mioc

NOTICE TO AUTHORS

ROMANIAN ASTRONOMICAL JOURNAL appears twice a year and is open to original contributions in Astronomy and related disciplines. The contributions – in English or French – can be accepted only if they were neither published before nor destined to another publication.

Manuscripts should, preferably, be submitted as e-mail attachments to roaj@aira.astro.ro, to the Editor in Chief (vmioc@aira.astro.ro), or to one of the members of the Editorial Board. They must be written in a well-known editor, preferably a recent version of Word. Authors who cannot submit an electronic version of their manuscript should sent it to the Editorial Board. In this case two copies of the manuscript (along with the text of the article on floppy disk) are required. The first page should contain: article's title (brief and informative), author's name and affiliation, followed by an *Abstract* in English and *Key words*. The text should be clear and concise (it is recommended not to exceed 10 pages). The *Abstract* will present clearly the principal conclusions on the work, in no more than 10–15 lines.

Chapters and Paragraphs. Papers, except short notes, should be divided into chapters, numbered by Arabic numerals. Chapters may be divided into paragraphs denoted by the number of the chapter and the number of the paragraph; each chapter and each paragraph should have a short descriptive title (e.g. "3.2. Results").

Formulae have to be centered and numbered consecutively in Arabic numerals, too, but included in brackets on the right-hand side of the manuscript.

Tables should be numbered consecutively in Arabic numerals; they should be introduced in the text at their appropriate place.

Figures and Illustrations should be submitted separately, in such a form as to permit reproduction without retouching. Any lettering should be large enough to be legible after the figure has been reduced in size for printing. Captions should be introduced in the text at their appropriate place. All figures should be numbered consecutively in Arabic numerals and referred to in the text, e.g. Fig. 2 or Figs. 2–5. Photographs should be given only if essential and should be enlarged enough to permit clear reproduction.

References are indicated in the text by the author's name and year of publication. They should be listed in alphabetic and chronologic order at the end of the paper, as follows: name and initials of the author(s), year of publication, suitable abbreviation of the journal (or title of the book and editing house), its volume and page.

The *fonts* to be used are: 11 for the text proper, 13 for the paper title, 9 for author's name and affiliation, abstract, key words, titles of chapters and paragraphs, figure captions, tables, running titles, and references.

Detailed instructions for the preparation of manuscripts can be found at http://www.astro.ro/~roaj.

Please pay attention to these recommendations; the manuscripts that do not observe them will be returned to the authors.

ROMANIAN
ASTRONOMICAL
JOURNAL

Vol. 16, No. 2, 2006

CONTENTS

ISSN 1220-5160

Rom. Astron. J., Vol. **16**, No. 2, p. 111–218, Bucharest, 2006